Retrofit for multi-period processes for practical heat exchanger network design

by Jan Andreas Stampfli

A thesis for the degree of
Doctor technicae

In the
Doctoral Program in Engineering Sciences – Mechanical Engineering

At the
Faculty of Mechanical and Industrial Engineering, TU-Wien

Under the supervision of
Prof. Dr. René Hofmann, TU-Wien

and
Prof. Dr. Beat Wellig, Lucerne University of Applied Sciences and Arts

Reviewed by
Dr. Timothy G. Walmsley, The University of Waikato

and
Prof. Dr. Paul R. Stuart, Polytechnique Montréal

Author
Jan Andreas Stampfli
Matr. Nr.: 11838514
jan.stampfli@hslu.ch

Supervisors
Prof. Dr. René Hofmann
rene.hofmann@tuwien.ac.at
TU Wien
Institute for Energy Systems and Thermodynamics
Getreidemarkt 9/E302
1060 Wien, Austria

Prof. Dr. Beat Wellig
beat.wellig@hslu.ch
Lucerne University of Applied Sciences and Arts
Competence Center Thermal Energy Systems and Process Engineering
Technikumstrasse 21
6048 Horw, Switzerland

Reviewers
Dr. Timothy G. Walmsley
tim.walmsley@waikato.ac.nz
The University of Waikato
Ahuora - Centre for Smart Energy Systems
Private Bag 3105
3240 Hamilton, New Zealand

Prof. Dr. Paul R. Stuart
paul.stuart@polymtl.ca
Polytechnique Montréal
Department of Chemical Engineering
2900 Édouard-Montpetit Boulevard
H3T 1J4 Montréal, Canada

Funding
This thesis is financially supported by the Swiss Innovation Agency Innosuisse and is part of the Swiss Competence Center for Energy Research – Efficiency of Industrial Processes SCCER EIP and the Swiss Federal Office of Energy's "SWEET" Programme (Call 1-2020) – Decarbonisation of Cooling and Heating, DeCarbCH. Further financial support is provided by the Lucerne University of Applied Sciences and Arts, Switzerland. This research is part of a collaboration between the Lucerne University of Applied Sciences and Arts and TU-Wien.

Going to press
I confirm that going to press of this thesis needs the confirmation of the examination committee.

Affidavit
I declare in lieu of oath, that I wrote this thesis and performed the associated research myself, using only literature cited in this volume. If text passages from sources are used literally, they are marked as such. I confirm that this work is original and has not been submitted elsewhere for any examination, nor is it currently under consideration for a thesis elsewhere.
I acknowledge that the submitted work will be checked electronically-technically using suitable and state-of-the-art means (plagiarism detection software). On the one hand, this ensures that the submitted work adheres to the high-quality standards of the current rules for ensuring good scientific practice "Code of Conduct" at the Vienna University of Technology. On the other hand, a comparison with other students' theses avoids violations of my copyright.

Horw, August 2023

Jan Stampfli

Abstract

Process integration addresses the challenge of reduction in energy consumption by heat recovery in the processing industry. Its main focus lies on the grassroot design for new plants. However, a large portion of existing plants were built during times with low energy prices and thus, little focus on energy efficiency. Hence, retrofitting existing plants has a high potential to improve the overall energy efficiency in the process industry. Due to the industry's orientation towards small volume, high value-added production demanding multi-product and multi-purpose plants, the focus of the process industry shifts to multi-period operation. Hence, process integration for such processes is more challenging as heat exchanger networks need to be flexible to handle multi-period operation. To overcome these challenges, research is also shifting more towards retrofitting existing plants and multi-period production. Further, for industry, it is more important to consider practical challenges within the optimization and be able to guide the optimization towards more practical plant designs rather than finding the best possible solution requiring complex and expensive controlling systems.

The research in this thesis focuses on developing a method addressing the challenge of retrofitting multi-period processes for practical heat exchanger network design. To ensure practical designs, additional constraints are considered in the optimization. These constraints increase the complexity of the already $\mathcal{NP}$-hard *in the strong sense* optimization problem. Hence, the developed method resorts to metaheuristic optimization algorithms. A possible hybrid trajectory-based as well as a hybrid evolutionary-based algorithm are investigated whereby the latter has prevailed. The implemented algorithm is split into two stages. A Genetic Algorithm optimizes the heat exchanger network topology and a Differential Evolution optimizes the heat loads for every operating period. To ensure feasible heat transfer in every operating period, bypass and admixer configurations, which ensure flexible operation of the heat exchangers, are analyzed to ensure feasible mixer temperatures by solving the logarithmic mean temperature analytically using the Lambert W-function. In recent years, reduction in greenhouse gas emissions has become more important for industry. Hence, greenhouse gas emissions are considered as a second objective in addition to the total annual cost. Therefore, the algorithm is using an NSGA-II sorting algorithm and hypervolume indicators to perform a Pareto optimization.

The developed algorithm is applied successfully to a case study from the literature and one from the industry. The results for the multi-objective optimization showed that the weighting between capital costs for retrofit and utility demand, causing operating costs and greenhouse gas emissions, has a large impact on the final design. This also implies that a change in energy costs or an improvement in the efficiency of the utility system has a significant impact on the final design.

Kurzfassung

Prozessintegration befasst sich mit der Reduzierung des Energiebedarfs durch Wärmerückgewinnung in der Prozessindustrie. Der Hauptfokus liegt auf der Planung neuer Anlagen. Allerdings wurde ein Grossteil der bestehenden Anlagen in Zeiten niedriger Energiepreise gebaut als Energieeffizienz in der Planung keine grosse Rolle gespielt hat. Daher besteht ein grosses Potenzial in der Nachrüstung bestehender Anlagen zur Verbesserung der Energieeffizienz in der Prozessindustrie. Aufgrund des Trends zur Herstellung von kleinen Produktmengen mit hoher Wertschöpfung werden Mehrproduktanlagen und Mehrzweck-Anlagen benötigt welche flexibel in verschiedenen Betriebsfällen betrieben werden können. Um den Betrieb für jedes Produkt gewährleisten zu können nimmt die Komplexität des Designs sowohl als auch der Optimierung mit der Anzahl der Betriebsfälle zu. Um diese Herausforderungen zu meistern setzt sich auch die Forschung mehr mit der Nachrüstung von bestehenden Anlagen und der Produktion mit mehreren Betriebsfällen auseinander. Weiter ist es für die Industrie wichtig, dass Herausforderungen aus der Praxis in die Optimierung mit einbezogen werden und dass die Optimierung in Richtung praxistauglichen Analgendesigns gelenkt werden, ohne dass auf komplexe Kontrollsysteme zurückgegriffen werden muss.

Der Fokus dieser Thesis liegt in der Entwicklung einer Optimierungsmethode für die Nachrüstung von Prozessen mit mehreren Betriebsfällen. Um praxisnahe Designs zu gewährleisten, werden zusätzliche Randbedingungen in der Optimierung mitberücksichtigt welche Herausforderungen aus der Praxis mit einbeziehen. Diese zusätzlichen Randbedingungen erhöhen die Komplexität des ohnehin schon $\mathcal{NP}$-schweren Optimierungsproblem. Daher verwendet der entwickelte Optimierungsansatz metaheuristische Algorithmen. Für den Algorithmus wurde ein hybrider, auf Trajektorien basierter, Algorithmus wie auch ein hybrider evolutionärer Algorithmus untersucht, wobei sich letzterer durchgesetzt hat. Dieser Algorithmus ist zweistufig wobei ein Genetischer Algorithmus für die Optimierung der Topologie des Wärmeübertragernetzwerkes und eine Differential Evolution für die Optimierung der Wärmeleistungen der Wärmeübertrager in jedem Betriebsfall eingesetzt wird. Mit der Integration von Beipass- und Beimischschaltungen kann die Flexibiltät des Wärmeübertragernetzwerkes gewährleistet werden. Dabei werden die Mischtemperaturen mithilfe der Lambert W-Funktion analytisch berechnet. Die Reduzierung von Treibhausgasemissionen hat in den letzten Jahren für die Industrie an Bedeutung gewonnen. Daher werden Treibhausgasemissionen, zusätzlich zu den jährlichen Gesamtkosten, als zweite Zielfunktion mitbetrachtet. Für die Pareto-Optimierung werden dafür ein NSGA-II-Sortieralgorithmus und Hypervolumenindikatoren verwendet.

Der entwickelte Algorithmus wurde erfolgreich auf ein Fallbeispiel aus der Literatur und ein Fallbeispiel aus der Industrie angewendet. Die Ergebnisse der multikriteriellen Optimierung zeigen, dass die Gewichtung zwischen den Nachrüstungkosten und dem Energiebedarf, der die Betriebskosten und Treibhausgasemissionen verursacht, einen grossen Einfluss auf das Design haben. Dies bedeutet auch, dass eine Änderung der Energiekosten oder eine Verbesserung der Effizienz des Versorgungssystems einen signifikanten Einfluss auf das Design haben.

Preface and Acknowledgments

This thesis was conducted as a collaboration between the Institute of Energy Systems and Thermodynamics at the Vienna University of Technology (TU-Wien) and the Competence Center Thermal Energy Systems and Process Engineering at the Lucerne University of Applied Sciences and Arts (HSLU) under the supervision of Prof. Dr. René Hofmann and Prof. Dr. Beat Wellig.

First, I would like to thank my supervisors René Hofmann and Beat Wellig for the provided support and advice. I also want to highlight the valuable inputs and support from Donald Olsen with his hands-on experiences in Process Integration. During this thesis, there were many insightful discussions, contributing to the accomplished research.

I would also like to thank all my colleagues both at HSLU and during my exchange at TU-Wien, with whom I had engaging conversations, for their inputs and support. A special thanks goes to Dr. Benjamin Ong, who was always willing to assist with guidance and support when needed.

Finally, I would like to thank my family and all of my friends for their unconditional support during this endeavor.

Contents

Nomenclature

Sets

$C = \{0 \dots j \dots NC\}$	Set of cold streams
$E = \{0 \dots e \dots NE\}$	Set of heat exchangers
$H = \{0 \dots i \dots NH\}$	Set of hot streams
$K = \{0 \dots k \dots NK\}$	Set of enthalpy stages
$OP = \{0 \dots op \dots NOP\}$	Set of operating periods
$S = \{0 \dots s \dots NS\}$	Set of splits

Parameter

A	Heat exchanger area (m^2)
OF	Objective function
Q	Thermal energy (kWh)
$\dot{Q}$	Heat flow (kW)
T	Temperature (°C)
U	Overall heat transfer coefficient ($W/(m^2\ K)$)
w	Weight factor
$\Delta\dot{H}$	Enthalpy flow change (kW)
ΔT_m	Logarithmic mean temperature difference (K)

Subscripts

a	Admixer existence (boolean)
b	Bypass existence (boolean)
c	Cold side
ex	Heat exchanger existence (boolean)
h	Hot side
in	Inlet
out	Outlet

Abbreviations

CAP	Capital costs
COP	Operating costs
DE	Differential Evolution
EAM	Exchanger address matrix
GA	Genetic Algorithm
GHG	Greenhous gas
HEN	Heat exchanger network
HENR	Heat Exchanger Network Retrofit
HENS	Heat Exchanger Network Synthesis
HEX	Heat exchanger
HR	Heat recovery
Ipopt	Interior Point Optimizer
KKT	Karush-Kuhn-Tucker
LMTD	Logarithmic mean temperature difference
LP	Linear Programming
MER	Maximum Energy Recovery
MINLP	Mixer-Integer Nonlinear Programming
MILP	Mixer-Integer Linear Programming
MOO	Multi-objective optimization
MP	Mathematical Programming
NLP	Nonlinear Programming
$\mathcal{NP}$	Non-deterministic polynomial-time
NSGA-II	Nondominated-sorting Genetic Algorithm
PA	Pinch Analysis
PI	Process Integration
TAC	Total annual cost
TAM	Time Average Model
TSM	Time Slice Model
SA	Simulated Annealing
SOO	Single-objective optimization
SWS	Stage-wise superstructure

Research Summary

This chapter serves as a guide through the thesis. Section 1 highlights the motivation for the research and discusses the topic of industrial energy efficiency in broader terms. In Section 2, the research background is provided as well as gaps in the literature are highlighted. The resulting problem statement including research questions is formulated in Section 3. Section 4 shows how the posed research questions are addressed in the publications and gives an overview of the developed algorithm. In Section 5, the used case studies are introduced and the findings from the application of the algorithm to said case studies are summarized. Finally, in Section 6, the findings of the research are discussed, conclusions are drawn, and an outlook for future work is given.

1 Introduction

Energy plays a key role in almost every aspect of life. In 2022, 41.3 Gt_{CO2eq} energy-related greenhouse gas (GHG) emissions were released worldwide (IEA, 2022). While increased CO_2 concentration in the atmosphere positively influences the greening of the Earth due to the carbon dioxide fertilization effect (Zhu et al., 2016), higher GHG concentrations (including CO_2) also amplify the greenhouse effect causing the global mean temperature to increase. In comparison to pre-industrial temperatures (1850-1900, a period chosen by the IPCC as reference due to the relatively widespread although still sparse, temperature observations (Hawkins et al., 2017)), the global mean temperature in 2017 has increased by approximately 1 °C (Allen et al., 2018). This correlation indicates that human-induced GHG emissions contribute to the global mean temperature rise. In 2015, at the 21st Conference of the Parties (COP21) of the United Nations Framework Convention on Climate Change (UNFCCC), 195 nations adopted the Paris Agreement to limit global warming to 1.5 °C. To reach this goal, Switzerland, among many other nations, aims to reach net-zero emissions by 2050 (The Federal Council, 2021). Climate policies tackle the reduction in various ways such as increased investment in research and development, carbon taxes, and technology bans. It is important to notice that global warming and the mitigation measures needed disproportionately affect the poor and vulnerable and therefore, effects on them must be observed and considered in the policy making. Lomborg (2020) showed, that the most cost-effective climate policy is to increase investment in green research and development to reduce the cost of decarbonization, rather than slowing down economic growth.

In 2022, the industry sector was the second largest contributor to global CO_2 emissions accounting for 26 % (9.15 Gt_{CO2}), after the energy sector accounting for 42 % (14.65 Gt_{CO2}) (IEA, 2022). Hence, decarbonization and electrification of the industrial sector are of large interest.

For the industry sector, increased profitability is an important incentive to improve energy efficiency. The COVID-19 pandemic and an energy supply shock, evoked by a gap between supply and demand, more volatile energy sources, and ineffective global strategic planning, caused the emergence of an energy crisis resulting in a significant increase in energy prices (Chofreh et al., 2021). As a result, a reduction in energy demand is of the highest priority to ensure competitiveness. Thereby, the interest to ensure energy-efficient production and the reduction of GHG emissions are closely linked.

In the process industry, improvement of energy efficiency and GHG emissions reduction is particularly challenging due to the high complexity of the systems, the heterogeneity within the sector, and in many cases, for the processes, required high temperature levels. To tackle these challenges, the use of methods from Process Integration (PI) is common. These methods usually tackle the challenge of finding a trade-off between capital costs for equipment and operating costs from energy consumption. Usually, PI methods focus on grassroot design. However, with the increase in energy prices and environmental awareness, brownfield design becomes more viable leading to an increase in the development of PI methods for retrofit (Sreepathi and Rangaiah, 2014b). The most recent energy crisis is likely to expedite this development even further.

The market drives towards high value-added products, demanding flexible plant designs for multi-period operation (Jiao et al., 2003). However, research in the field of PI focusing on retrofit and multi-period operation simultaneously is rather sparse, hence creating a need for the development of such methods.

2 Context

This section provides the background to this thesis. First, in Section 2.1, PI is introduced and some of the key contributions are highlighted. Optimization is a core part of PI. Hence, in Section 2.2 optimization problems are characterized based on their properties. Further, an overview of optimization techniques to tackle these problems is given, and in PI commonly used optimization techniques are highlighted.

2.1 Process Integration

In this thesis, PI only refers to energetic PI and thus, can be referred to as a holistic thermo-economic approach aimed at improving efficiency in the process industry by analyzing the heating and cooling demands of an entire system and exploring possible heat recovery (HR) rather than improving the efficiency of individual components.

Traditionally, the goal is to minimize the total annual cost (TAC) of the system, which is a trade-off between annualized capital costs and operating costs (Smith, 2005). As Gundersen (2000) stated, the International Energy Agency (IEA) defines PI as follows:

> *"Systematic and General Methods for Designing Integrated Production Systems, ranging from Individual Processes to Total Sites, with special emphasis on the Efficient Use of Energy and reducing Environmental Effect."*
>
> (IEA, 1993)

In response to the oil crisis and the resulting increase in energy prices in the early 1970s, energy efficiency technologies gained more interest. The field of PI emerged in this period. Early works involved the development of the insight-based method called Pinch Analysis (PA). Hohmann (1971) introduced the concept of Heat Integration which laid the foundation for the integration of energy conversion units such as heat pumps. Linnhoff and Flower (1978) and Linnhoff (1979) introduced the Problem Table Algorithm and the concept of the Pinch which led to the foundation of the PA (Linnhoff and Hindmarsh, 1983). Umeda et al. (1978) and Umeda et al. (1979) developed the concept of the T-$\dot{Q}$ diagram and the Composite Curves, which is a visualization of the heating and cooling demand, and are up to this day a crucial part of PA and PI. In the early days of PI, PA was seen as controversial as it uses simple techniques rather than complex mathematical approaches. However, the method has proven itself useful in its practical application in industry and is now generally accepted among researchers and consultants (Kemp and Lim, 2020).

Another branch of PI, which was initially in opposition to PA, but later complemented it, approaches the problem from the mathematical optimization side and is called Heat Exchange Network Synthesis (HENS). The problem of HENS was introduced by Broeck (1944). Hwa (1965) and Ponton and Donaldson (1974) were among the first to study how to solve the HENS problem.

Bogataj et al. (2023) summarized the key developments in PI in the last 50 years, with the focus on PA and Mathematical Programming (MP) showing that for both approaches the research has advanced from simple continuous process synthesis towards more complex problems considering multi-period operation, detailed heat exchanger (HEX) design, retrofit, and multi-objective optimization. Due to the high complexity, methods tend to simplify or break down the problem into smaller sub-problems. Thereby, it is also not uncommon to combine PA and MP techniques to take advantage of both approaches.

With the increase of complexity in PI, new approaches addressing the HENS problem using metaheuristic optimization techniques started to emerge with Dolan et al. (1989) being the first to use a Simulated Annealing (SA) algorithm for HENS. Toimil and Gómez (2017) provide a comprehensive review of recent metaheuristic approaches to the HENS problem.

2.1.1 Heat Exchanger Network Synthesis

HENS can be seen as the core sub-problem of PI. It addresses the problem of designing a heat exchanger network (HEN) for HR of a defined system with regard to minimal TAC. In his review paper on HENS, Furman and Sahinidis (2002) stated that Masso and Rudd (1969) defined HENS as follows:

> *"Given (i) a set H of hot process streams to be cooled from the inlet temperatures to the outlet temperatures, (ii) a set C of cold process streams to be heated from the inlet temperatures to the outlet temperatures, (iii) the heat capacities and flow rates of the hot and cold process streams, (iv) the utilities available and the temperatures or temperature ranges and the costs for these utilities, and, (v) heat-exchanger cost data, develop a network of heat exchangers with minimum annualized investment and operating costs."*
>
> (Masso and Rudd, 1969)

Among others, Shenoy (1995) and Biegler et al. (1997) provide a comprehensive introduction to the topic of HENS. In general, HENS can be divided into sequential and simultaneous approaches. Thereby, early published works such as by Floudas et al. (1986) usually address the problem sequentially to reduce the computation cost. Therefore, HENS is decomposed into three sub-problems which have to be solved in sequence using the transshipment model by Papoulias and Grossmann (1983):

1. The minimum utility demand / Maximum Energy Recovery (MER)
2. The minimum number of HEX
3. The minimum area/capital costs of the HEN

The result of the sub-problems is used in the initial conditions for the next sub-problem. A global optimum of one of the sub-problems might lead to a local optimum of the whole problem. Therefore, this approach might lead to convergence to a local optimum, rather than the global optimum (Ciric and Floudas, 1991). In opposition, simultaneous HENS formulations address the problem without decomposition to omit convergence in a local optimum. Simultaneous HENS is usually posed as a minimization of TAC which is a combination of annualized capital costs and operating costs. A simultaneous HENS formulation widely used to date is the stage-wise superstructure (SWS; shown in Fig. 1) by Yee and Grossmann (1990). The SWS formulation divides the HEN into enthalpy stages in which each hot steam can be connected to each cold stream. The number of enthalpy stages directly influences the number of possible HEXs and is, therefore, an important parameter to find the optimal solutions but also affects the complexity of the system and thus, computation costs. To fulfill the energy balance a balance utility HEX is placed at the end of each stream. Inlet and outlet temperatures for the HEX are determined using the energy balance of each process stream in each enthalpy stage. The outlet temperature can be determined using the enthalpy change of the stream caused by the heat loads of the HEX connected to the stream. This formulation for

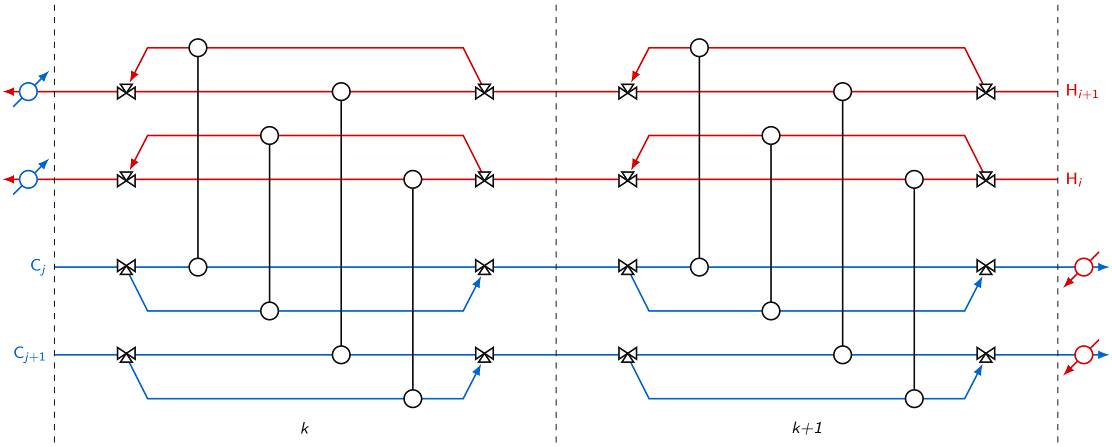

Fig. 1 Stage-wise superstructure with two hot streams (H_i) and two cold streams (C_j) and two enthalpy stages (k) proposed by Yee and Grossmann (1990)

the calculation of the outlet temperatures only allows isothermal mixing. With this limitation, the problem can be represented in a linear formulation with except of the objective function. The nonlinearity is caused by the logarithmic mean temperature differences (LMTDs), which are needed to determine the HEX areas, the heat transfer equation used to determine the areas, and the cost functions used to determine the capital costs for the needed area. Among others, Ciric and Floudas (1991) proposed a HENS approach that includes mass balance equations for the stream splitting to include non-isothermal mixing as well. Such formulations add additional non-convex equations, which increase the complexity of the solution space and thus, the difficulty of finding the global optimum.

Furman and Sahinidis (2001) showed that the complexity of the HENS problem is $\mathcal{NP}$-hard (non-deterministic polynomial-time hard) *in the strong sense*. The high complexity evoked due to the non-linearity, non-convexity, and combinatorial discontinuities, led to explore other optimization approaches such as metaheuristic algorithms. Dolan et al. (1989) were the first to propose an approach using a SA algorithm for HENS which found better solutions compared to current available MP approaches. The first approach using a Genetic Algorithm (GA) for HENS was published by Lewin et al. (1998). Thereby, the approach consisted of two stages using GA for the topology optimization of the HEN and a Linear Programming (LP) model to address the MER problem. Lewin (1998) also extended the model using a cascaded LP model to minimize TAC.

2.1.2 Retrofit

For companies, profitability is one of the key motivations. For a long time, energy prices were rather low and thus, there was no incentive for energy-efficient production. Hence, a large share of existing plants were built without having energy efficiency in mind. Such plants have usually a high HR potential. To improve the overall energy efficiency of the industry, Heat Exchanger Network Retrofit (HENR) methods are needed.

In retrofit the HEN is modified rather than designed from the ground up. Thereby, the topology of the HEN can be modified by re-piping or re-sequencing existing HEXs. Usually, existing HEXs can also be removed and new HEXs can be added. To address the changes in heat loads, HEXs can also be retrofitted by extending their area. In addition to considering the capital costs for new HEXs and operating costs for utility consumption, modification costs for the retrofit and added area need to be considered as well. An example of such a HENR formulation can be found in Article 2.

Sreepathi and Rangaiah (2014b) showed that a trend in research towards retrofit is evident, as the amount of published articles in the field has doubled within 5 years. The first research in the field of retrofit was done by Ciric and Floudas (1989), which adopted the sequential transshipment model (Papoulias and Grossmann, 1983). Thereby, the investment costs for new HEXs, additional HEX area, and piping costs for a fixed HR were minimized. The first simultaneous approach was proposed by Ciric and Floudas (1990). As the objective function, reassignment costs for existing HEXs, investment costs for new HEXs, and piping costs are minimized. Another simultaneous approach was proposed by Yee and Grossmann (1991) by extending the SWS (Yee and Grossmann, 1990) to a retrofit formulation.

By extending the HENS formulation (Athier et al., 1997), Athier et al. (1998) proposed one of the first metaheuristic approaches to HENR using a two-stage SA in combination with a Nonlinear Programming (NLP) formulation. Thereby, the SA is used to optimize the topology of the HEN and the NLP formulation optimizes the needed areas. Bochenek and Jezowski (2006) proposed a two-stage HENR method using GA for the top-level as well as for the sub-level. It has been shown that the results of both approaches are better in comparison to current available MP-based methods. Sreepathi and Rangaiah (2014b) provides a comprehensive review of HENR methods including MP as well as metaheuristic approaches.

2.1.3 Multi-Period Operation

PI was first developed for continuous processes only. However, market trends towards high value-added products (e.g., fine chemicals, pharma, food, beverages) and thus, the demand for flexible production to address dynamic customer demands and highly customized products, require more flexible plant designs (Jiao et al., 2003). This adds an additional time dimension and thus constraints for HR. A non-continuous operation may also arise in total site heat integration. Inter-plant HR between continuous plants can cause time constraints for HR due to different scheduling of the plants. In such cases, inter-plant HR is often achieved using intermediate loops to bypass the time constraints for HR (e.g., Stampfli et al., 2019b). In this thesis, the focus lies on HR within single plants and, therefore does not consider inter-plant HR. In general, non-continuous production within a single plant can be categorized into batch and multi-period processing. Batch processes are characterized as a sequence of operations or tasks to treat a charge, also called a batch. A certain step could take an extended period of time to complete (e.g., a chemical reaction) before the next step can be started. Therefore, batch processes can be characterized as *distributed in time* (Majozi, 2010). On the other hand, multi-period processes, also known as processes with multiple operating cases (Olsen et al., 2017) or multiple base cases (Jones, 1991), can also be referred to as *continuous in periods*. In Fig. 2, the multi-period behavior is categorized into the following three process types:

- A *single-product* process refers to a single plant used to produce one product. The production can be influenced by changes in the material feed (depending on customer demands) or changes in properties of streams from the outside (caused by seasonal changes) such as temperature and humidity of intake of ambient air, or of material stored outside.
- A *multi-product* process refers to a single plant used to produce various products passing through the equipment in the same order. The production can be influenced by the different temperature or mass flow requirements of each product.
- A *multi-purpose* process refers to a single plant used to produce various products passing through the equipment in a changed order. Due to the completely different characteristics of each process and its requirements, the re-arrangement of the equipment can influence production significantly.

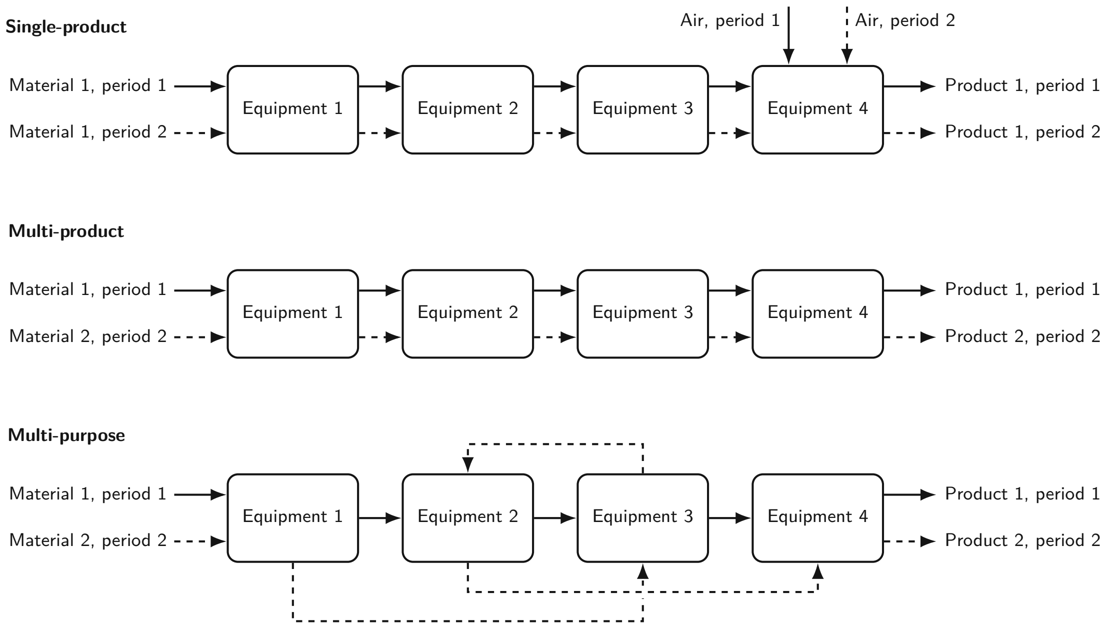

Fig. 2 Categorization of multi-period plants with four exemplary equipment (in this case equipment do not include HEXs)

The time dependence in processes can be addressed in two ways. Either the process is decomposed in periods with continuous operation using the Time Slice Model (TSM), introduced by Linnhoff et al. (1988), or is analyzed as if all the heating and cooling demands would occur at the same time using the Time Average Model (TAM), introduced by Clayton (1986). The two models have distinct advantages for either direct or indirect HR. By the use of the TSM, direct HR potential between simultaneously existing streams can be analyzed. The TAM on the other hand is used to analyze the total HR potential (including direct and indirect) of the process and can be used to explore the potential of thermal energy storage integration (Kemp and Deakin, 1989). Some approaches also combine the two concepts to explore direct HR potential with the TSM in a first step and analyze the residual indirect HR with the TAM for storage integration (e.g., Krummenacher, 2001).

Due to the characteristics of multi-period processes, their time slices (continuous periods) tend to be rather long (e.g., in a multi-product plant the switch between two products might occur every few weeks or months). Hence, the potential for direct HR is more interesting than indirect HR between time slices which might lead to significant losses due to long storage periods. Even though the TSM is typically used in PA, HENS utilizes the same concept to formulate the multi-period problem. Thereby, heat loads and temperatures are split into continuous periods called operating periods. The HENS formulation is therefore extended by an additional dimension in time. Grossmann and Sargent (1979) were the first to introduce a mathematical formulation for the multi-period HENS problem. By adapting the sequential transshipment model (Papoulias and Grossmann, 1983) for multi-period operation, Floudas and Grossmann (1986) proposed a systematic approach to solve the formulation. Based on the SWS by Yee and Grossmann (1990), Aaltola (2002) proposed a simultaneous framework to multi-period HENS minimizing TAC and flexibility.

Kang and Liu (2014) proposed a two-stage sequential approach to solve the multi-period HENR problem using a reverse order matching method minimizing TAC. Thereby, in the first step, the multi-period HENS formulation by Verheyen and Zhang (2006) is solved. In the second step, the required HEX areas of the new HEN design are matched with the HEX areas of the existing design in reversed order. In the third step, the minimization of capital costs for the additional area is substituted by minimizing the additional needed area of existing HEXs. This substitution was later replaced by minimizing the capital costs instead (Kang and Liu, 2015). Isafiade (2018) proposed a similar approach using a two-stage sequential reduced superstructure synthesis approach to solve the multi-period HENR problem. Like Kang and Liu, Isafiade solved the multi-period HENS model by Verheyen and Zhang (2006) in the first step. In the second step, instead of only matching the areas of the HEXs in the new HEN with the areas of the HEXs in the existing HEN, Isafiade solves the reduced superstructure as a Mixed-Integer Nonlinear Programming (MINLP) model. This allows the model to update the topology and remove the no longer needed HEXs or add new HEXs. Langner et al. (2020) splits the multi-period HENR problem into five sequential steps to consider the temperature of process variables such as the inlet temperatures. Thereby, the problem is broken down into simpler sub-problems that can be solved with well-established single-period HENR methods.

2.1.4 Multi-Objective Optimization

In the industry there are often multiple, with each other conflicting, objectives. A prime example from PI is minimizing annualized capital costs and operating costs. Other examples of conflicting objectives are maximizing HR and minimizing space requirements or maximizing safety. Only limited research on multi-objective multi-period HENR has been conducted. Sreepathi and Rangaiah (2015) extended the single-period multi-objective optimization (MOO) for HENR (Sreepathi and Rangaiah, 2014a), which uses the non-dominated sorting Genetic Algorithm (NSGA-II) for the Pareto optimization, to consider variations in heat capacities. Thereby, annualized capital costs and utility costs are used as the objectives. Kang and Liu (2017) proposed an approach to solve the MOO multi-period HENR problem using a three-stage sequential procedure to minimize TAC and GHG emissions based on the reverse order matching method. The first stage solves a simplified formulation of the multi-period HENS (Kang et al., 2016). In the second step, the GHG emissions are included as a second objective in the multi-objective HENS model. Therefore, the ε-constraint method is adopted to solve the new formulation. In the last step, the reverse order matching method is applied to match HEX areas of the new HEN design with HEX areas from the existing HEN by considering the four objectives minimizing the modifications of the existing HEN structure, maximizing the number of substituted HEXs, minimizing the additional required areas, and minimize the annualized capital costs for the retrofit.

2.2 Optimization and Mathematical Programming

Optimization is a core part of PI, hence, this section introduces the concept and challenges of mathematical optimization as well as commonly used optimization techniques. Optimization is a branch of mathematics concerned with the search for the optimal solution of a mathematical model. Research in optimization dates back to ancient times. Notable contributions in the 18th century helped to lay the foundation of the field. Bernoulli (1713) introduced the concept of probability theory and its application in the field of optimization, while Euler (1744) introduced the concept of the Euler-Lagrange equation which has become a fundamental tool in the field of optimization. Lagrange (1797) introduced the concept for calculus of variations and Gauss (1809) the concept of least squares.

With the introduction of the simplex algorithm for solving linear problems, Dantzig (1948) laid the foundation of MP and revolutionized the field of optimization. In contrast to solving optimization problems using calculus, Dantzig's work focused on formulating the problem as a mathematical model which can be solved using an algorithm. Since then, a variety of algorithms has been developed, tackling not only linear problems but also nonlinear or mixed-integer problems. In general, an MP can be formulated as a minimization problem (Floudas, 1995)

$$\min_{\mathbf{x},\mathbf{y}} f(\mathbf{x},\mathbf{y}) \qquad \mathbf{x} \in \mathcal{X} \subseteq \mathbb{R}^n,\ \mathbf{y} \in \mathcal{Y} \subseteq \mathbb{Z}^m \tag{2.1a}$$

$$\text{s.t. } h_i(\mathbf{x},\mathbf{y}) = 0 \qquad i = 1,\dots,p \tag{2.1b}$$

$$g_j(\mathbf{x},\mathbf{y}) \leq 0 \qquad j = 1,\dots,q \tag{2.1c}$$

whereby, Eq. 2.1a is the objective function, based on a vector of n continuous variables $\mathbf{x}$ and m integer variables $\mathbf{y}$ contained in the feasible regions $\mathcal{X}$ and $\mathcal{Y}$. These regions can be constrained by a set of equality constraints, Eq. 2.1b, and a set of inequality constraints, Eq. 2.1c. For unconstrained problems, Eq. 2.1b and Eq. 2.1c do not exist resulting in $\mathcal{X} = \mathbb{R}^n$ and $\mathcal{Y} = \mathbb{Z}^m$. For maximization problems, the objective function (Eq. 2.1a) can be rewritten as

$$\max_{\mathbf{x},\mathbf{y}} f(\mathbf{x},\mathbf{y}) = \min_{\mathbf{x},\mathbf{y}} -f(\mathbf{x},\mathbf{y}) \tag{2.2}$$

2.2.1 Characterization of Optimization Problems

Optimization problems are classified based on their attributes which determine what techniques can be used. One major distinction is between continuous and discrete solution spaces. Discrete optimization, dealing with decision processes represented using integer variables ($\mathbb{Z}$), is commonly used in operations research for combinatorial problems such as the Traveling Salesman Problem or the Bin Packing Problem. On the other hand, continuous optimization problems deals with real numbers ($\mathbb{R}$). Thereby, linear and nonlinear problems are distinguished. To determine if a continuous optimization problem is linear, the objective function, as well as all constraints, need to satisfy the superposition principle (according to Brillouin (1946), introduced by D. Bernoulli in 1753):

- *Additivity*: $f(x_1 + x_2, y_1 + y_2) = f(x_1, y_1) + f(x_2, y_2)$
- *Homogeneity*: $f(a\,x, a\,y) = a\,f(x, y)$

whereby, x_1, x_2 and y_1, y_2 are two different variables evaluated at two points (1 and 2) and a is a constant parameter. Linear optimization problems can usually be solved with ease. In contrast, nonlinear problems are more complex and require more demanding approaches in general based on gradients of the objective function. To find extreme points, the methods search for stationary points $\mathbf{x}^*$ where the gradient is zero $\nabla f(\mathbf{x}^*) = \mathbf{0}$. Fig. 3, visualizes stationary points for the Peaks and hyperbolic paraboloid functions. To find such stationary points, the nonlinear problem needs to be twofold continuously differentiable ($f \in C^2$).

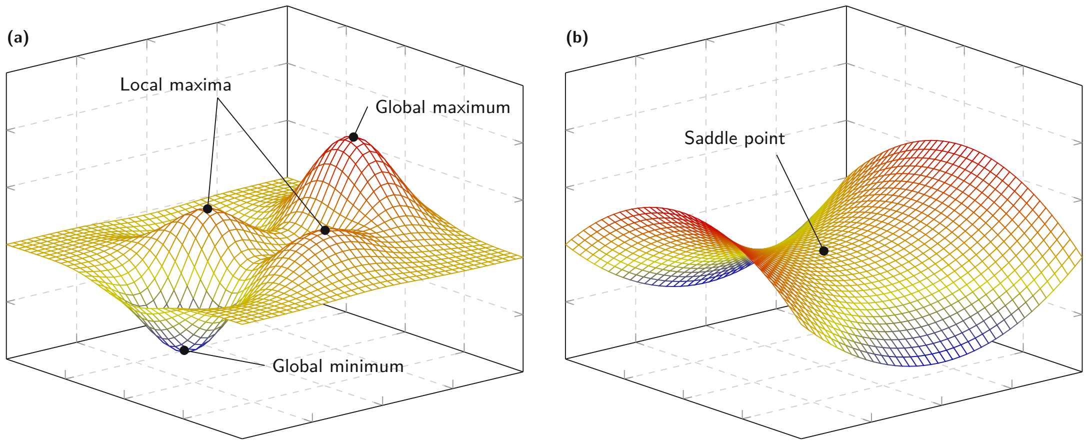

Fig. 3 **(a)** Peaks function marked with its global maximum, its global minimum, and local maxima as stationary points and **(b)** hyperbolic paraboloid function with its saddle point as its only stationary point

To determine the type of a stationary point, all Eigenvalues λ_i with $i = 1, \ldots, n$ of the Hessian $\nabla^2 f(\mathbf{x}^*)$ need to be considered:

- *Positive definite* Hessian ($\forall i : \lambda_i > 0$): $\mathbf{x}^*$ is a local minima
- *Negative definite* Hessian ($\forall i : \lambda_i < 0$): $\mathbf{x}^*$ is a local maxima
- *Indefinite* Hessian ($\forall i : (\exists \lambda_i > 0) \wedge (\exists \lambda_i < 0) \wedge (\forall \lambda_i \neq 0)$): $\mathbf{x}^*$ is a saddle point

For cases where some Eigenvalues are zero and others are either positive or negative, the Hessian is *semi-definite*. In these cases, it cannot be said if $\mathbf{x}^*$ is a local extremum or a saddle point. Hence, gradient and Hessian can only identify local extrema. However, for convex problems, a local extremum is always a global extremum. For a problem to be convex, its solution space as well as its objective function need to be convex. The solution space $\mathcal{X} \subseteq \mathbb{R}^n$ is convex if for all $x_1, x_2 \in \mathcal{X}$ and all reel numbers α with $0 < \alpha < 1$,

$$(\alpha\, x_1 + (1 - \alpha)\, x_2) \in \mathcal{X} \tag{2.3}$$

is fulfilled. For a convex solution space a function $f(x)$ is convex if for all $x_1 \neq x_2 \in \mathcal{X}$,

$$f(\alpha\, x_1 + (1 - \alpha)\, x_2) < \alpha\, f(x_1) + (1 - \alpha)\, f(x_2) \tag{2.4}$$

is fulfilled. If one of these conditions is not fulfilled, the problem is non-convex and might contain local optima in which a gradient-based algorithm, depending on its step size, can converge prematurely. Hence, solving non-convex problems is more complex and is usually considered $\mathcal{NP}$-hard (Murty and Kabadi, 1987). The topic of extrema and convexity is widely documented in various optimization-themed books, such as in *Nonlinear and Mixed-Integer Optimization* by Floudas (1995).

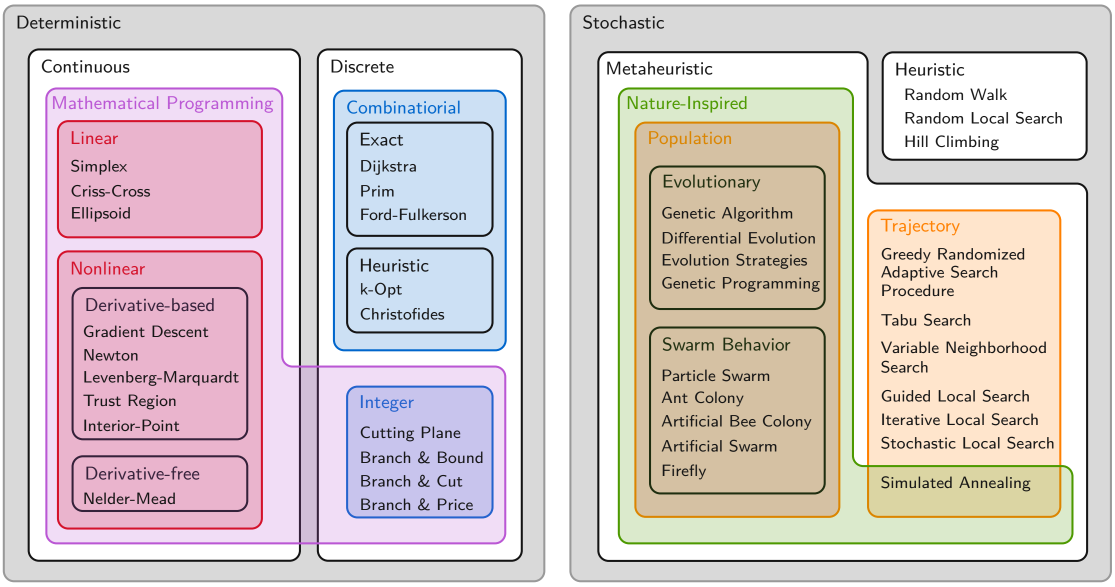

Fig. 4 Classification of exemplary optimization algorithms based on the problems attributes and algorithm techniques (non-exhaustive)

2.2.2 Classification of Optimization Techniques

To adapt to the different characteristics of optimization problems, various optimization techniques have been developed. Fig. 4 gives an overview of optimization techniques classified by their attributes and techniques. The major distinction is drawn between deterministic and stochastic optimization. A deterministic algorithm follows a given procedure and will always generate the same output for a specific input. In contrast, a stochastic algorithm includes randomness in the optimization to explore a broader solution space to omit premature convergence in local optima. This is especially useful for discontinuous and non-convex problems.

In literature, Pinch Analysis is sometimes referred to as an insight-based heuristic approach. It is important to notice that PA is an algorithm because it only provides a set of rules which have to be followed rather than a complete procedure for PI. Hence, PA is not treated as an optimization technique and is therefore not included in this chapter and in Fig. 4.

2.2.2.1 Deterministic Optimization

Deterministic optimization is subdivided by variable type. In the field of continuous optimization ($\mathbb{R}$), mainly linear and nonlinear problems are distinguished. Thus, all linear problems are convex, simple algorithms such as the Dantzig's Simplex (Dantzig, 1948) can be used to find the global optimum. In contrast, nonlinear problems are usually addressed using gradient-based methods such as Newton's Method (Newton, 1711). As an alternative, derivative-free algorithms, such as the Simplex method by Nelder and Mead (1965) can be used.

Convex nonlinear problems are usually easy to solve with conventional nonlinear algorithms, however, for non-convex problems, such methods might converge prematurely in local optima. Most nonlinear algorithms can be extended for global optimization. Therefore, additional methods for analyzing, or simplifying the problem are incorporated. Methods that analyze the solution space are for e.g., interval analysis which can be used to verify the optimality of a local optimum or a multi-start approach which performs the optimization multiple times with various initial conditions, usually determined using stochastic methods. Other methods approach the problem by simplification for e.g., convex relaxation which solves a convex approximation of the non-convex problem, surrogate modeling replacing complex functions with easier-to-evaluate functions, or dividing the search space into smaller regions to optimize separately with divide-and-conquer or branch and bound methods. Deterministic global optimization methods are discussed in detail in various books such as *Deterministic Global Optimization: Theroy, Methods and Applications*, by Floudas (2013).

Discrete optimization ($\mathbb{Z}$) is widely used in combinatorial optimization for example Dijkstra's algorithm (Dijkstra, 1959) which is a greedy algorithm used to find the shortest path for graphs such as the Traveling Salesman Problem. Another branch of discrete optimization addresses the optimization of integer problems. These problems are usually formulated, similar to continuous problems, in the form of a mathematical program. Branch and bound as well as cutting plane algorithms are usually used in this field. The field of integer optimization is commonly combined with either linear or nonlinear algorithms to solve MI(N)LP problems whereby the integer algorithm subdivides the solution space into continuous problems which are then solved by a linear or nonlinear solver. In the field of MP, in general, deterministic continuous linear as well as nonlinear, and discrete integer optimization techniques are used.

Constraint Handling Techniques: In MP, constraint problems are usually transformed into unconstrained problems by incorporating their constraints into the objective function using Lagrange multipliers (Lagrange, 1775) and the Karush-Kuhn-Tucker (KKT) condition to ensure a well-posed problem and that the solution satisfies the primal-dual problem (Karush, 1939; Kuhn and Tucker, 1951). The KKT conditions are a set of necessary conditions for optimality in constraint optimization and can be stated as follows:

1. *Stationarity condition* is fulfilled if the gradient of the objective function is orthogonal to the tangent space of the feasible region defined by the constraints at the point $\mathbf{x}^*$:

$$\nabla f(\mathbf{x}^*) + \boldsymbol{\lambda}^\mathsf{T} \nabla \mathbf{h}(\mathbf{x}^*) + \boldsymbol{\mu}^\mathsf{T} \nabla \mathbf{g}(\mathbf{x}^*) = \mathbf{0} \tag{2.5}$$

whereby $\nabla \mathbf{h}(\mathbf{x}^*)$ is the gradient of all equality constraints, $\nabla \mathbf{g}(\mathbf{x}^*)$ is the gradient of all inequality constraints, and $\boldsymbol{\lambda}$, $\boldsymbol{\mu}$ are vectors containing the associated Lagrange multiplier.

2. *Primal feasibility* is fulfilled if none of the equality $\mathbf{h}(\mathbf{x}^*)$ and inequality constraints $\mathbf{g}(\mathbf{x}^*)$ are violated at the point $\mathbf{x}^*$:

$$\mathbf{h}(\mathbf{x}^*) = \mathbf{0} \tag{2.6a}$$
$$\mathbf{g}(\mathbf{x}^*) \leq \mathbf{0} \tag{2.6b}$$

3. *Dual feasibility* is fulfilled if the Lagrange multipliers of all inequality constraints are positive:

$$\boldsymbol{\mu} \geq \mathbf{0} \tag{2.7}$$

4. *Complementary slackness* is fulfilled if the product of the Lagrange multipliers and the inequality constraints is zero:

$$\boldsymbol{\mu}^{\mathsf{T}} \mathbf{g}(\mathbf{x}^*) = 0 \tag{2.8}$$

It is important to notice that KKT conditions are necessary but not sufficient conditions for optimality. KKT constraints are an essential part of many constraint-handling procedures. Floudas (1995) summarized constraint handling techniques for MP as follows:

- *Penalty methods* add a term to the objective function for any violation of a constraint. The penalization of the violations ensures that the optimization is guided towards the feasible region.
- *Barrier methods* generate a wall around the feasible region to omit the algorithm leaving the feasible space. Therefore, the value of the objective functions increases drastically towards the constraints by incorporating the constraints with e.g., logarithmic penalty functions.
- *Successive linear/quadratic programming methods* approximate the objective function and constraints using Taylor first-order (linear) or second-order (quadratic) series approximation. The approximation is used to generate the search direction and is repeated for every step. In this approach, the constraints are incorporated into the objective function by penalization.
- *Gradient projection methods* project the gradient of infeasible solutions onto the closest feasible point and perform a gradient decent step. Hence, it is ensured that the algorithm is not leaving the feasible region. This approach does not integrate the constraints into the objective function.

- *Generalized reduced gradient methods* compute the reduced gradient by considering the objective and constraints simultaneously and using first-order Taylor approximation. If the current point is infeasible, gradient projection methods are used toward the feasible region. As long the solution is infeasible a new approximation of the gradient is performed which is then used for a new gradient projection step.

2.2.2.2 Stochastic Optimization

Stochastic algorithms can generally be subdivided into heuristic and metaheuristic algorithms. Thereby, heuristic algorithms are usually simpler problem-specific algorithms that use practical knowledge of the problem and thus, commonly suffer from premature convergence in local optima. In contrast, metaheuristic algorithms are high-level methods that combine local and global search methods. Often probabilistic techniques are incorporated to explore complex solution spaces or escape local optima. Among others, in *Methaheuristics From Design to Implementation*, Talbi (2009) provides an exhaustive overview and guidelines on how to design metaheuristic algorithms. Metaheuristic algorithms can generally be subdivided into population-based and trajectory-based algorithms.

Population-based algorithms are usually inspired by processes in nature and work with a set of solutions that are compared, recombined, and modified. Two major types of population-based algorithms are evolutionary-based and swarm-behavior-based algorithms. Evolutionary algorithms follow the concept of natural selection in which fitter individuals from the population are more likely to survive. Typical evolutionary algorithms such as Genetic Algorithms or Differential Evolution are based on the evolution of genes over generations in organisms. Swarm behavior algorithms are inspired by the collective behavior of social animals such as swarms of insects, flocks of birds, or schools of fish. Individuals of the population, usually called agents or particles, move based on their and other closeby individuals' position and velocity.

In contrast to population-based algorithms, trajectory-based algorithms usually follow a single agent iteratively updating and evaluating the solution. The decision in which direction the agent is moving is usually determined using neighborhood functions that describe possible movements from the actual point in the solution space. The decision of which neighborhood move is performed is decided by comparing the results between various moves. A typical trajectory-based algorithm is SA which is inspired by the annealing process in metallurgy which is a heat treatment process to alter the physical properties of the material.

Constraint Handling Techniques: In stochastic optimization, constrained optimization problems are usually approached with metaheuristics, however, simpler problems can also be addressed using heuristics. Talbi (2009) provides an overview of commonly used constrained handling techniques for metaheuristics:

- *Reject strategies* discard all solutions which violate constraints. This means for population-based methods, only feasible individuals are considered in the selection process and trajectory-based algorithms reject neighborhood moves resulting in infeasible solutions. This strategy is only possible for constraints that are violated rarely and thus does not restrict the search excessively.
- *Penalizing strategies* include the constraints as an additional term in the objective function or replace the objective function if the constraints are violated. Thereby, it is possible to only count the number of violations or to consider the distance to the feasible region. The latter guides the algorithm towards the feasible region. The penalization function can either be constant, linear, or quadratic.
- *Repair strategies* consist of an additional optimization that modifies the infeasible solutions by minimizing the constraint violations. To ensure only feasible solutions, repair strategies are often combined with reject strategies whereby, irreparable solutions are rejected after a repair attempt.
- *Decoding strategies* extend the search to infeasible regions and, similar to repair strategies, try to repair the solution. However, decoding strategies identify a reason for the infeasibility and transform the solution based on the reason into the feasible region. Decoding strategies are usually very problem specific in contrast to repair strategies.
- *Preserving Strategies* limit the search space by forbidding variables to reach certain regions which are known to be infeasible. Preserving strategies do not only ensure feasible solutions but might also improve the performance of the algorithm by not wasting computational resources on infeasible regions. However, this approach might lead to small feasible regions which can limit a sufficient exploration.

2.2.3 Optimization in Process Integration

In Section 2.1, various optimization approaches for HEN design were discussed. Due to the high complexity, the optimization of such formulations can be approached in two different ways. On one hand, the problem is simplified by decomposition or linearization. Therefore, well-established models such as the SWS by Yee and Grossmann (1991), are modified. Such models are usually formulated using Algebraic Modeling Languages such as AMPL (Fourer et al., 1990) or Pyomo (Bynum et al., 2021), which are used to transform the equations into MP solver readable matrix formulations. Due to the simplifications, such approaches tend to neglect practical influences such as mixer configurations as they increase the complexity of the problem. On the other hand, rather than simplify the problem, the optimization approach is changed by using stochastic methods instead which can deal better with highly complex problems. This approach can handle the additional complexity resulting from practical constraints, but it cannot guarantee to find the global optimal solutions. The most commonly used stochastic algorithms in PI are GA and SA.

3 Problem Statement

In Section 1, the need for the development of PI methods, dedicated to retrofit of multi-period processes for practical heat exchanger network design, was emphasized. In Section 2, existing PI methods and optimization approaches from literature are reviewed. Derived from these two chapters, the aim of this thesis can be formulated as:

Aim: *Development of an approach for retrofit of multi-period processes for practical heat exchanger network designs.*

To achieve this aim, two main objectives are proposed. *Objective 1* focuses on the practical design aspect and *Objective 2* focuses on the implementation of the optimization method and how measures to achieve *Objective 1* can be incorporated into the optimization.

Objective 1: *Identification of the key aspects to incorporate in an approach to practical heat exchanger network design for industrial application.*

- **Q 1.1:** *What are the key challenges to consider when retrofitting multi-period processes for the industry?*
- **Q 1.2:** *What assumptions in the modeling of retrofit for multi-period processes have a significant impact on the final design?*
- **Q 1.3:** *What specific steps in the optimization should be considered to find more practical designs?*

Objective 2: *Development of an optimization approach for practical heat exchanger network retrofit in industry.*

- **Q 2.1:** *Which optimization techniques should the approach be based on?*
- **Q 2.2:** *Which practical measures need to be included in the optimization for practical designs?*
- **Q 2.3:** *Which objective functions are needed to find relevant solutions?*

4 Research Approach

This section covers the development of a method for HENR for multi-period processes based on the aim and objectives defined in the problem statement (Section 3). An overview of the contributions in the form of articles and developed software, and how they are connected, is provided in Fig. 5.

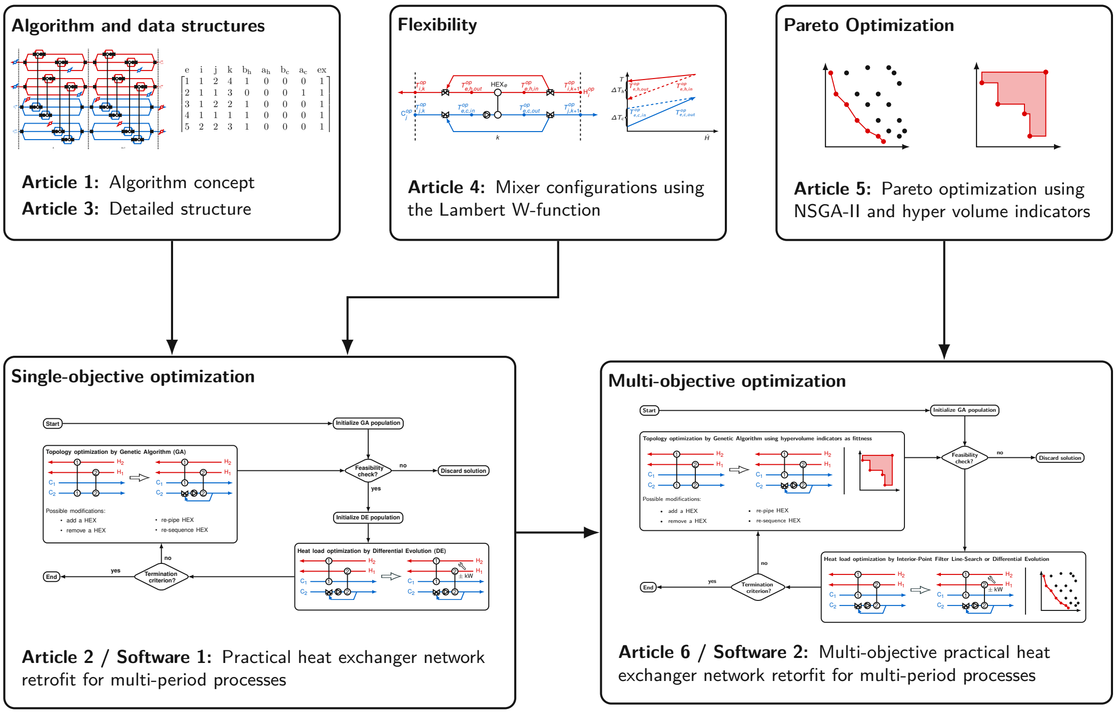

Fig. 5 Overview of the development of the method and related articles

Article 1 introduces the concept of a two-stage GA/DE algorithm for HENR for multi-period processes using a metaheuristic approach. The article includes the structure of the algorithm as well as the fitness function for minimizing TAC and how constraints are incorporated in the metaheuristic approach. The algorithm is applied to an illustrative case study from the literature. In Article 3, the algorithm and data structures used for the optimization are introduced. To ensure flexible HEN designs, Article 4 explains how mixer configurations are integrated into the network design. Thereby, the approach for the mixer configuration selection as well as the analytical calculation of the mixer temperatures using Lambert W-functions are introduced. The single-objective optimization (SOO) approach, introduced in Article 2 and Software 1, combines the flexible HEN designs and algorithm and data structures into one. Further, practical constraints and additional costs such as piping are introduced and the results are analyzed in detail by applying the algorithm to a case study from industry.

Article 5 introduces a multi-objective optimization (MOO) approach using NSGA-II and hypervolume indicators for a Pareto optimization considering GHG emissions besides TAC. With Article 6 and Software 2, the SOO is extended with the multi-objective approach. Thereby, both optimization approaches are compared to each other as well as the selection of objective functions is discussed.

The following sections serve as the guide through the thesis and cover how the objectives, from the problem statement, can be achieved. Thereby, Section 4.1 identified which practical key points need to be addressed in the method to achieve *Objective 1*. In Section 4.2, the optimization concepts to achieve *Objective 2* are introduced, and in Section 4.3 shows how the method can be integrated into a practical workflow.

4.1 Practical Design

This section discusses how *Objective 1* can be achieved. Hence, practical aspects of the retrofit of multi-period processes are illustrated. In Section 4.1.1, the demand for flexibility of multi-period processes is introduced. Section 4.1.2, discusses what practical measures need to be included in the optimization to ensure practical HEN design. Finally, in Section 4.1.3, the topic of multi-objective optimization is addressed.

4.1.1 Flexibility

Multi-period plants need to have a flexible HEN design to ensure feasible heat transfer in every operating period. Therefore, the mass flow in HEXs needs to be adaptable to account for varying heating and cooling demands and temperature levels for a fixed HEX area. In industry there are three commonly used approaches to ensure flexibility:

1. Utility compensation to address the varying heating and cooling demands
2. Bypassing a HEX with a fraction of the mass flow
3. Admixing a fraction of the outlet mass flow of a HEX back to the inlet

To address varying heating or cooling demands, industry plants feature utility HEXs within the process for utility compensation (1). Another option is the integration mixer configurations. An example of a possible mixer configuration is shown in Fig. 6. This example shows how a bypass configuration (2) on the hot stream and an admixer configuration (3) on the cold stream can be integrated into the SWS model (Yee and Grossmann, 1990). Besides the enthalpy stage temperatures ($T^{op}_{i,k}$, $T^{op}_{j,k}$) from the SWS model, each mixer configuration introduces an inlet $T^{op}_{e,h,in}$, $T^{op}_{e,c,in}$ and outlet $T^{op}_{e,h,out}$, $T^{op}_{e,c,out}$ temperature for the HEX. Fig. 6(b) shows how the temperatures $T^{op}_{e,h,out}$ and $T^{op}_{e,c,in}$ can be adjusted for the depicted mixer configuration. If $T^{op}_{e,h,in}$ or $T^{op}_{e,c,out}$ has to be adjusted, an admixer configuration on the hot steam or a bypass configuration on the

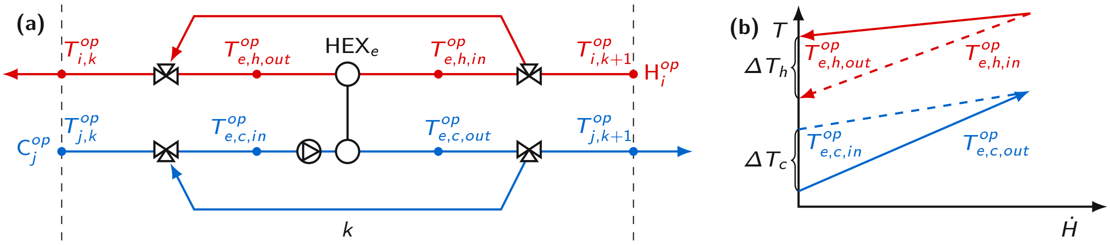

Fig. 6 Example mixer configuration **(a)** with a bypass configuration on the hot stream and admixer configuration on the cold stream (published in Article 2) and **(b)** associated possible temperature modifications

cold stream is needed. If the heat load of a HEX is different in an operating period, one of the temperatures has to be adjusted to fulfill the heat transfer equation

$$\dot{Q}_e^{op} = U_e^{op} \max_{op \in OP} (A_e^{op}) \, \Delta T_{m,e}^{op}. \tag{4.1}$$

The logarithmic mean temperature difference (LMTD), in Eq. 4.1, can conventionally only be solved implicitly for one of the inlet or outlet temperatures. However, Chen (2019) developed a method utilizing the Lambert W-function (Lambert, 1758; Euler, 1779) to solve the LMTD analytically which can be incorporated into a HEN formulation.

By reducing the mass flow in a HEX with a bypass, the inlet or outlet temperatures can reach unrealistic high or low levels. The adjusted temperature is limited due to a minimal possible mass flow within the HEX, but also other limitations such as material constraints of the equipment or process stream (phase change, chemical reactions). To omit such temperatures, extreme temperatures for process streams are introduced as constraints. More details on flexibility and how it is implemented in the optimization approach is published in Article 2 and 4.

4.1.2 Practical Retrofit Measures

Besides the flexibility aspect of the multi-period behavior, practical aspects of plant design are to be considered in the HEN model. Process streams in multi-period plants might not be active or do not have heating or cooling demands in some of the operating periods. In such cases, a bypass mixer configuration is needed which completely bypasses the still active streams connected to the inactive process stream to omit unwanted effects on the temperature and unnecessary pressure drops.

Another aspect of the practical design is soft streams. In contrast, to process streams, these streams do not have required heating or cooling demands but can be used for HR. Examples of soft streams are flue gas, exhaust air, or wastewater streams, which can but do not have to be cooled down before releasing it into the environment. Soft streams are to be considered in the optimization as potential matches with process streams, however, cannot be connected to utility streams as they do not have a target temperature that needs to be reached.

Another important factor is the complexity of the plant. For example, having a higher number of splits in the plant might decrease the TAC but increases the complexity and thus, demands a more sophisticated control system of which costs are usually neglected in the TAC. Therefore, the HEN model has to include practical constraints to limit the complexity that can be adjusted depending on the demands of the plant. First, the number of splits a stream can have at one point has to be restricted. Hence, the number of HEXs connected to a stream in one enthalpy stage is limited by a user-defined value. Further, the number of possible HEXs of the HEN can be limited to omit a high number of HEXs which cover only a small fraction of the HR.

In addition to these constraints, further costs for the retrofit are included in the TAC. Besides the usual costs of new HEXs and added HEX area, also costs for splits and mixer configurations are considered. Thereby, modification costs for adding, or removing equipment, as well as re-piping, and re-sequencing are determined. Depending on the layout of the plant, process streams might have a large distance between each other leading to high match costs for these streams. On average, piping accounts for 13 % of capital costs of fluid-processing plants (Peters and Timmerhaus, 1991). For multi-period processes, some connections might be only in use for a short amount of time, depending on the scheduling of the process. Therefore, it is important to consider these additional match costs (piping costs) in the HEN model. More details on the implementation of practical retrofit measures is published in Article 2.

4.1.3 Multi-Objective Problems

Multiple objective problems are common occurrences in industry. Besides cost reductions, common objectives in PI are reduction in GHG emissions, space, or complexity. The latter two are difficult to quantify and are therefore, accounted for with extensions and constraints in the HEN model. GHG emissions are accounted for by Pareto optimization. The implementation of the multi-objective optimization (MOO) as well as the objective functions selection is discussed in Article 5 and 6.

4.2 Optimization Approach

As discussed in Section 2, due to its complexity, HENS is usually tackled either by simplification of the problem or by the use of stochastic algorithms. Thus the objectives of this thesis explore the extensions demanding flexibility of the HEN and require further practical measures and constraints, the developed algorithm rather uses stochastic algorithms than a simplification of the problem.

Within the scope of this thesis, two different hybrid metaheuristic nature-inspired optimization approaches are analyzed to achieve *Objective 2*. The resulting algorithm is published in Article 3. To ensure the availability of the algorithm to the industry, the optimization model is available online (Software 1). The extended model for the MOO is published in Article 6 and is also available online (Software 2).

4.2.1 Hybrid Evolutionary-Based Approach

Evolutionary algorithms are based on the process of how populations evolve over generations in nature. Hence, these algorithms optimize a population (set of individual solutions, called chromosomes) with each other based on the concept of *survival of the fittest*. Thereby, three evolutionary operators are applied in the optimization process: (1) selection, (2) recombination, and (3) mutation. The selection process (1) is usually based on the fitness (objective) of the chromosomes, whereby also a certain amount of random selection is included to ensure a broader exploration of the solution space. In the recombination process (2), two or more parent chromosomes mate, meaning a child chromosome is generated by recombining genes (type of information; e.g., containing all the information on how a HEX is integrated into the HEN) of the parent solutions. In nature, during this process copying errors might occur which are called mutations (3). Thereby, single alleles (values in the genes), might randomly change. This operation helps to broaden the search in the solution space. An overview of this approach is shown in Fig. 7. The proposed algorithm is separated into two-stages. In the top-level algorithm, all integer variables representing the topology of the HEN are optimized.

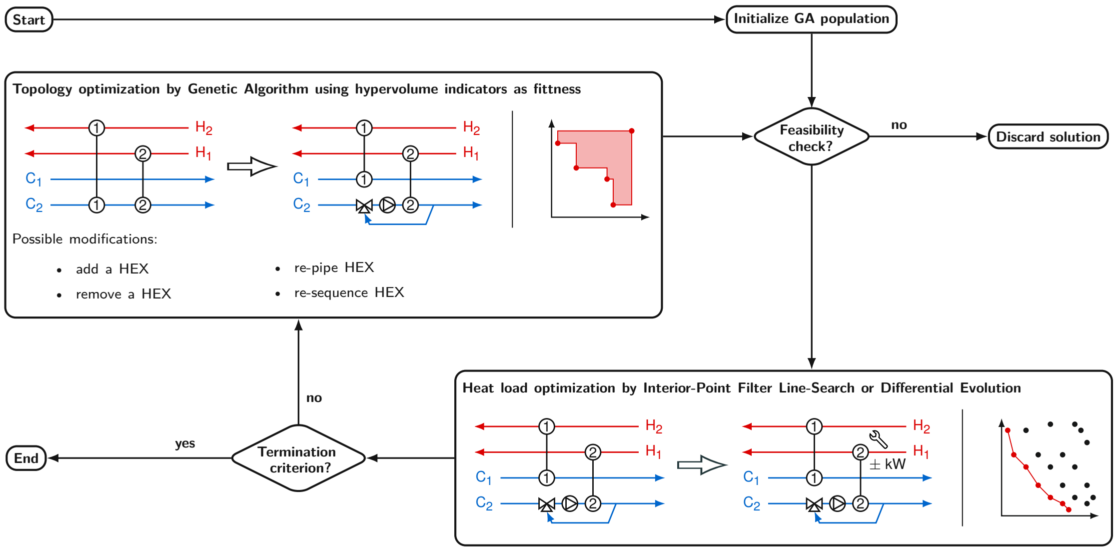

Fig. 7 Overview of the two-stage hybrid evolutionary algorithm for multi-objective optimization (adapted from Article 6)

In the sub-level algorithm, the heat loads of the HEXs in each operating period are optimized (continuous variables). While for the top-level algorithm, a GA is used, for the sub-level algorithm two potential approaches are analyzed. The first approach uses Ipopt (Interior Point Optimizer) solver developed by Wächter and Biegler (2006). Ipopt is an open-source software using the interior point line search filter method, which is a gradient-based deterministic algorithm, to solve continuous large-scale nonlinear problems. The second approach uses DE which is another population-based algorithm based on evolution.

Population-based approaches are predestined for parallel computing as all the chromosomes in the population need to be evaluated before their fitness can be compared in the selection process. With a two-stage algorithm, it is predestined to distribute the chromosomes of the top-level algorithm, in this case, HEN topologies, to multiple threads on which the sub-level algorithm will optimize the heat loads and evaluate the chromosomes based on the given topology from the top-level algorithm simultaneously.

4.2.1.1 Topology Optimization with Genetic Algorithm

The chromosome (topology of the HEN) can be represented in the form of an exchanger address matrix (EAM). This is a common approach often used in HEN synthesis (among others used by Rezaei and Shafiei (2009), and Soltani and Shafiei (2011)). An example of an EAM is shown in Fig. 8. The chromosome consists of all the information needed to design the HEN, whereby each gene stores the needed information to place a HEX. A gene consists of the following information: HEX number (e), hot stream the HEX is connected to (i), cold stream the HEX is connected to (j), and enthalpy stage the HEX is placed in (k). Binary information about the mixer configuration and the existence of the HEX (1 if existing, 0 is not existing) is stored as follows: bypass configuration on the hot side (b_h), admixer configuration on the hot side (a_h), bypass configuration on the cold side (b_c), admixer configuration on the cold side (a_c), and HEX exists (ex).

The optimization with the GA starts by initialing a population of random chromosomes (EAMs). For all feasible topologies, the sub-level algorithm optimizes the heat loads and evaluates the fitness based on the HEN model (more details on the HEN model are published in Article 2). The fitness of the chromosomes in the selection step of the GA is determined using the objective function, thereby a tournament selection is performed. This means that a given number of randomly selected chromosomes is compared based on

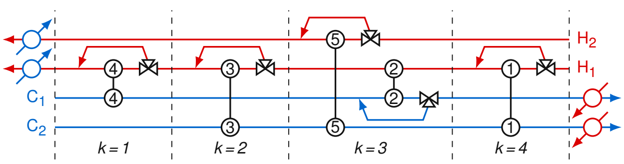

$$\textbf{EAM} = \begin{array}{c} \begin{array}{ccccccccc} e & i & j & k & b_h & a_h & b_c & a_c & ex \end{array} \\ \begin{bmatrix} 1 & 1 & 2 & 4 & 1 & 0 & 0 & 0 & 1 \\ 2 & 1 & 1 & 3 & 0 & 0 & 0 & 1 & 1 \\ 3 & 1 & 2 & 2 & 1 & 0 & 0 & 0 & 1 \\ 4 & 1 & 1 & 1 & 1 & 0 & 0 & 0 & 1 \\ 5 & 2 & 2 & 3 & 1 & 0 & 0 & 0 & 1 \end{bmatrix} \end{array}$$

Fig. 8 Example of a exchanger address matrix for the GA (published in Article 2) their fitness and the fittest of them are selected and used as parents for the recombination. In the recombination step, a one-point crossover is performed. Thereby, a random gene number (HEX number) is selected. The selected gene is used to split both parent chromosomes at its position. All genes, above the selected gene, in parent 1 and all genes, below the selected gene, in parent 2 are recombined into a new child chromosome. Next, the mutation step is performed, in which alleles in the new child chromosome are modified with a certain probability. These three evolutionary operators together represent one generation of the GA. The algorithm repeats these generations till a stopping criteria is fulfilled. To keep track of the best solutions, a Hall of Fame list keeps track of the best-found solution and is updated at the end of every generation.

In order to consider constraints decoding and penalizing strategies are implemented. For the latter, a quadratic penalty function is used which replaces the objective function if a constraint is violated.

For multi-objective optimization the sub-level algorithm returns a list of Pareto-optimal solutions rather than a single best solution. Therefore, the selection process in the GA needs to be adapted. The fitness of each Pareto front is determined using hypervolume indicators (Zitzler et al., 2007). The hypervolume of a Pareto front is defined as the volume between all points of the Pareto front and a selected reference point that is worse than all found solutions. If there are only two objective functions, the hypervolume reduces itself to an area. By comparing the size of the hypervolume, the quality and thus, the fitness of the Pareto front can be determined.

This algorithm is implemented in Software 1 and 2. A detailed explanation of the implementation is published in Article 3 and the extension for multi-objective optimization in Article 6.

4.2.1.2 Heat Load Optimization with Interior-Point Filter Line-Search Algorithm

In the sub-level algorithm, the HEN model (explained in Article 2) is optimized with a fixed HEN topology. Thus, the problem is simplified to a nonlinear, non-convex problem. This problem can be tackled using a global optimizer such as Ipopt (Wächter and Biegler, 2006), comparable to commercial solvers such as BARON. Ipopt is based on the Newton method, whereby the derivative of the objective function is used to direct the algorithm to the optimal solution. This approach is extended using barrier methods to account for the constraints. Thereby, the constraints of the problem are incorporated into the objective function as a logarithmic penalty function. With the line-search method, the barrier problem is interpreted as a bi-objective optimization, whereby the second objective represents the barrier function of the constraints. To ensure global convergence and avoid premature convergence at a point where the KKT condition is fulfilled, the backtracking line-search method is used to determine the step size by exploring a decreasing sequence of trial step sizes. With the filter method, only trial step sizes that improve the objective function or the barrier function are accepted.

To extend this approach to cover multi-objective problems, the objective function needs to be adapted using linear scalarization:

$$\min_{x \in X} \sum_{i=1}^{i=I} (w_i \, OF_i(x)) \qquad \text{with} \quad \sum_{i=1}^{i=I} w_i = 1 \text{ and } 1 \geq w_i \geq 0 \; \forall \, w_i \tag{4.2}$$

By varying the weight factors w_i of each objective $OF_i(x)$, a Pareto front containing all the non-dominated results can be produced.

4.2.1.3 Heat Load Optimization with Differential Evolution

Another approach to solving the nonlinear, non-convex optimization problem is using DE, which is an evolutionary algorithm designed to handle continuous variables. In contrast to a deterministic algorithm, like the Interior-Point method, DE does not need any gradient information. DE instead, uses the same three evolutionary operators as GA but in the reversed order: mutation, recombination, and selection. The chromosome for the DE (called heat load matrix), consists of the heat loads of every existing HEX in each operating period, resulting in a two-dimensional matrix. For every feasible topology from the GA, the DE algorithm initializes a population of random heat load chromosomes, which are then evaluated using the HEN model from Article 2. After the initialization, the evolutionary process starts by randomly selecting three non-equal chromosomes. A new donor chromosome is generated by combining the three selected chromosomes using a perturbation factor. In the recombination step, a new trial chromosome is generated by replacing alleles in the first of the three selected chromosomes with alleles from the donor chromosome. The newly generated trial chromosome is then evaluated using the HEN model and compared to the first of the three randomly selected chromosomes. The fitter of these chromosomes is chosen using a greedy selection process. If the trial chromosome is fitter than the first of the three randomly selected chromosomes, it is therefore replaced in the population, otherwise the first of the three randomly selected chromosomes stays in the population. The three evolutionary operators are applied in this order for every generation till the termination criteria are fulfilled.

The constraints for continuous variables such as energy balances are usually violated, hence penalizing strategies are used in the sub-level algorithm. This helps to guide the search toward the feasible region.

To extend the DE for multi-objective optimization, the selection process needs to be adapted. To find the Pareto-optimal chromosomes, the greedy selection is updated to include the non-dominated sorting Genetic Algorithm (NSGA-II). Instead of choosing the chromosome with the fittest objective, NSGA-II determines all the chromosomes which are not dominated by another chromosome (no other chromosome exists that is better in one objective without being worse in other objectives). In the greedy optimization step the population is then updated accordingly to only include non-dominated chromosomes generating a Pareto front.

This algorithm is implemented in Software 1 and 2. A detailed explanation of the implementation is published in Article 3 and the extension for multi-objective optimization in Article 6.

4.2.2 Hybrid Trajectory-Based Approach

The research on using a trajectory-based instead of an evolutionary-based algorithm was initiated by the application of the single-objective algorithm to the case studies published in Article 1 and 2. The results showed that the optimized topology differs significantly from the initial design. The more different the networks are, the more retrofit work is needed. This is an important factor for the practical application as it increases the down times of the plant. For evolutionary-based algorithms, it is difficult to limit the number of modifications as randomly initialized topologies are used in the optimization. In contrast, a trajectory-based algorithm starts the optimization with the initial design and modifies it to find better solutions. Hence, with a trajectory-based algorithm, the number of modifications and therefore, the needed retrofit work can be limited.

Trajectory-based algorithms have only a single agent (solution) which moves through the solution space. Thereby, improved solutions are always accepted and worse solutions are only accepted with a given probability. In this approach uses SA. Possible moves of the agent in the solution space are called neighborhood moves and need to be tailored to the problem. Often violated constraints are addressed using a repair strategy. Hence, a repair algorithm is used as a sub-level algorithm for the SA. Therefore, the constraints

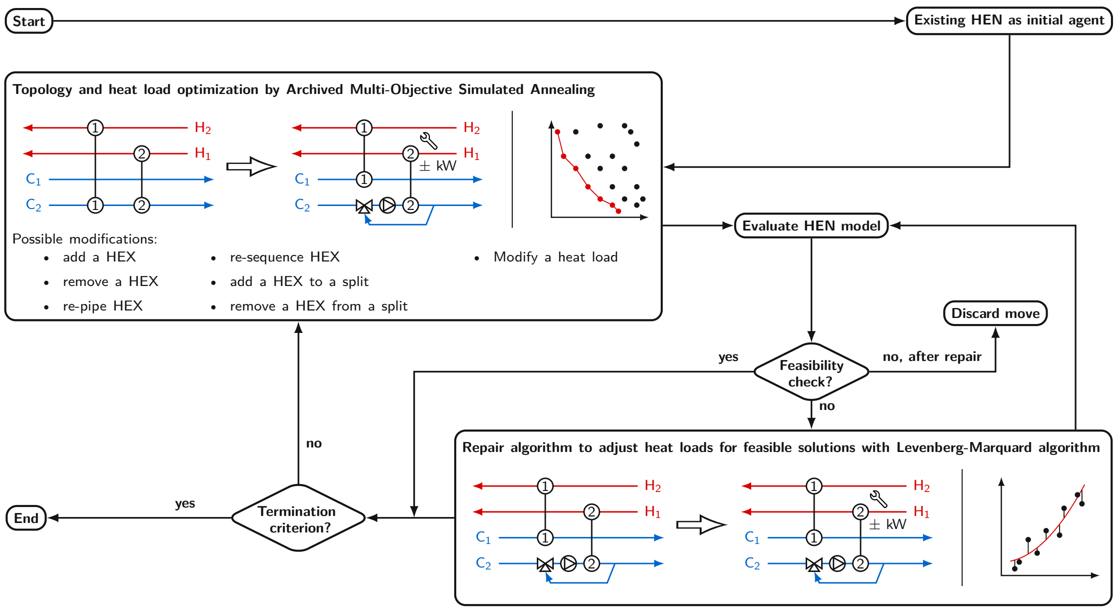

Fig. 9 Overview of the two-stage hybrid trajectory algorithm for multi-objective optimization.

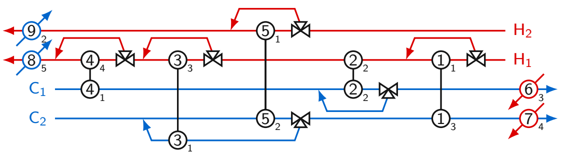

$$
\mathbf{EAM} = \begin{array}{c}
\begin{array}{cccccccccccc} \mathrm{e} & \mathrm{i} & \mathrm{j} & \mathrm{e_i} & \mathrm{e_j} & \mathrm{s_i} & \mathrm{s_j} & \mathrm{b_h} & \mathrm{a_h} & \mathrm{b_c} & \mathrm{a_c} & \mathrm{ex} \end{array} \\
\begin{bmatrix}
1 & 1 & 2 & 1 & 3 & 0 & 0 & 1 & 0 & 0 & 0 & 1 \\
2 & 1 & 1 & 2 & 2 & 0 & 0 & 0 & 0 & 0 & 1 & 1 \\
3 & 1 & 2 & 3 & 1 & 0 & 1 & 1 & 0 & 0 & 0 & 1 \\
4 & 1 & 1 & 4 & 1 & 0 & 0 & 1 & 0 & 0 & 0 & 1 \\
5 & 2 & 2 & 1 & 2 & 0 & 1 & 1 & 0 & 0 & 0 & 1 \\
6 & 2 & 2 & 1 & 3 & 0 & 0 & 1 & 0 & 0 & 0 & 1 \\
7 & 2 & 2 & 2 & 4 & 0 & 0 & 1 & 0 & 0 & 0 & 1 \\
8 & 2 & 2 & 5 & 1 & 0 & 0 & 1 & 0 & 0 & 0 & 1 \\
9 & 2 & 2 & 2 & 2 & 0 & 0 & 1 & 0 & 0 & 0 & 1
\end{bmatrix}
\end{array}
$$

Fig. 10 Example of a exchanger address matrix for the SA

are reformulated as a nonlinear least-squares problem. If the repair algorithm is not able to find a feasible solution, the solution is rejected and another neighborhood move is performed. An overview of the algorithm is shown in Fig. 9. The here presented algorithm procedure is similar to the approach published by Ochoa-Estopier et al. (2015). However, in contrast to Ochoa-Estopier et al. (2015), the EAM is used to represent the HEN topology and further, the HEN model includes multi-period operation and addresses multi-objective problems.

4.2.2.1 Topology and Heat Load Optimization with Simulated Annealing

The general idea of SA is having one individual, called agent, moving through the solution space. The agent has a similar format as in the evolutionary algorithm (EAM and heat load matrix) shown in Fig. 10. However, instead of enthalpy stages (k), the HEXs are numbered on each hot (e_i) and cold stream (e_j) and an additional split number (s_i) and (s_j) is added to keep track of in which split the HEX is. Possible moves in the solution

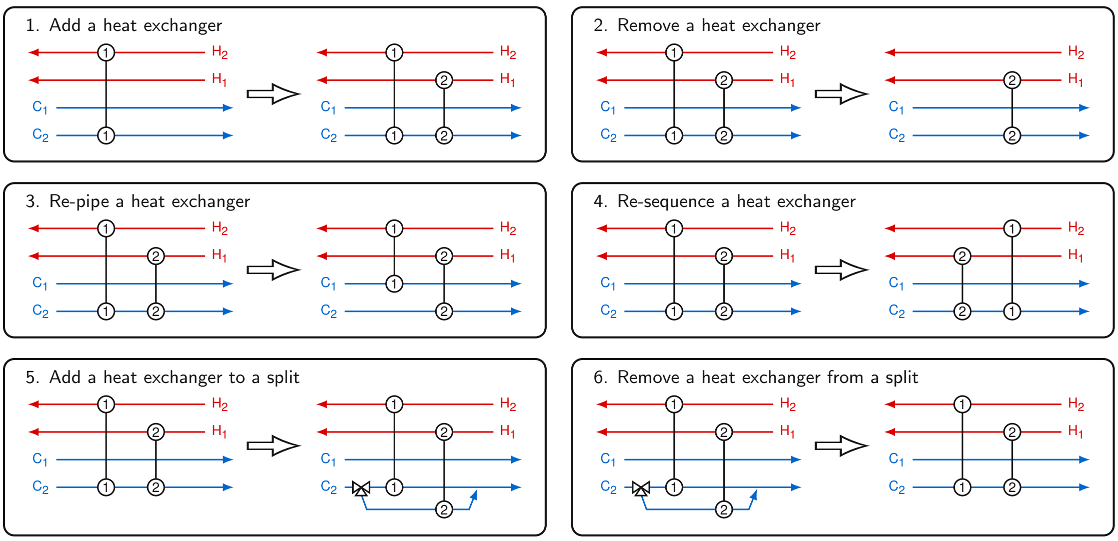

Fig. 11 Topology neighborhood moves for the SA

space are called neighborhood moves. These moves describe modifications on the network which are reachable from the existing design. The following 7 neighborhood moves are considered in the optimization (all topology-based neighborhood moves are visualized in Fig. 11):

1. *Add a HEX:* For a random non-existing HEX (ex = 0), hot and cold stream (i,j), stream HEX numbers (e_i, e_j) are randomly chosen from a set of possible new stream matches. The stream HEX numbers of all existing HEXs, including and above the chosen number, are increased by one. The heat load for each operating period is defined by

$$\dot{Q}_e^{op} = \text{random.uniform}\left(\dot{Q}_{min}, \min\left(\Delta\dot{H}_{i\in e}^{op}, \Delta\dot{H}_{j\in e}^{op}\right)\right) \tag{4.3}$$

   whereby, $\dot{Q}_{min}$ is a user-defined variable to omit HEXs with small heat loads. $\dot{H}_{i\in e}^{op}$ and $\dot{H}_{j\in e}^{op}$ are the enthalpy flows of the connected streams. If the new HEX is connected to a utility, it is connected in parallel to another utility HEX. To ensure a feasible mass balance the split fraction for all HEXs in the utility split is updated using the Dirichlet distribution (the sum of all random variables always adds up to 1). If no new match is possible, instead, the move *remove a HEX* is performed.
   Constraints:

   - Number of HEXs: if all HEXs are existing, no new HEX can be added.
   - Forbidden matches: matches which are infeasible ($T_{i,in}^{oc} \leq T_{j,in}^{oc}\, \forall\, i, j, oc$) and restricted by the user due to practical reasons are not possible.

2. *Remove a HEX:* First, fixed HEXs are updated to include HEX which are the sole ones on a stream (to omit infeasible solutions where the energy balance of a stream cannot be fulfilled). An existing HEX (ex = 1) is randomly chosen and its stream numbers (i and j), stream HEX numbers (e_i, e_j), and existence of the HEX (ex) are set to 0 and the mixer configuration is set to no mixer ($b_h/a_h/b_c/a_c = 0$). Stream HEX numbers (e_i, e_j) above the removed HEX are decreased by one. If the HEX is in a split, the split fraction of the remaining HEXs is recalculated using the Dirichlet distribution. If there is only one additional HEX in the split, it is removed (s_i and/or e_j are set to 0). If no HEX can be removed, instead, the move *add a new HEX* is performed.
   Constraints:

   - Fixed HEXs: HEXs which are the sole ones on a stream cannot be removed to fulfill the energy balance of the stream and user-defined fixed HEXs which cannot be removed due to specific practical reasons.

3. *Re-pipe a HEX:* First, it is randomly decided if the hot or cold side of a HEX is re-piped. In the next step, re-pipeable HEXs are identified (depending on the HEX side: HEXs which are the sole ones on a stream can only be re-piped on the other side) by creating a new set

$$X_{re-pipe} = (X_{match,fixed} \cup X_{forb})^C \tag{4.4}$$

which contains all re-pipable HEXs. Next, a random re-pipeable HEX as well as a random new stream are chosen. On the old stream, the stream HEX numbers ($\mathrm{e_i}$, $\mathrm{e_j}$) above the selected HEX are reduced by one and on the new stream increased by one. If the HEX was in a split and there is more than one remaining HEX, the split fractions for the remaining HEXs are updated with the Dirichlet distribution. If there is only one remaining HEX in the split, the split is removed. The mixer configuration on the new stream is set to no mixer ($\mathrm{b_h/a_h/b_c/a_c} = 0$) and its fraction to 0. If the move is not possible, instead, the move *modify a heat load* is performed.
Constraints:

   - Forbidden matches: matches which are infeasible ($T^{oc}_{i,in} \leq T^{oc}_{j,in} \,\forall\, i, j, oc$) or restricted by the user due to practical reasons are not possible.
   - Fixed matches: HEXs which are the sole ones on a stream cannot be re-piped and user-defined fixed HEXs cannot be re-piped.

4. *Re-sequence a HEX*: First, it is randomly decided which side of a HEX is re-sequenced. Next, fixed matches are updated with HEXs which are between two fixed HEXs. Then, a HEX is randomly chosen to be re-sequenced. By default, the HEX is always re-sequenced with the HEX below on the stream as far as it is not the first HEX or the HEX below is fixed. The stream HEX number ($\mathrm{e_i}$, $\mathrm{e_j}$), the split number ($\mathrm{s_i}$ and/or $\mathrm{e_j}$), and the mixer configuration ($\mathrm{b_h/a_h/b_c/a_c}$) for both matches are switched with each other. If the move is not possible, instead, the move *modify a heat load* is performed.
Constraints:

   - Fixed matches: HEXs which are in between two fixed HEXs and user-defined fixed HEXs due to practical reasons.

5. *Add a HEX to a split:* First, it is randomly decided which side of a HEX is added to a split. Next, possible HEXs for a split are identified (HEXs without splits excluding utility streams). Two HEXs which are next to each other on a stream are chosen randomly. If one of the chosen HEX already is in a split, the other is added to this split as long the number of HEXs in the split does not exceed a user-defined maximum of HEXs. If both HEXs are not in a split, a new split, with the lowest non-existing split number is created. The split fractions of all HEXs are updated using the Dirichlet distribution. The mixer configuration and fraction are updated if the mixer configuration for one HEXs has changed. If the move is not possible,

instead, the move *remove a HEX from a split* is performed.
Constraints:

- Number of HEXs in a split: if the user-defined value is reached no additional HEX can be added to a split.
- No new utility splits: all utility HEXs are already in parallel and therefore, no new split on utility streams is possible.

6. *Remove a HEX from a split*: First, it is randomly decided which side of a HEX is removed from a split. If there are more than two HEXs left in the split, the split fraction is updated using the Dirichlet distribution, otherwise, the split is removed and the split fractions are set to zero. The mixer configuration of the removed HEX is set to no mixer ($\mathrm{b_h}/\mathrm{a_h}/\mathrm{b_c}/\mathrm{a_c} = 0$) and the mixer fraction to zero. If the move is not possible, instead, the move *add a HEX to a split* is performed.
Constraints:

   - No utility splits are removed: utility splits HEXs are considered to be always in parallel and therefore, no splits on utility streams can be removed.

7. *Modify a heat load:* First, non-modifiable HEXs are identified. In a next step, an existing modifiable HEX ($\mathrm{ex}= 1$), as well as an operating period are chosen randomly. The heat load is modified according to Eq. 4.3. If the chosen HEX is connected to a split, split fractions are updated accordingly to the heat load distribution. This move can always be performed.
Constraints:

   - Non-modifiable HEXs: HEXs which are the sole ones on a streams cannot be modified (user-defined fixed matches are not included).

For the start of the SA, the existing plant design is used as the initial position of the agent. For every iteration, neighborhood moves are performed till the equilibrium condition is satisfied. This is usually a number of iterations such as a multiple of the neighborhood size. In each iteration it is chosen which neighborhood move is performed based on their probabilities. During the iteration, the agent makes a move if the objective improves. To explore the solution space, also worse solutions are accepted if the Metropolis-criterion (Metropolis et al., 1953) is fulfilled:

$$P < \exp \frac{-|f(x') - f(x)|}{T} \tag{4.5}$$

whereby, P is a random number between 0 and 1, $f(x)$ is the current objective value, $f(x')$ the objective value after the move x', and T is the temperature. The temperature is an algorithmic parameter controlling the likelihood of replacing the actual solution with a worse solution. The temperature parameter is degrading using geometric cooling

$$T_{+1} = T\,\alpha \qquad \text{with } \alpha < 1 \tag{4.6}$$

each time the equilibrium condition is satisfied and is initialized to reject 3 % of the moves. By using the annealing of the temperature, the likelihood of accepting a worse solution decreases until the stopping criteria, usually a final temperature, is satisfied. This process allows the SA to narrow the search over time from global to local optimization.

To extend SA for multi-objective optimization, various approaches are proposed in the literature. One promising approach is to incorporate an archive that keeps track of non-dominated solutions (Bandyopadhyay et al., 2008). Thereby, the probability to accept worse solutions is adapted to consider the distance to the non-dominated solutions.

4.2.2.2 Nonlinear Least-Squares Repair Algorithm

By modifying the topology and heat loads of the HEN, constraints such as the energy balance of the streams or feasible heat transfer will usually be violated due to the randomness of the neighborhood moves. To still fulfill these constraints a repair algorithm is needed to adjust the heat loads. The constraints (stream energy balances and feasible temperature differences) are reformulated as an objective function:

$$\begin{aligned} OF(\dot{Q}_e^{op}) = &\sum_{\forall i} \left(\Delta \dot{H}_i^{op} - \sum_{\forall e \in i} \dot{Q}_e^{op} \right)^2 + \sum_{\forall j} \left(\Delta \dot{H}_j^{op} - \sum_{\forall e \in j} \dot{Q}_e^{op} \right)^2 \\ &+ \sum_{\forall e} \sum_{\forall op} \min \left(T_{e,h,b}^{op} - T_{e,c,a}^{op} - \Delta T_{min}, T_{e,h,a}^{op} - T_{e,c,b}^{op} - \Delta T_{min}, 0 \right)^2 \end{aligned} \tag{4.7}$$

whereby, the subscripts a and b indicate here the enthalpy stage temperatures ($T_{i,k}^{op}, T_{j,k}^{op}$) before ($b$) and after ($a$) the mixer configuration of HEX e. If this function is solved successfully, the feasibility of the HEN without mixer configurations is guaranteed. Including the mixer configurations into the objectives would require solving the LMTD and thus lead to a non-convex problem which cannot be solved with nonlinear least-squares solver such as the Levenberg-Marquard algorithm (Levenberg, 1944; Marquardt, 1963), defeating the concept of having a simple solver in the sub-level.

To ensure feasibility, all constraints (including the constraints for the mixer temperatures published in Article 2) need to be checked for violation. If the solution is still infeasible after the repair attempt, the neighborhood move is rejected and a new move is performed.

4.2.3 Comparison of the Optimization Approaches

Both algorithms have two stages to break down the problem into smaller sub-problems and simplify the solution process while still solving the problem simultaneously. In contrast to the evolutionary-based approach, which splits the stages between integer and continuous variables and handles constraints directly within the respective algorithms, the trajectory-based algorithm optimizes integer and continuous variables in the top-level algorithm and uses the sub-level to ensure feasibility. A key advantage for HEN retrofit with the trajectory-based algorithm is that the existing design can be used as the initial solution of the algorithm and the neighborhood moves can be defined to represent actual modifications to the HEN that would need to be implemented in the actual retrofit of the plant. Further, it is beneficial that the sub-level can be modeled as a nonlinear least-squares problem. However, the fact that not all constraints can be included, without increasing the complexity significantly, finding feasible solutions cannot be guaranteed. If the non-convex constraints would be included, a more complex solver would be needed, losing the advantage of having an algorithm with low computation cost in the sub-level. Therefore, the evolutionary-based approach is pursued instead. Further, the evolutionary-based approach is that the algorithm provides multiple solutions at once. Despite the increased computation cost, multiple solutions also have their benefits. Multiple near-optimum solutions can be provided as a result. This is beneficial for the application of the approach as the user can still decide which of the solutions is more suitable to implement. Another advantage is that the adaption to multi-objective optimization is simple as the solutions for generating a Pareto front already exist and only have to be sorted considering the additional objectives. This simplifies the implementation of multi-period problems significantly.

To optimize the continuous variables in the evolutionary-based approach a deterministic and an evolutionary algorithm are compared. While a deterministic algorithm such as Ipopt is generally faster at finding solutions, gradient-based approaches have difficulties finding feasible solutions for highly complex problems such as HENR problems. In contrast to this, DE is able to find feasible solutions but might not find the global optimal solutions. However, as Objective 1 focuses on practical design rather than global optimum, this is not a substantial problem. By considering the interaction between the two levels, the GA algorithm produces with the random initialized networks a lot of infeasible solutions for the sub-level algorithm. This leads to a problem for a deterministic algorithm, whereby, the evolutionary-based algorithm does not need to converge and thus can use the penalty function to guide the algorithm towards the feasible region.

4.3 Integration into a Practical Workflow

In this section, it is shown how the evolutionary-based optimization approach can be integrated into a workflow for the conceptual design in a retrofit project. An exemplary workflow with the integrated optimization approach is shown in Fig. 12.

Step 1: System Boundary: First, the system boundaries for the project need to be determined. The boundaries are usually based on plant layout, environment, and production schedules. Further, access to existent heat sinks and sources such as utility systems, district heating, geothermal probes, ambient air, or waters can influence retrofit possibilities and thus, are an important factor in the selection of the system boundary.

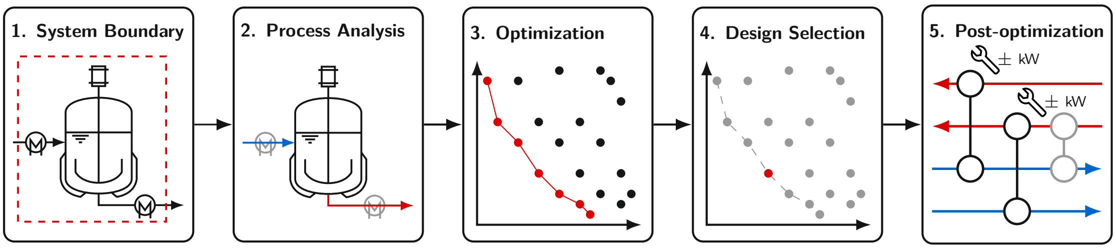

Fig. 12 Overview of a practical workflow for a retrofit project with integrated optimization approach

Step 2: Process Analysis: As soon as the system boundaries are set, essential process requirements such as stream temperatures, mass flows, and the multi-period behavior, need to be determined. This is usually done by identifying crucial process and soft streams within the boundaries. Depending on the plant, the needed stream data might be accessible via a process control system. However, this is uncommon in small and medium-sized production plants and process data usually needs to be determined by directly measuring the parameters. A further important part of this step is the plant layout. New pipes might be required for the retrofit. Therefore, distances between heat sources and sinks need to be clarified to estimate match costs. Further, costs for potential new equipment as well as utilities need to be determined, which is usually done using quotes and invoices. With this information coefficients for the cost functions can be estimated. Process simulation can be a helpful tool for this step. For example, if the plant also has to be adapted for a new production scenario such as a new product, part load operation, or a different schedule.

Step 3: Optimization: In the optimization step, first, suitable objectives for the project specifications need to be determined. Usually in retrofit, TAC and GHG emissions are the most relevant. Depending on the problem size the algorithm parameters need to be adapted. Therefore, usually, rules of thumb are used as a first guess. Due to the randomness of the algorithm, to achieve confident results, a statistical analysis with multiple computations for each configuration would need to be performed. This is a time-consuming process and might be, due to that the global optimum does not have to be found, abbreviated by the use of sensitivity and convergence analysis of the actual solution as shown in Article 2 and 6. As soon as all the parameters are fixed, the actual optimization using the multi-objective hybrid evolutionary algorithm based on GA and DE can be used to solve the problem.

Step 4: Design Selection: After the optimization, there are multiple near-optimum Pareto fronts stored in the Hall of Fame list. Out of these, the user has to decide which solution should be implemented. Decision factors for this might be the payback period, which equipment need to be retrofitted, how many modifications on the plant are needed, how long the plant needs to be shut down for the retrofit, as well as not-in-use HEX area which indicates how well the HEX area is utilized in each operating period (for more detail see Article 6).

Step 5: Post-optimization: The selected HEN design might contain a high number of small HEXs. These HEXs increase the complexity of the HEN and the control system. Therefore, it is reasonable to analyze the HEN using relaxation concepts from graph theory such as loops and paths (Smith, 2005; Kemp and Lim, 2020). For large HENs, MP-based algorithms might be used to simplify this process.

5 Case Studies

In this section, the case studies used to illustrate the application of the developed algorithm are introduced and the results are summarized.

5.1 Crude Oil Production

This case study was introduced by Jones (1991) in his PhD thesis. The case study is a simple multi-period process from the crude oil industry. The case study has been anonymized and therefore, only limited information is provided. It consists of four process streams of which two are hot and two are cold streams and with two operating periods. All process streams are active in both operating periods. The temperatures differ significantly between both operating periods suggesting that the data is most likely from a multi-product or multi-purpose plant. Process requirements and cost data are provided in Article 1. Due to its size and simplicity, this case study was selected to introduce the GA/DE algorithm at the 30th European Symposium on Computer Aided Process Engineering (ESCAPE). Since Jones studied the grassroot design of multi-period processes no information about the existing HEN was provided. Hence, an initial HEN, shown in Fig. 13, was designed using PA. The best and the second best-found solution by the algorithm are shown in Fig. 14. Compared to the PA design, both of solutions can

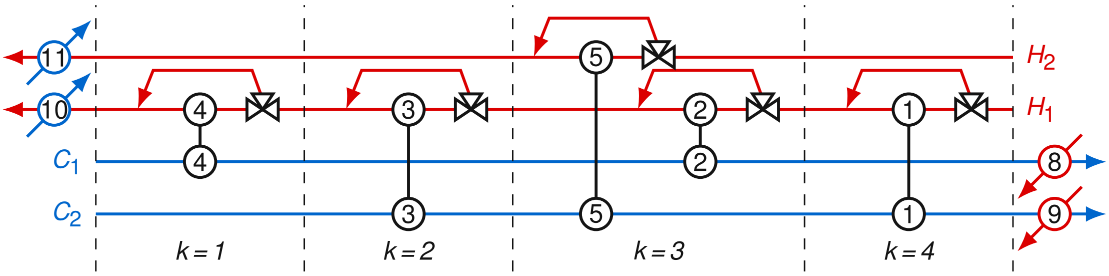

Fig. 13 Existent HEN design established using PA (published in Article 1)

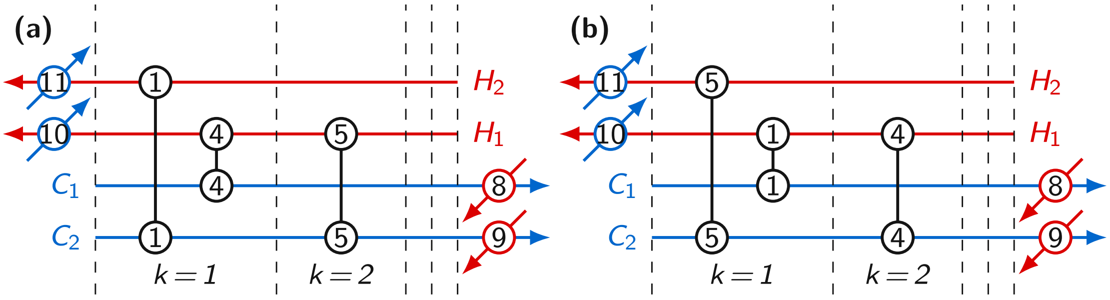

Fig. 14 Optimized HEN design for the **(a)** best and **(b)** second best solution using the GA/DE algorithm (published in Article 1)

reduce TAC by around 55 %. However, the designs are significantly different compared to the existing design leading to long down times for retrofit work. Due to the random initialization of HEN topologies in the GA/DE algorithm, the number of modifications cannot simply be limited. By including more cost factors such as piping, the number of unfavorable results can be reduced. Hence, the plant layout should be considered by accounting for piping costs in the optimization.

5.2 Potato Chips Production

This case study is based on a PA from industry conducted by Fotsch (2006). In the PA, the fritter line 1 of a potato chips production plant from the company Zweifel Pomy-Chips AG is optimized. The flow chart of the process is shown in Fig. 15. The core part of the plant is the fritter which has its associated utility system which cannot be modified. The waste gas of the boiler from the fritter utility system is a soft stream that can but does not have a target temperature to which it has to be cooled down. Its excess heat can be released into the environment. The plant is used to produce chips with two different oil contents: regular chips ($w_{oil} = 0.35$) and Cractive chips ($w_{oil} = 0.25$).

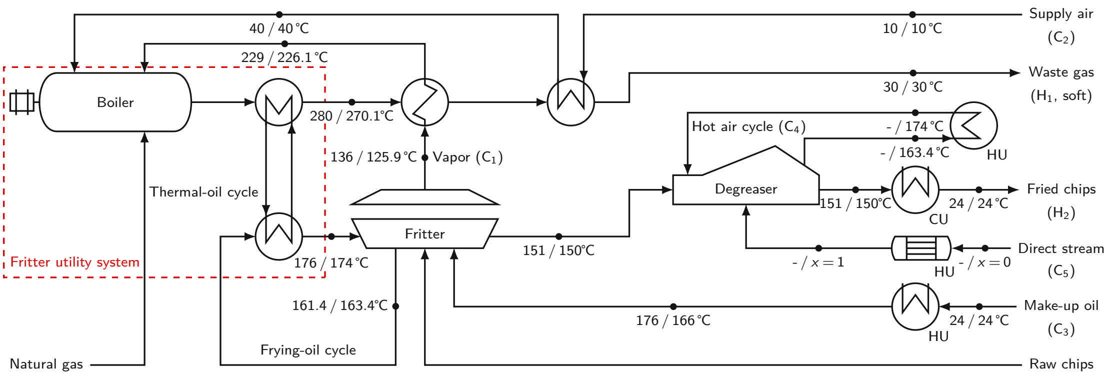

Fig. 15 Flow chart of the fritter line 1 for chips production (published in Article 6)

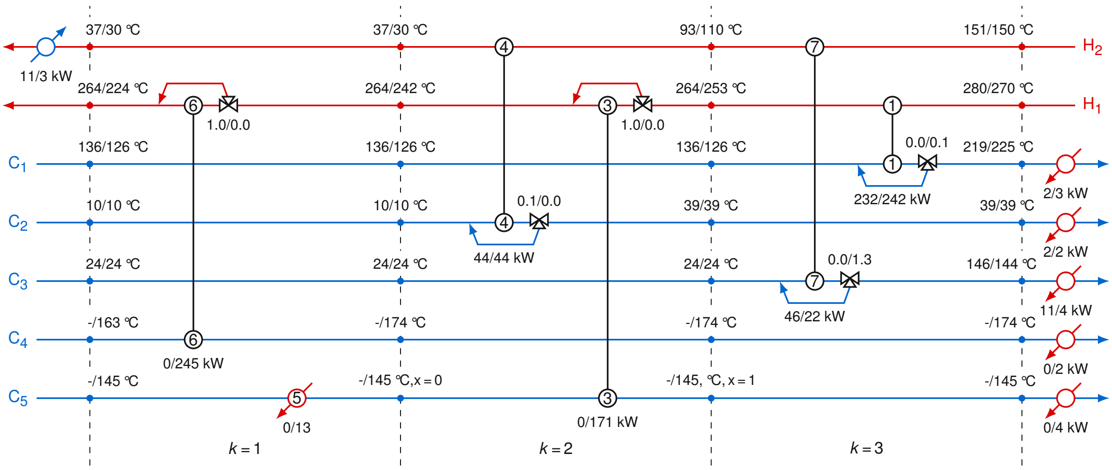

Fig. 16 Resulting retrofitted HEN design using the single-objective GA/DE algorithm (published in Article 6)

Therefore, two operating periods are needed whereby, in the second operating period, an additional degreaser unit is used to reduce the oil content of the chips. The degreaser has additional process requirements extending the number of streams in one of the operating periods. Since the degreaser unit is not running in every operating period it can be argued that this process can be categorized as a multi-purpose plant. The case study consists of seven streams of which two are hot and five are cold streams and has two operating periods. A more detailed process explanation including process requirements and cost data is provided in Article 2 and the GHG emission factors needed for the multi-objective optimization are provided in Article 6.

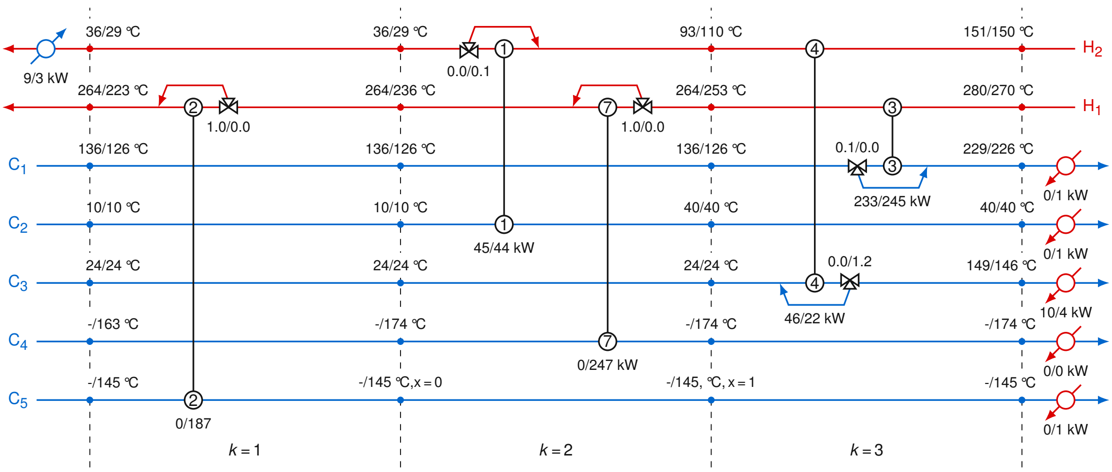

Fig. 17 Resulting retrofitted HEN design using the multi-objective GA/DE algorithm (published in Article 6)

Tab. 1 Comparison of results between the resulting designs of the SOO and MOO optimization and the initial design

Design	TAC (CHF/y)	CAP (CHF/y)	COP (CHF/y)	GHG (t_{CO2e}/y)	Q_{HU} (MWh/y)	Q_{CU} (MWh/y)
Initial	141,080	0	141,080	331.68	1451	623
SOO_{TAC}	48,198	35,419	12,780	30.14	132	55
$MOO_{TAC,GHG}$	61,341	54,453	6,888	15.04	62	48

This case study was selected because it is a real, but not a too extensive case study from the industry on which the practicability of the algorithm can be tested. It includes important occurring factors from the industry such as streams that not only have changing temperatures between operating periods but also streams that are inactive in certain operating periods, or soft streams which cannot be connected with utility streams. Hence, constraints that forbid certain connections such as soft streams and utility streams or no heat transfer for HEX connected to inactive steams, can be tested. Further, its manageable size allows computation times to stay within a reasonable range, qualifying it as an ideal selection as the main case study for the thesis.

In Article 2 and 4 the single-objective GA/DE algorithm is applied to this case study and the resulting optimized HEN design is shown in Fig. 16. In Article 5, and 6 the multi-objective GA/DE algorithm is applied to this case study and the resulting optimized HEN design is shown in Fig. 16. In Tab. 1, the results for both approaches are compared. It can be seen that both approaches improve TAC and GHG emissions significantly compared to the initial design.

The only difference between the approaches is that in addition to the TAC, GHG emissions are considered as a second objective. By comparing Fig. 16 and Fig. 17, it can be seen that the topology for both is similar. The MOO has a higher weight on the utility demand as it is part of the TAC (operating costs) and GHG emissions. Hence, the utility demand is reduced significantly which is also evident in Tab. 1. It can be seen, that the utility demand and the GHG emissions are about halved, however the capital costs and thus, the TAC is increased due to the higher weight on the utility demand. In Article 6, various combinations of objectives have been compared to show their influence on the results. It has been shown that by adjusting the weights using capital costs and operating costs as objectives, similar results as for the SOO can be achieved verifying the MOO algorithm and illustrating the importance of the objective function selection.

6 Conclusions and Outlook

This thesis contributes to the research topic of heat exchanger networks retrofit of processes with multi-period operation. The aim of this thesis is to develop a method, with a focus on practical application. Hence, key extensions, for practical design, to the multi-period heat exchanger network retrofit formulation are identified and implemented. One of the major extensions is the detailed analysis of the mixer configurations to ensure flexibility. Therefore, logarithmic mean temperatures are determined analytically using the Lambert W-functions. To ensure practicality, mixer temperatures are limited by constraints that omit unrealistic temperature levels and split fractions. Another key extension is to allow the user to have some degree of control over the decision-making process. Hence, constraints limiting the complexity of the heat exchanger network, such as a maximal number of splits or a maximum number of total heat exchangers, are included in the formulation. To ensure practical heat exchanger network designs, additional costs, such as costs for splits, mixers, or piping costs, are considered in the optimization. Decision-making factors in the process industry are often based on multiple objectives, therefore the formulation also includes a multi-objective approach analyzing total annual cost and greenhouse gas emissions simultaneously. To generate a Pareto front, a non-dominated sorting Genetic Algorithm and hypervolume indicators are used. The resulting HEN designs are stored in a Hall of Fame list to help the user in the decision-making process. Due to the high complexity of the formulation, a two-stage hybrid evolutionary-based algorithm, using Genetic Algorithm for the topology optimization and Differential Evolution for the heat load optimization, is developed.

The algorithm is applied to two case studies. Thereby, an illustrative case study from the crude oil industry and a real case study from the food industry are analyzed. The crude oil industry case study is optimized using the single-objective algorithm. The algorithm was able to reduce total annual cost by 55 % compared to the existing design created by Pinch Analysis. The second case study from the food industry is more complex and features challenges from the industry. The analyzed process is a fritter line in a potato chips production plant whereby two types of chips with different oil content are produced. This case study is optimized by the single-objective algorithm as well as the multi-objective algorithm. The single-objective optimization is able to reduce total annual cost by 66 %. With the extension to multi-objective optimization, greenhouse gas emissions can be halved. However, the reduction in greenhouse gas emissions increases the total annual cost by 27 % (compared to the single-objective solution). The application to the case study showed the importance of the selection of the objective functions. By minimizing total annual cost and greenhouse gas emissions simultaneously, a higher weight is given to utility consumption as it is part of both objectives. Hence, minimizing capital costs and greenhouse gas emissions as well as minimizing capital costs and operating costs are analyzed as alternative objective functions. As expected, the latter optimization provides similar results as the single-objective optimization minimizing total annual cost. The analysis shows that the selection of the objective function is an important part of the optimization. It also showed that the solution is highly dependent on operation costs and greenhouse gas emission factors. Hence, a change in energy prices or an improvement in the efficiency of utility systems has a high impact on the final network design.

The computation cost for the algorithm strongly depends on the algorithm and model parameters. Due to limited computational resources, it was not possible to perform a detailed parameter study. Hence, the algorithm parameters, which depend on the problem size, are chosen based on experience and convergence. The industrial case study has 7 streams and 2 operating periods. Computation times for the single-objective optimization are between 6 to 8 hours. These are rather high values but could possibly be improved with a comprehensive parameter study. Combining two population-based algorithms increases the number of heat exchanger network solutions that need to be evaluated drastically as for every feasible topology a population of heat load distributions is introduced. Even though the heat load distributions are evaluated in parallel on multiple threads, the resulting computation times are still high. Replacing the Differential Evolution with a nonlinear programming solver could reduce the computation times. However, the random initialized topologies by the Genetic Algorithm are likely to cause many infeasible solutions for the heat load distributions. Therefore, a large share of the population would have to be discarded as the deterministic algorithm would not be able to converge. On the other hand, Differential Evolution works with a penalty function considering infeasible solutions and uses them as a guide toward the feasible region. A possible solution to this problem would be to start the optimization using the Differential Evolution until a major part of the solutions is feasible and then switch from the Differential Evolution to a Nonlinear Programming solver to speed up the optimization.

In order to ensure practicality in the industry and minimize modifications to the heat exchanger network, ideally, the retrofitted design is as close as possible to the existing design. The application to the case study showed, that due to the random initialization of the Genetic Algorithm, final solutions are often quite different from the existing design. An approach to control the number of modifications is to introduce another objective that minimized the number of modifications. However, a more practical approach would be to explore the trajectory-based algorithm further using Simulated Annealing because its neighborhood moves can be defined in such a way that they represent actual retrofit modification steps such as re-piping a heat exchanger. Although, the problem with the Simulated Annealing approach using a repair algorithm is that the sub-stage is non-convex and therefore needs a global nonlinear programming solver. Hence, the benefit of the simple quadratic convex problem is lost and thus, the repair algorithm in the sub-stage could also include the computation of the mixer temperatures using the Lambert W-function.

In summary, this thesis addresses the demand for a broader understanding of flexible plant design and practical retrofit of such plants. Further, the application of the algorithm to a real case study from the industry demonstrated the importance of retrofit for companies to ensure energy-efficient production and reduction in greenhouse gas emissions to ensure competitiveness while the industry is transitioning towards the net-zero goal.

References

Aaltola, J. (2002). Simultaneous synthesis of flexible heat exchanger network. *Applied Thermal Engineering* 22 (8), pp. 907–918.
DOI: 10.1016/S1359-4311(02)00008-X

Agner, R., Ong, B. H. Y., Stampfli, J. A., and Krummenacher, P. (2021). Integration of heat pumps with thermal energy storage in non-continuous processes. In: *Proceedings of the 24 th Conference on Process Integration, Modelling and Optimisation for Energy Saving and Pollution Reduction*, pp. 1–10.

Agner, R., Ong, B. H. Y., Stampfli, J. A., Krummenacher, P., and Wellig, B. (2022). A graphical method for combined heat pump and indirect heat recovery integration. *Energies* 15 (8), p. 2829.
DOI: 10.3390/en15082829

Allen, M. R., Dube, O. P., Solecki, W., Aragón-Durand, F., Cramer, W., Humphreys, S., Kainuma, M., Kala, J., Mahowald, N., Mulugetta, Y., Perez, R., Wairiu, M., and Zickfeld, K. (May 2018). Framing and context. In: *Global Warming of 1.5°C*. Cambridge University Press, pp. 49–92.
DOI: 10.1017/9781009157940.003

Athier, G., Floquet, P., Pibouleau, L., and Domenech, S. (1997). Synthesis of heat-exchanger network by simulated annealing and nlp procedures. *AIChE Journal* 43 (11), pp. 3007–3020.
DOI: 10.1002/aic.690431113

Athier, G., Floquet, P., Pibouleau, L., and Domenech, S. (1998). A mixed method for retrofiting heat-exchanger networks. *Computers and Chemical Engineering* 22, Supplement 1, pp. 505–511.
DOI: 10.1016/S0098-1354(98)00094-5

Bandyopadhyay, S., Saha, S., Maulik, U., and Deb, K. (2008). A simulated annealing-based multiobjective optimization algorithm: amosa. *IEEE Transactions on Evolutionary Computation* 12 (3), pp. 269–283.
DOI: 10.1109/TEVC.2007.900837

Bernoulli, J. (1713). Ars conjectandi, opus posthumum. Thurnisius & Tauber.

Biegler, L. T., Grossmann, I. E., and Westerberg, A. W. (1997). Systematic methods for chemical process design. Prentice Hall. ISBN: 0132723379.

Bochenek, R. and Jezowski, J. M. (2006). Genetic algorithms approach for retrofitting heat exchanger network with standard heat exchangers. *Computer Aided Chemical Engineering* 21, pp. 871–876.
DOI: 10.1016/S1570-7946(06)80155-0

Bogataj, M., Klemeš, J., and Kravanja, Z. (2023). Fifty years of heat integration: pinch analysis and mathematical programming. In: *Handbook of Process Integration (PI)*. Woodhead Publishing, pp. 73–99. ISBN: 9780128238509.
DOI: 10.1016/B978-0-12-823850-9.00020-7

Brillouin, L. (1946). Wave propagation in periodic structures: electric filters and crystal lattices. McGraw–Hill.

Broeck, H. T. (1944). Economic selection of exchanger sizes. *Industrial and Engineering Chemistry* 36 (1), pp. 64–67.
DOI: 10.1021/ie50409a013

Bynum, M. L., Hackebeil, G. A., Hart, W. E., Laird, C. D., Nicholson, B. L., Siirola, J. D., Watson, J.-P., and Woodruff, D. L. (2021). Pyomo - optimization modeling in python. 3rd. Springer Science & Business Media. ISBN: 9783030689278.

Chen, J. J. J. (2019). Logarithmic mean: chen's approximation or explicit solution? *Computers and Chemical Engineering* 120, pp. 1–3.
DOI: 10.1016/j.compchemeng.2018.10.002

Chofreh, A. G., Goni, F. A., Klemeš, J. J., Moosavi, S. M. S., Davoudi, M., and Zeinalnezhad, M. (Apr. 2021). Covid-19 shock: development of strategic management framework for global energy. *Renewable and Sustainable Energy Reviews* 139, p. 110643.
DOI: 10.1016/j.rser.2020.110643

Ciric, A. R. and Floudas, C. A. (1989). A retrofit approach for heat exchanger networks. *Computers and Chemical Engineering* 13 (6), pp. 703–715.
DOI: 10.1016/0098-1354(89)80008-0

Ciric, A. R. and Floudas, C. A. (1990). A mixed integer nonlinear programming model for retrofitting heat-exchanger networks. *Industrial and Engineering Chemistry Research* 29 (2), pp. 239–251.
DOI: 10.1021/ie00098a014

Ciric, A. R. and Floudas, C. A. (1991). Heat exchanger network synthesis without decomposition. *Compurers and Chemical Engineering* 15 (6), pp. 385–396.
DOI: 10.1016/0098-1354(91)87017-4

Clayton, R. W. (1986). Cost reductions on an edible oil refinery identified by a process integration study at van den berghs and jurgens ltd. Energy Efficiency Office R&D, Energy Technology Support Unit (ETSU), Harwell Laboratory, pp. 1–37.

Dantzig, G. B. (1948). Programming in a linear structure.

Dijkstra, E. W. (1959). A note on two problems in connexion with graphs. *Numerische Mathematik* 1, pp. 269–271.

Dolan, W. B., Cummings, P. T., and LeVan, M. D. (1989). Process optimization via simulated annealing: application to network design. *AlChE Journal* 35 (5), pp. 725–736.
DOI: 10.1002/aic.690350504

Euler, L. (1744). Methodus inveniendi lineas curvas maximi minimive proprietate gaudentes, sive solutio problematis isoperimetrici lattissimo sensu accepti: cum exemplis illustrium virorum. Marc-Michel Bousquet.

Euler, L. (1779). De serie lambertina plurismique eius insignibus propretatibus. *Acta Academiae Scientiarum Imperialis Petropolitanae* 6, pp. 29–51.

Floudas, C. A., Ciric, A. R., and Grossmann, I. E. (1986). Automatic synthesis of optimum heat exchanger network configurations. *AIChE Journal* 32 (2), pp. 276–290.
DOI: 10.1002/aic.690320215

Floudas, C. A. and Grossmann, I. E. (1986). Synthesis of flexible heat exchanger networks for multiperiod operation. *Computers and Chemical Engineering* 10 (2), pp. 153–168.
DOI: 10.1016/0098-1354(86)85027-X

Floudas, C. A. (2013). Deterministic global optimization: theroy, methods and applications. Springer Science & Buisness Media. ISBN: 9781475749496.

Floudas, C. A. (1995). Nonlinear and mixed-integer optimization. 1st. Oxford University Press. ISBN: 9780195100563.

Fotsch, P. (2006). Pilotphase Pinch-Methodik 2006/07: Zweifel Pomy-Chips AG. Swiss Federal Office of Energy SFOE, pp. 1–71.

Fourer, R., Gay, D. M., and Kernighan, B. W. (1990). A modeling langugae for mathematical programming. *Management Science* 36 (5), pp. 519–554. DOI: 10.1287/mnsc.36.5.519

Furman, K. C. and Sahinidis, N. V. (2001). Computational complexity of heat exchanger network synthesis. *Computers and Chemical Engineering* 25 (9-10), pp. 1371–1390. DOI: 10.1016/S0098-1354(01)00681-0

Furman, K. C. and Sahinidis, N. V. (2002). A critical review and annotated bibliography for heat exchanger network synthesis in the 20th century. *Industrial and Engineering Chemistry Research* 41 (10), pp. 2335–2370. DOI: 10.1021/ie010389e

Gauss, C. F. (1809). Theoria motus corporum coelestium in sectionibus conicis solem ambientum. Perthes et Besser.

Grossmann, I. E. and Sargent, R. W. H. (1979). Optimum design of multipurpose chemical plants. *Industrial & Engineering Chemistry Process Design and Development* 18 (2), pp. 343–348. DOI: 10.1021/i260070a031

Gundersen, T. (2000). A process integration primer. International Energy Agency, pp. 1–90.

Hawkins, E., Ortega, P., Suckling, E., Schurer, A., Hegerl, G., Jones, P., Joshi, M., Osborn, T. J., Masson-Delmotte, V., Mignot, J., Thorne, P., and Oldenborgh, G. J. V. (Sept. 2017). Estimating changes in global temperature since the preindustrial period. *Bulletin of the American Meteorological Society* 98 (9), pp. 1841–1856. DOI: 10.1175/BAMS-D-16-0007.1

Hohmann, E. C. J. (1971). Optimum networks for heat exchange. PhD thesis. University of Southern California.

Hwa, C. S. (1965). Mathematical formulation and optimization of heat exchanger networks using separable programming. In: *AIChE IChemE Symposium Series 4*, pp. 101–106.

IEA (2022). Co2 emissions in 2022. International Energy Agency.

Isafiade, A. J. (2018). Retrofitting multi-period heat exchanger networks using the reduced superstructure synthesis approach. *Chemical Engineering Transactions* 70, pp. 133–138. DOI: 10.3303/CET1870023

Jiao, J., Ma, Q., and Tseng, M. M. (2003). Towards high value-added products and services: mass customization and beyond. *Technovation* 23 (10), pp. 809–821. DOI: 10.1016/S0166-4972(02)00023-8

Jones, P. S. (1991). Targeting and design of heat exchanger networks under multiple base case operation. MA thesis. University of Manchester Institute of Science and Technology (UMIST).

Kang, L. and Liu, Y. (2014). Retrofit of heat exchanger networks for multiperiod operations by matching heat transfer areas in reverse order. *Industrial and Engineering Chemistry Research* 53 (12), pp. 4792–4804.
DOI: 10.1021/ie4041143

Kang, L. and Liu, Y. (2015). Multi-objective optimization on a heat exchanger network retrofit with a heat pump and analysis of co2 emissions control. *Applied Energy* 154, pp. 696–708.
DOI: 10.1016/j.apenergy.2015.05.050

Kang, L., Liu, Y., and Wu, L. (2016). Synthesis of multi-period heat exchanger networks based on features of sub-period durations. *Energy* 116, pp. 1302–1311.
DOI: 10.1016/j.energy.2016.06.047

Kang, L. and Liu, Y. (2017). A systematic strategy for multi-period heat exchanger network retrofit under multiple practical restrictions. *Chinese Journal of Chemical Engineering* 25 (8), pp. 1043–1051.
DOI: 10.1016/j.cjche.2017.01.002

Karush, W. (1939). Minima of functions of several variables with inequalities as side conditions. MA thesis. University of Chicago.

Kemp, I. C. and Lim, J. S. (2020). Pinch analysis for energy and carbon footprint reduction: user guide to process integration for the efficient use of energy. 3rd. Butterworth-Heinemann, pp. 1–566. ISBN: 9780081025369.

Kemp, I. C. and Deakin, A. W. (1989). The cascade analysis for energy and process integration of batch processes. ii: network design and process scheduling. *Chemical Engineering Research and Design* 67 (5), pp. 510–516.

Krummenacher, P. (2001). Contribution to the heat integration of batch processes (with or without heat storage). PhD thesis. École polytechnique féderale de Lausanne (EPFL).

Kuhn, H. W. and Tucker, A. W. (1951). Nonlinear programming. In: *Proceedings of 2nd Berkeley Symposium on Mathematical Statistics and Probability*, pp. 481–492.

Lagrange, J.-L. (1775). Recherches d'arithmétique. *Nouveaux Mémoires de l'Académie Royale des Sciences et Belles-Lettres de Berlin*.

Lagrange, J.-L. (1797). Théorie des fonctions analytiques. Courcier.

Lambert, J. H. (1758). Observationes variae in mathesin puram. *Acta Helvetica* 3 (1), pp. 128–168.

Langner, C., Svensson, E., and Harvey, S. (2020). A framework for flexible and cost-efficient retrofit measures of heat exchanger networks. *Energies* 13 (6), pp. 1–24.
DOI: 10.3390/en13061472

Levenberg, K. (1944). A method for the solution of certain non-linear problems in least squares. *Quarterly of Applied Mathematics* 2, pp. 164–168.

Lewin, D. R., Wang, H., and Shalev, O. (1998). A generalized method for hen synthesis using stochastic optimization – i. general framework and mer optimal synthesis. *Computers and Chemical Engineering* 22 (10), pp. 1503–1513.
DOI: 10.1016/S0098-1354(98)00220-8

Lewin, D. R. (1998). A generalized method for hen synthesis using stochastic optimization - ii. the synthesis of cost-optimal networks. *Computers and Chemical Engineering* 22 (10), pp. 1387–1405.
DOI: 10.1016/S0098-1354(98)00221-X

Linnhoff, B. and Flower, J. (1978). Synthesis of heat exchanger networks i: systematic generation of energy optimal networks. *AIChE Journal* 24, pp. 633–642.
DOI: 10.1002/aic.690240411

Linnhoff, B. and Hindmarsh, E. (1983). The pinch design method for heat exchanger networks. *Chemical Engineering Science* 38 (5), pp. 745–763.
DOI: 10.1016/0009-2509(83)80185-7

Linnhoff, B., Ashton, G. J., and Obeng, E. D. A. (1988). Process integration of batch processes. In: *IChemE Symposium Series 109*. Vol. 109, pp. 221–237.

Linnhoff, B. (1979). Thermodynamic analysis in the design of process networks. PhD thesis. The University of Leeds.

Lomborg, B. (2020). Welfare in the 21st century: increasing development, reducing inequality, the impact of climate change, and the cost of climate policies. *Technological Forecasting and Social Change* 156, p. 119981.
DOI: 10.1016/j.techfore.2020.119981

Lucas, E. J., Stampfli, J. A., Rast, L. P., Agner, R., and Wellig, B. (2021). Heat pump and thermal energy storage integration in non-continuous processes – an application to the food industry. In: *Proceedings of the 13th IEA Heat Pump Conference*, pp. 1478–1490.

Majozi, T. (2010). Batch chemical process integration. Springer Dordrecht Heidelberg, pp. 1–282. ISBN: 9789048125876.

Marquardt, D. W. (1963). An algorithm for least-squares estinmation of nonlinear parameters. *J. Soc. Indust. Appl. Math* 11 (2), pp. 431–441.
DOI: 10.1137/0111030

Masso, A. H. and Rudd, D. F. (1969). The synthesis of system design – ii. heuristic structuring. *AIChE Journal* 15 (1), pp. 10–17.
DOI: 10.1002/aic.690150108

Metropolis, N., Rosenbluth, A. W., Rosenbluth, M. N., Teller, A. H., and Teller, E. (1953). Equation of state calculations by fast computing machines. *The Journal of Chemical Physics* 21 (6), pp. 1087–1092. ISSN: 00219606.
DOI: 10.1063/1.1699114

Murty, K. G. and Kabadi, S. N. (1987). Some np-complete problems in quadratic and nonlinear programming. *Mathematical Programming* 39, pp. 117–129.

Nelder, J. A. and Mead, R. (1965). A simplex method for function minimization. *Computer Journal* 7 (4), pp. 308–313.
DOI: 10.1093/comjnl/7.4.308

Newton, I. (1711). De analysi per aequationes numero terminorum infinitas. William Jones.

Ochoa-Estopier, L. M., Jobson, M., Chen, L., Rodríguez-Forero, C. A., and Smith, R. (2015). Optimization of heat-integrated crude oil distillation systems. part ii: heat

exchanger network retrofit model. *Industrial and Engineering Chemistry Research* 54 (18), pp. 5001–5017.
DOI: 10.1021/ie503804u

Olsen, D., Abdelouadoud, Y. L., Liem, P., Hoffmann, S., and Wellig, B. (2017). Integration of heat pumps in industrial processes. In: *IEA Heat Pump Conference 12*, pp. 1–12.

Papoulias, S. A. and Grossmann, I. E. (1983). A structural optimization approach in process synthesis – ii: heat recovery networks. *Computers and Chemical Engineering* 7 (6), pp. 707–721.
DOI: 10.1016/0098-1354(83)85023-6

Peters, M. S. and Timmerhaus, K. D. (1991). Plant design and economics for chemical engineers. 4th. McGraw-Hill. ISBN: 0071008713.

Ponton, J. W. and Donaldson, R. A. B. (1974). A fast method for the synthesis of optimal heat exchanger networks. *Chemical Engineering Science* 29 (12), pp. 2375–2377.

Rezaei, E. and Shafiei, S. (2009). Heat exchanger networks retrofit by coupling genetic algorithm with nlp and ilp methods. *Computers and Chemical Engineering* 33 (9), pp. 1451–1459.
DOI: 10.1016/j.compchemeng.2009.03.009

Shenoy, U. V. (1995). Heat exchanger network synthesis: process optimization by energy and resource analysis. Gulf Publishing Company. ISBN: 0881453196.

Smith, R. (2005). Chemical process design and integration. 2nd. John Wiley and Sons, Ltd, p. 712. ISBN: 0471486809.

Soltani, H. and Shafiei, S. (2011). Heat exchanger networks retrofit with considering pressure drop by coupling genetic algorithm with lp (linear programming) and ilp (integer linear programming) methods. *Energy* 36 (5), pp. 2381–2391.
DOI: 10.1016/j.energy.2011.01.017

Sreepathi, B. K. and Rangaiah, G. P. (2014a). Improved heat exchanger network retrofitting using exchanger reassignment strategies and multi-objective optimization. *Energy* 67, pp. 584–594.
DOI: 10.1016/j.energy.2014.01.088

Sreepathi, B. K. and Rangaiah, G. P. (2014b). Review of heat exchanger network retrofitting methodologies and their applications. *Industrial and Engineering Chemistry Research* 53 (28), pp. 11205–11220.
DOI: 10.1021/ie403075c

Sreepathi, B. K. and Rangaiah, G. P. (2015). Retrofitting of heat exchanger networks involving streams with variable heat capacity: application of single and multi-objective optimization. *Applied Thermal Engineering* 75, pp. 677–684.
DOI: 10.1016/j.applthermaleng.2014.09.067

Stampfli, J. A., Lucas, E. J., Olsen, D. G., and Krummenacher, P. (2019a). Batch process integration: management of capacity-limited thermal energy storage by optimization of heat recovery. *Chemical Engineering Transactions* 76, pp. 1027–1032.
DOI: 10.3303/CET1976172

Stampfli, J. A., Atkins, M. J., Olsen, D. G., Walmsley, M. R., and Wellig, B. (2019b). Practical heat pump and storage integration into non-continuous processes: a hybrid

approach utilizing insight based and nonlinear programming techniques. *Energy* 182, pp. 236–253.
DOI: 10.1016/j.energy.2019.05.218

Stampfli, J. A., Olsen, D. G., Wellig, B., and Hofmann, R. (2020a). Heat exchanger network retrofit for processes with multiple operating cases : a metaheuristic approach. *Computer Aided Chemical Engineering* 48, pp. 781–786.
DOI: 10.1016/B978-0-12-823377-1.50131-2

Stampfli, J. A., Lucas, E. J., Ong, B. H. Y., Olsen, D. G., Krummenacher, P., and Wellig, B. (2020b). Optimization of volume-limited thermal energy storage in non-continuous processes. *Energy* 203, p. 117805.
DOI: 10.1016/j.energy.2020.117805

Stampfli, J. A., Ong, B. H. Y., Olsen, D. G., Wellig, B., and Hofmann, R. (2021). A hybrid evolutionary algorithm for heat exchanger network retrofit for processes with multiple operating cases. In: *Proceedings of the 16th Conference on Sustainable Development of Energy, Water and Environment Systems*, p. 116.

Stampfli, J. A., Olsen, D. G., Wellig, B., and Hofmann, R. (2022a). A parallelized hybrid genetic algorithm with differential evolution for heat exchanger network retrofit. *MethodsX* 9, p. 101711.
DOI: 10.1016/j.mex.2022.101711

Stampfli, J. A., Ong, B. H. Y., Olsen, D. G., Wellig, B., and Hofmann, R. (2022b). A hybrid evolutionary algorithm for multi-objective heat exchanger network retrofit for multi-period processes. In: *Proceedings of the 25th Conference on Process Integration, Modelling and Optimisation for Energy Saving and Pollution Reduction*, pp. 1–8.

Stampfli, J. A., Ong, B. H. Y., Olsen, D. G., Wellig, B., and Hofmann, R. (2022c). Applied heat exchanger network retrofit for multi-period processes in industry: a hybrid evolutionary algorithm. *Computers and Chemical Engineering* 161, p. 107771.
DOI: 10.1016/j.compchemeng.2022.107771

Stampfli, J. A., Ong, B. H., Olsen, D. G., Wellig, B., and Hofmann, R. (2023). Multi-objective evolutionary optimization for multi-period heat exchanger network retrofit. *Energy* 281, p. 128175.
DOI: 10.1016/j.energy.2023.128175

Stampfli, J. A. (2021). J-a-st/moc_retrofit_ga_de: v1.0. Zenodo.
DOI: 10.5281/zenodo.4441140

Stampfli, J. A. (2023). J-a-st/moc_retrofit_ga_de: v2.0. Zenodo.
DOI: 10.5281/zenodo.7568479

Talbi, E.-G. (2009). Methaheuristics from design to implementation. John Wiley and Sons Inc, p. 593. ISBN: 9780470278581.

The Federal Council (2021). Switzerland's long-term climate strategy. Schweizerische Eidgenossenschaft, pp. 1–60.

Toimil, D. and Gómez, A. (2017). Review of metaheuristics applied to heat exchanger network design. *International Transactions in Operational Research* 24 (1-2), pp. 7–26.
DOI: 10.1111/itor.12296

Umeda, T., Itoh, J., and Shiroko, K. (1978). Heat exchange system synthesis. *Chemical Engineering Progress* 74, pp. 70–76.

Umeda, T., Harada, T., and Shiroko, K. (1979). A thermodynamic approach to the synthesis of heat integration systems in chemical processes. *Computers and Chemical Enginrenng* 3 (1-4), pp. 273–282.
DOI: 10.1016/0098-1354(79)80046-0

Verheyen, W. and Zhang, N. (2006). Design of flexible heat exchanger network for multi-period operation. *Chemical Engineering Science* 61 (23), pp. 7730–7753.
DOI: 10.1016/j.ces.2006.09.028

Wächter, A. and Biegler, L. (2006). On the implementation of a primal-dual interior-point filter line-search algorithm for large-scale nonlinear programming. *Mathematical Programming* 106, pp. 25–57.
DOI: 10.1007/s10107-004-0559-y

Wellig, B., Agner, R., Ong, B. H. Y., Stampfli, J. A., Olsen, D. G., and Krummenacher, P. (2021). Integration von wärmepumpen und speichern zur effizienzsteigerung nicht-kontinuierlicher prozesse. In: *27. Tagung des BFE-Forschungsprogramms "Wärmepumpen und Kältetechnik"*, pp. 1–14.

Yee, T. F. and Grossmann, I. E. (1990). Simultaneous optimization models for heat integration - ii. heat exchanger network synthesis. *Computers and Chemical Engineering* 14 (10), pp. 1165–1184.
DOI: 10.1016/0098-1354(90)85010-8

Yee, T. F. and Grossmann, I. E. (1991). A screening and optimization approach for the retrofit of heat-exchanger networks. *Industrial and Engineering Chemistry Research* 30 (1), pp. 146–162.
DOI: 10.1021/ie00049a023

Zhu, Z., Piao, S., Myneni, R. B., Huang, M., Zeng, Z., Canadell, J. G., Ciais, P., Sitch, S., Friedlingstein, P., Arneth, A., Cao, C., Cheng, L., Kato, E., Koven, C., Li, Y., Lian, X., Liu, Y., Liu, R., Mao, J., Pan, Y., Peng, S., Peuelas, J., Poulter, B., Pugh, T. A., Stocker, B. D., Viovy, N., Wang, X., Wang, Y., Xiao, Z., Yang, H., Zaehle, S., and Zeng, N. (Aug. 2016). Greening of the earth and its drivers. *Nature Climate Change* 6 (8), pp. 791–795.
DOI: 10.1038/nclimate3004

Zitzler, E., Brockhoff, D., and Thiele, L. (2007). The hypervolume indicator revisited: on the design of pareto-compliant indicators via weighted integration. *Lecture Notes in Computer Science (including subseries Lecture Notes in Artificial Intelligence and Lecture Notes in Bioinformatics)* 4403 LNCS, pp. 862–876. ISSN: 16113349.
DOI: 10.1007/978-3-540-70928-2_64

Publications and Software

This chapter contains all the core publications of this thesis including three journal articles and three conference proceedings as well as the associated developed software packages. Further, publications and software not directly related to the thesis, are included. For all the publications a summary and a CRediT author statement [1] are provided.

[1] According to the Elsevier CRediT author statement: https://www.elsevier.com/authors/policies-and-guidelines/credit-author-statement

Article 1

Heat Exchanger Network Retrofit for Processes with Multiple Operating Cases: a Metaheuristic Approach

published in Computer Aided Chemical Engineering in collaboration with Donald G. Olsen, Beat Wellig, and René Hofmann

The research in this conference article was presented in the form of a talk by Jan A. Stampfli at the 30th European Symposium on Computer Aided Process Engineering, in Milan, Italy. This contribution to the conference introduces the two-stage GA/DE algorithm. Thereby, the focus lays on the algorithmic implementation, the constraint handling, and its application to the crude oil production case study from literature (Jones, 1991). The comparison of the retrofitted design to the existing design shows that the algorithm was able to halve TAC.

My contribution: Conceptualization, Methodology, Software, Validation, Formal analysis, Investigation, Data curation, Writing –original draft, Visualization, Writing –review & editing.

Stampfli, J. A., Olsen, D. G., Wellig, B., and Hofmann, R. (2020a). Heat exchanger network retrofit for processes with multiple operating cases : a metaheuristic approach. Computer Aided Chemical Engineering *48, pp. 781–786.*

DOI: 10.1016/B978-0-12-823377-1.50131-2

PROCEEDINGS OF THE 30th European Symposium on Computer Aided Process Engineering (ESCAPE30), May 24-27, 2020, Milano, Italy

Heat Exchanger Network Retrofit for Processes with Multiple Operating Cases: A Metaheuristic Approach

Jan A. Stampfli,[a,b,*] Donald G. Olsen,[a] Beat Wellig,[a] René Hofmann[b,c]

[a]*Lucerne University of Applied Sciences and Arts, Competence Center Thermal Energy Systems and Process Engineering, Technikumstrasse 21, 6048 Horw, Switzerland*
[b]*Vienna University of Technology, Institute for Energy Systems and Thermodynamics, Getreidemarkt 9/BA, 1060 Vienna, Austria*
[c]*AIT Austrian Institute of Technology GmbH, Center for Energy, Sustainable Thermal Energy Systems, Giefinggasse 2, 1210 Vienna, Austria*
jan.stampfli@hslu.ch

Abstract

An essential method to improve industrial energy efficiency is through the retrofitting of existing heat exchanger networks. This method presents a difficult challenge that is often compounded by the need to handle multiple operating cases behavior as well. Most research has been tackling retrofitting of such processes by deterministic mathematical approaches. With the increase in size and complexity, however, metaheuristic algorithms provide advantages in the search for the global optimum due to their exhaustive exploration of the search space. Hence, this research provides a two-level metaheuristic approach for the retrofit of processes with multiple operating cases. The retrofit problem is decomposed into a master and slave problem, whereby a genetic algorithm optimizes the network topology, and a differential evolution algorithm optimizes continuous variables such as the heat loads of heat exchangers. The developed algorithm has been successfully applied to a case study from literature with results showing that the incorporation of the suggested modifications can halve the total annual cost of the process.

Keywords: heat exchanger network (HEN), retrofit, multiple operating cases, genetic algorithm, differential evolution

1. Introduction

Energy optimization of industrial processes is an essential aspect of the general goal of improving energy efficiency worldwide. A key approach to help reach this goal is to use process integration techniques that focus on the network of heat exchangers (HEXs) used extensively in industry. A large portion of these process integration projects involves the retrofitting of existing industrial plants. However, industrial processes also exhibit multiple operating cases (MOCs) over time such as in the pharmaceutical, chemical, food, and beverage industries. Methods to help optimize MOCs design for the retrofit case are needed. To date, most research has focused on each challenge individually. Both are commonly solved as optimization problems using mathematical programming (MP). The MP approach can also be used to optimize for the retrofit case subject to MOCs behavior. The resulting mixed-integer nonlinear programming (MINLP) problem formulation can be solved using either deterministic or metaheuristic algorithms. Common deterministic methods that address retrofit MOCs design are the reverse matching approach (Kang and

Liu, 2014) and the reduced superstructure synthesis (Isafiade, 2018). However, the search for the global optimum is hampered by the increase in problem size and complexity, in particular by the implementation of mixers (bypassing and admixing). Metaheuristic algorithms are capable of a broader exploration of the search space owing to their ability to escape local optima by generating a random new solution. Aguitoni et al. (2018), in particular, showed the applicability of a metaheuristic for heat exchanger network (HEN) synthesis.

The specific contribution of this research to literature is to use a metaheuristic approach for the retrofit MOCs design. Thereby a two-level optimization approach is used based on a genetic algorithm (GA) for topology optimization and a differential evolution (DE) algorithm for continuous optimization.

2. Methodology

2.1. Heat Exchanger Network Retrofit of Processes with Multiple Operating Cases

In processes with multiple operating cases, the mass flows, specific heat capacity, supply, and target temperatures change over the course of the production period. To ensure a feasible HEN for each operating case, bypassing as well as admixing around key HEXs is often needed. There are basically five distinct operations to modify the existing HEN design which are often combined together: (1) re-piping of a HEX, (2) re-sequencing of a HEX, (3) modifying the area of a HEX, (4) adding bypasses or admixers to a HEX, and (5) incorporating a new HEX into the design. In practice, the cost to modify the area may differ between HEXs. Therefore, it is necessary to have different cost factors for each HEX. Fig. 1 shows the associated superstructure model of the retrofitting of MOCs design. In each enthalpy stage *k*, every hot process stream *i* can be matched with every cold process stream *j* and utility matches are possible (utility optimization). To ensure the energy balance of every process stream is balanced, utilities are also placed at the streams end. Each HEX can be bypassed (shown in stage 2) or admixed (shown in stage 1).

2.2. Metaheuristic approach

The metaheuristic approach uses an evolutionary concept of survival of the fittest. Thereby, a population of solutions (chromosomes) is initialized. In each generation, evolutionary operations (selection, crossover, and mutation) are applied. During the evolution, *n* best solutions are stored in a list, which is updated as soon as a better solution is found. As a result, several near-optimal solutions are determined, which can be compared in terms of practicability for detail engineering. The MINLP problem is decomposed into a master and slave problem (two-level optimization). To solve the master problem (modification of the HEN topology) a GA, and to solve the slave problem (modification of heat loads, bypassing, and admixing of fractions) a DE algorithm is used.

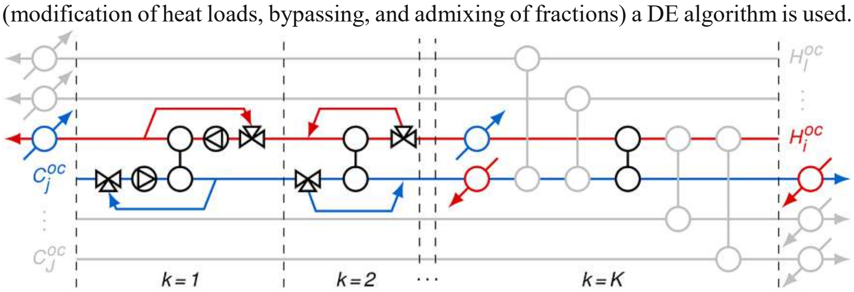

Fig. 1: Superstructure for retrofit of MOCs design (*i*: hot process streams, *j*: cold process streams, *k*: enthalpy stages, *oc*: operating cases)

The algorithm is implemented in Python 3.7 using by using the Distributed Evolutionary Algorithms in Python (DEAP) library (Fortin et al. 2012). Experiments are run on a 2.8 GHz Intel i7 computer with 16 GB RAM.

2.2.1. Master Problem: Topology Optimization by Genetic Algorithm

A GA is used to optimize integer variables of the topology (HEX matches as well as the existence of bypassing or admixing). Thereby, the exchanger address matrix (EAM) represents individual solutions (chromosomes). Among others, Rezaei and Shafiei (2009) have used this approach. For the selection of a new chromosome, tournament selection is performed. Thereby, the fittest among n randomly chosen chromosome is selected. For evaluation of the fitness of each chromosome, the DE algorithm (described in section 2.2.2) solves the slave problem. With the probability of crossover P_C, selected parents mate to generate new children using the one-point crossover operation. By the probability of mutation P_M, genes (vector which, e.g., represents matches of a HEX to a process stream) in a chromosome are mutated based on a uniform distribution.

2.2.2. Slave Problem: Continuous Optimization by Differential Evolution

The DE algorithm initializes individuals consisting of continuous optimization variables (heat loads and split fractions for bypassing and admixing). The standard algorithm is configured as *DE/rand/1/bin*. This means that individuals for mutation are selected randomly, only one difference for perturbation (F_P: perturbation factor) is considered, and a binomial crossover is performed. Further, a stopping criterion is implemented, which terminates the DE evolution if no improvement in fitness after n generations is achieved.

2.2.3. Fitness Function and Constraints

For evaluation of the population, the fitness (maximization) is given by the inverse of the total annual cost (TAC) composed of yearly utility cost and annualized retrofit cost for area extensions, splits, re-piping, bypasses, admixers, and new HEXs:

$$fitness = \frac{1}{TAC} \tag{1}$$

In order to ensure thermodynamically feasible solutions, some constraints must be defined. First, the energy balance for all process streams i, j is fulfilled in each OC by:

$$\sum_k \sum_j \dot{Q}^{oc}_{i,j,k} \leq CP^{oc}_i (T^{oc}_S - T^{oc}_T) \qquad \forall i \tag{2}$$

$$\sum_k \sum_i \dot{Q}^{oc}_{i,j,k} \leq CP^{oc}_j (T^{oc}_T - T^{oc}_S) \qquad \forall j \tag{3}$$

Thereby, the sum of all heat loads matched with the actual process stream $\dot{Q}$ needs to be smaller or equal to the enthalpy flow of the process stream, which is given by the heat capacity flow CP and supply and target temperatures T_S, T_T. Further in each HEX e, feasible heat transfer is ensured by having a temperature difference between hot and cold process stream, which is larger than the minimum allowed temperature difference ΔT_{min}:

$$T^{oc}_{e,i,in} - T^{oc}_{e,j,out} \geq \Delta T_{min} \qquad \forall e \tag{4}$$

$$T^{oc}_{e,i,out} - T^{oc}_{e,j,in} \geq \Delta T_{min} \qquad \forall e\,. \tag{5}$$

Tab. 1: Stream data of OC 1 (4,664 h/y)

#	T_S (°C)	T_T (°C)	CP (kW/K)
H_1	280	50	50
H_2	210	100	70
C_1	30	190	40
C_2	150	280	60

For all streams: h = 0.1 kW/(m^{2}K)

Tab. 2: Stream data of OC 2 (3,336 h/y)

#	T_S (°C)	T_T (°C)	CP (kW/K)
H_1	290	80	60
H_2	180	110	50
C_1	160	300	40
C_2	70	130	60

For all streams: h = 0.1 kW/(m^{2}K)

In order to ensure practicality, the number of splits (corresponds to the sum of *Match*) per stage k and process stream is limited by

$$\sum_j Match_{i,j,k}^{oc} + 1 \leq MaxSplits \qquad \forall i,k,oc \qquad (6)$$

$$\sum_i Match_{i,j,k}^{oc} + 1 \leq MaxSplits \qquad \forall j,k,oc \qquad (7)$$

whereby *MaxSplit* is a user-defined parameter. All constraints are implemented using quadratic penalty functions described by

$$penalty = \Delta(X_{opt} - X_{viol})^2 . \qquad (8)$$

This penalty function is applied to the fitness of each infeasible chromosome. X_{viol} describes the violation of the constraints (distance to the feasible region). X_{opt} describes the optimal value of X_{viol}. The weight Δ ensures that an infeasible solution is always larger than a feasible solution.

3. Illustrative Case Study

The introduced methodology is applied to a case study first introduced by Jones (1991). Stream data for the two operating cases (OCs) are shown in Tab. 1 and Tab. 2. Tab. 3 provides utility and cost data.

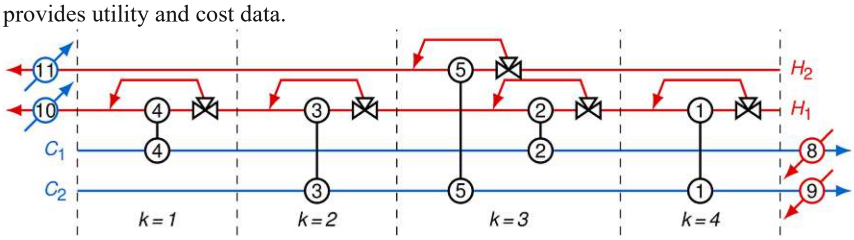

Fig. 2: Existent HEN design

Tab. 3: Optimization parameters

Alg.	Pop. size	P_C	P_M	F_P	Max. iterations
GA	50	0.9	0.1	-	50
DE	100	0.9	-	0.5	200

Tab. 4: Utility and cost data

Utility stream	T_S (°C)	T_T (°C)	h (kW/m²/K)	c_{UT} (CHF/MWh)
Steam (HU)	350	349	6	80
Cooling water (CU)	10	11	2	8

Cost for area extension of existing HEX (CHF): $1{,}474A_{ext}^{0.63}$; Cost for new HEX (CHF): $18{,}920+1{,}474A^{0.63}$; Split, bypassing, admixing, and re-piping cost per changed stream (CHF): 4,000; Plant lifetime: $n = 5$ y; Interest rate: $i = 10\%$

Tab. 4 includes optimization parameters of for the algorithm. Fig. 2 shows the actual MOCs design established by Pinch Analysis. The investment cost of the existent plant is depreciated, and thus resulting in TAC of 2,295,000 CHF/y.

4. Results and Discussion

Depending on the size of the EAM, it can be defined how many new HEX can be integrated during the retrofit process. For the actual case study, it was decided to have the possibility to integrate two new HEX (6 and 7). In Fig. 3, the resulting HENs for the best and the 2nd best solution are shown. Thereby, it can be seen that only existent HEXs are re-piped, re-sequenced, and extended but no new HEXs, splits, bypasses, or admixers are incorporated. A comparison of heat loads and corresponding areas of the retrofitted networks, as well as the existing design, is shown in Tab. 5. The TAC for the best solution amounts to 1,038,000 CHF/y, which is composed of 538,000 CHF investment cost and 896,000 CHF/y yearly operating cost. For the 2nd best solution, TAC accumulates to 1,046,000 CHF/y consisting of 555,000 CHF investment cost and 900,000 CHF/y yearly operating cost. It is imperative to notice that due to the assumption of constant re-piping cost, it cannot be clearly determined which of these solutions would be favorable to implement in practice. Nevertheless, compared to the existing design, a reduction of TAC of around 55 % can be achieved. For both solutions, substantial modifications to the HEN are needed.

Tab. 5: Comparison of heat loads and installed area of existent design with optimized solutions

	Existing design			Best solution			2nd best solution		
HEX	$\dot{Q}_{OC1}$ (kW)	$\dot{Q}_{OC2}$ (kW)	A (m²)	$\dot{Q}_{OC1}$ (kW)	$\dot{Q}_{OC2}$ (kW)	A (m²)	$\dot{Q}_{OC1}$ (kW)	$\dot{Q}_{OC2}$ (kW)	A (m²)
1	3,500	0	1,726	2,803	3,500	1,726	6,400	5,080	4,222
2	0	3,800	1,546	-	-	-	-	-	-
3	0	100	13	-	-	-	-	-	-
4	5,800	0	2,414	6,400	5,070	4,022	4,143	100	7,107
5	1,500	3,500	1,594	4,096	100	7,264	2,741	3,500	1,594
8	600	1,800	708	0	530	708	0	520	708
9	2,800	0	505	901	0	505	916	0	505
10	2,200	8,700	262	1,004	7,430	736	958	7,420	735
11	6,200	0	313	4,897	0	485	4,959	0	490

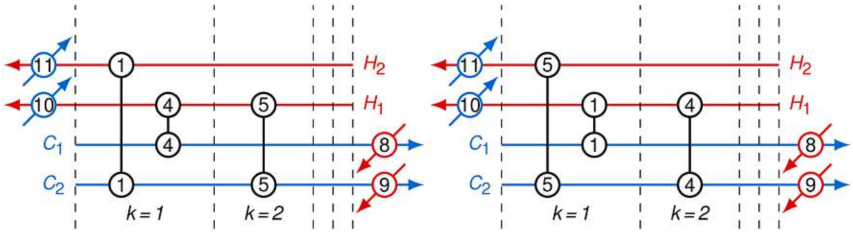

Fig. 3: Optimized HEN design for the best solution (left) and 2nd best solution (right)

5. Conclusions

The presented approach introduces metaheuristic algorithms to the retrofitting of MOCs HEN designs. The method has been successfully applied to the case study. However, due to the assumption of fixed costs for splitting, re-piping, bypassing, and admixing, it cannot be clearly stated which solution is most beneficial to implement in practice. Therefore, these costs should be refined by making them dependent on plant layout, mass flow, and pressure drop. Using an evolutionary-based algorithm for topology optimization leads to substantially different solutions compared to the existing design. It should be investigated whether algorithms based on neighborhood structures (e.g., simulated annealing or variable neighborhood search) would be more appropriate to use. Such algorithms apply retrofit modifications such as re-piping and re-sequencing as neighborhood moves on the existing design.

6. Acknowledgments

This research project is financially supported by the Swiss Innovation Agency Innosuisse and is part of the Swiss Competence Center for Energy Research – Efficiency of Industrial Processes SCCER EIP. Further support is provided by the Lucerne University of Applied Sciences and Arts, Switzerland.

References

A.J. Isafiade, 2018, Retrofitting Multi-Period Heat Exchanger Networks using the Reduced Superstructure Synthesis Approach, Chemical Engineering Transactions, 70, 133-138.

E. Rezaei, S. Shafiei, 2009, Heat exchanger networks retrofit by coupling genetic algorithm with NLP and ILP methods, Computers and Chemical Engineering, 33, 1451-1459.

F.-A. Fortin, F.-M. De Rainville, M.-A. Gardner, M. Parizeau, C. Gagné, 2012, DEAP : Evolutionary algorithms made easy, Journal of Machine Learning Research, 13, 2171-2175.

L. Kang, Y. Liu, 2014, Retrofit of Heat Exchanger Networks for Multiperiod Operations by Matching Heat Transfer Areas in Reverse Order, Industrial & Engineering Chemistry Research, 53(12), 4792-4804.

M.C. Aguitoni, L.V. Pavão, P.H. Siqueira, L. Jiménez, M.A.S.S. Ravagnani, 2018, Heat exchanger network synthesis using genetic algorithm and differential evolution, Computers and Chemical Engineering, 117, 82-96.

P.S. Jones, 1991, Targeting and design for heat exchanger networks under multiple base case operation, PhD Thesis, University of Manchester Institute of Science and Technology, Manchester, United Kingdom of Great Britain and Northern Ireland.

Article 2

Applied Heat Exchanger Network Retrofit for Multi-Period Processes in Industry: a Hybrid Evolutionary Algorithm

published in Computers and Chemical Engineering in collaboration with Benjamin H.Y. Ong, Donald G. Olsen, Beat Wellig, and René Hofmann

This journal article is an invited contribution to the special issue of the 30th European Symposium on Computer Aided Process Engineering of the Computers and Chemical Engineering journal. The work in this article extends the research from Article 1. The HEN model is extended using the Lambert W-function to analytically determine mixer temperatures. Further, the algorithm is able to handle soft streams and streams which are inactive in certain operating cases. Additionally, practical constraints such as extreme temperatures of streams and additional costs for piping are considered in the optimization. For demonstration purposes, the algorithm is applied to the potato chips production case study from the industry (Fotsch, 2006).

My contribution: Conceptualization, Methodology, Software, Validation, Formal analysis, Investigation, Data curation, Writing –original draft, Visualization, Writing –review & editing.

Stampfli, J. A., Ong, B. H. Y., Olsen, D. G., Wellig, B., and Hofmann, R. (2022c). Applied heat exchanger network retrofit for multi-period processes in industry: a hybrid evolutionary algorithm. Computers and Chemical Engineering *161, p. 107771.*

DOI: 10.1016/j.compchemeng.2022.107771

Computers and Chemical Engineering 161 (2022) 107771

Contents lists available at ScienceDirect

Computers and Chemical Engineering

journal homepage: www.elsevier.com/locate/compchemeng

Applied heat exchanger network retrofit for multi-period processes in industry: A hybrid evolutionary algorithm

Jan A. Stampfli[a,b,*], Benjamin H.Y. Ong[a], Donald G. Olsen[a], Beat Wellig[a], René Hofmann[b]

[a] Lucerne University of Applied Sciences and Arts, Competence Center Thermal Energy Systems and Process Engineering, Technikumstrasse 21, Horw 6048, Switzerland
[b] TU-Wien, Institute of Energy Systems and Thermodynamics, Getreidemarkt 9/BA, Vienna 1060, Austria

ARTICLE INFO

Article history:
Received 15 January 2021
Revised 9 February 2022
Accepted 11 March 2022
Available online 14 March 2022

Keywords:
Heat exchanger network (HEN)
Retrofit
Multi-period
Meta-heuristics
Genetic algorithm
Differential evolution
Parallel processing
Lambert W-function

ABSTRACT

In Swiss process industry, process integration is often applied to retrofit existing plants with multi-period operation. Such periods may experience a high degree of variation in temperature or mass flow. Some process streams may not exist in every period or are soft streams. The resulting retrofitted network needs to be able to ensure feasible heat transfer in each period by the integration of mixer configurations to control the temperature. These attributes increase the complexity of the solution space. Hence, this work proposes an evolutionary two-level algorithm for heat exchanger network retrofit. Genetic algorithm is used for topology optimization and a differential evolution algorithm handles the heat loads. The algorithm is extended with practical constraints such as a maximum number of heat exchangers. Explicit mixer temperature calculations are implemented using the Lambert W-function. The algorithm was successfully applied to an industrial case study, reducing its total annual cost by approximately 66%.

1. Introduction

With the growing awareness on the need to mitigate greenhouse gas (GHG) emissions and the inevitable depletion of fossil fuel, the world is transitioning towards more sustainable and energy-efficient alternatives. The current global focus is to optimize energy production and consumption with their associated sustainability and environmental impacts, which provides industry the incentive and necessary policies to improve their processes (Zore et al., 2017). The European Commission established a set of binding measures to help the EU to reach its energy efficiency target by 2030, where EU countries will have to achieve energy savings of at least 0.8% each year for the period of 2021–2030 (European Commission, 2020). To offset the deficit, one of the key steps is to increase energy efficiency (Maus et al., 2020). The Swiss industrial sector is responsible for 18% of total Swiss energy consumption, with more than half used for process heating, contributing 20% to Swiss CO_2 emissions (Kemmler and Spillmann, 2020). Since industry is a major consumer in the Swiss energy system, optimizing heat recovery (HR) is the first crucial step in achieving deep decarbonization. One methodology addressing this challenge is Process Integration, which was developed during the oil crisis in the 1970's. The methodology focused on reducing hot and cold utility consumption to help improve energy efficiency and energy savings. Reducing process heat demand of industrial processing plants is a critical step for emissions reduction, with multiple long-term economic and environmental benefits. These targets can be realized with heat exchanger networks (HEN) (Klemeš, 2013). Most current project improvements are dedicated to retrofitting of existing industrial plants rather than grassroots design. As a result, the focus of this contribution is on HEN retrofit of multi-period processes in industry. The chemical, pharmaceutical, food, and beverage industries cover 45% of the total Swiss energy for process heat demand (Kemmler and Spillmann, 2020). These processes often have multiple periods due to production of multiple products in the same plant as well as seasonal changes in ambient temperatures.

Numerous studies have been carried out to improve the efficiency of HEN design. There are three notable methods to

* Corresponding author at: Lucerne University of Applied Sciences and Arts, Competence Center Thermal Energy Systems and Process Engineering, Technikumstrasse 21, Horw 6048, Switzerland.
E-mail addresses: jan.stampfli@hslu.ch (J.A. Stampfli), benjamin.ong@hslu.ch (B.H.Y. Ong), donald.olsen@hslu.ch (D.G. Olsen), beat.wellig@hslu.ch (B. Wellig), rene.hofmann@tuwien.ac.at (R. Hofmann).

https://doi.org/10.1016/j.compchemeng.2022.107771

Sets

$C = \{0 \ldots j \ldots NC\}$	Set of cold streams
$CH = \{1 \ldots ch \ldots NCH\}$	Set of heat load chromosomes
$CT = \{1 \ldots ct \ldots NCT\}$	Set of topology chromosomes
$E = \{0 \ldots e \ldots NE\}$	Set of heat exchangers
$H = \{0 \ldots i \ldots NH\}$	Set of hot streams
$K = \{0 \ldots k \ldots NK\}$	Set of enthalpy stages
$GH = \{1 \ldots gh \ldots NGH\}$	Set of heat loads generatrions
$GT = \{1 \ldots gt \ldots NGT\}$	Set of topology generatrions
$OP = \{0 \ldots op \ldots NOP\}$	Set of operating periods

Parameter

A	Heat exchanger area (m^2)
C	Cost coefficient (CHF)
CR	Crossover probability (–)
c	Specific cost coefficient (e.g., CHF/m^2)
c_p	Specific heat capacity (kJ/kg K)
f_d	Degression factor (–)
$\dot{H}$	Enthalpy flow (kW)
HoF	Hall of fame list (–)
h	Film heat transfer coefficient (W/(m^2 K))
i_r	Interest rate (–)
$LMTD$	Logarithmic mean temperature difference (K)
MT	Mutation probability (–)
$\dot{m}$	Mass flow (kg/s)
n	Deprecation lifetime (y)
$\dot{Q}$	Heat flow (kW)
T	Temperatures (°C)
TAC	Total annual costs (CHF)
U	Overall heat transfer coefficient (W/(m^2 K))
W	Lambert W-function (–)
w	mass fraction (–)

Greek letters

Δ	Penalty constant (–)
ΔT	Temperature difference (K)
Δt	Time duration (s)
ψ	Temperature difference ratio (–)

Subscripts

a	Annualized
c	Cold side
h	Hot side
in	Inlet
out	Outlet
S	Supply
T	Target

Abbreviations

CU	Cold utility
DE	Differential evolution
GA	Genetic algorithm
HEN	Heat exchanger network
HENR	Heat exchanger network retrofit
HENS	Heat exchanger network synthesis
HEX	Heat exchanger
HR	Heat recovery
HU	Hot utility
MINLP	Mixed-integer nonlinear programming
OP	Operating period

retrofit a HEN (Sreepathi and Rangaiah, 2014): 1) Pinch-based HEN retrofit analysis, 2) Mathematical Programming (MP), and 3) hybrid of graphical-insight based and MP approach. Asante and Zhu (1996) developed Network Pinch retrofit, a two-stage pinching approach that ensures minimal structural changes and capital-energy optimization. Jiang et al. (2014) uses sensitivity analysis to improve HEN energy performance by increasing of HEX area with fixed network structure to improve utility savings. Akpomiemie and Smith (2015) developed a retrofit methodology on the installation of heat transfer enhancement without additional heat transfer area to reduce the implementation time.

Pinch-Analysis (PA) relies on thermodynamic and physical insights of processes to identify the potential energy savings from retrofitting a HEN using graphs (composite curves, grand composite curves). One of the key advantages of this method is the efficient visualization of the problem, which allows stakeholder internal communication and development of practical solutions based on the engineers inputs. There are several developments in the graphical-insight based approach from the recent years. The Retrofit Thermodynamic Diagram (RTD) plots the heat loads and driving forces of the HEN (Lakshmanan and Bañares-Alcántara, 1996), which was later modified to incorporate thermodynamic feasibility representation and minimum allowed temperature difference, known as Shifted RTD (SRTD) (Yong et al., 2014). Yong et al. (2015) later extended the SRTD to include Grid Diagram to accurately visualize the HEN arrangements and key parameters, known as the Shifted Retrofit Thermodynamic Grid Diagram (SRTGD), with the inclusion of maintenance planning by Chin et al. (2020). Wan Alwi and Manan (2010) presented Stream Temperature vs. Enthalpy plots (STEP), a graphical tool that simultaneously carries out targeting and design of HEN, and was further extended to include HEN retrofit by allowing users to simultaneously diagnose and retrofit existing HEN (Lai et al., 2018). Lai et al. (2019) further extends STEP to include heat exchanger (HEX) area versus enthalpy to minimize the overall required HEX area to reduce the payback period. Kamel et al. (2017) presented temperature driving force (TDF) that revamps the graphical approach of Network Pinch (Gadalla, 2015) by structural and non-structural modifications. Bonhivers et al. (2016) links PA and bridge analysis to develop a retrofit tool, energy transfer diagram (ETD), to identify suitable HEN configuration based on the rate of cascaded heat through each existing HEX. Lal et al. (2018) modified the ETD by adding the support of Heat Surplus-Deficit Table for high potential energy savings.

According to Sreepathi and Rangaiah (2014), MP-based methods are generally divided into two optimization methods, stochastic methods or deterministic methods. The focus of the review for MP is only on genetic algorithm (GA) and differential evolution (DE), as this paper develops its method based on those two stochastic algorithms. For more detailed reviews, Sreepathi and Rangaiah (2014) reviewed the different methodologies for retrofits and Toimil and Gómez (2017) reviewed on metaheuristics used for HEN retrofit. The genetic algorithm (GA) is based on the evolution in nature (Holland, 1975). Lewin uses GA to synthesize HENs in a two part series. Lewin et al. (1998) used GA to determine the structure of the HEN and rate the efficiency of the maximum energy recovery units, without resorting to stream splitting. In the second part, Lewin (1998) aimed to obtain a family of cost-optimum HEN where stream splitting was supported.

The optimization of retrofitting of HEN is usually solved with deterministic method, however, due to complex, non-linear, non-convexity of the vast solution space; GA can be applied to solve the problem. Liu et al. (2014) combines GA with deterministic method to solve the mixed-integer nonlinear programming (MINLP) problem of minimizing the cost of newly added HEXs, utilities, and repiping, this is also applied to MINLP problem for retrofitting HEN in crude oil distillation unit (Liu et al., 2016). Björk and Nordman (2005) developed a hybrid optimization method that uses GA and MINLP to solve a large-scale retrofit heat exchanger network problem. GA divides the large retrofit HEN problem into sub-systems and find the optimal structure for each subsystem. This reduces the computational time and effort for a large-scale optimization problem. Rezaei and Shafiei (2009) retrofits HEN by coupling GA with NLP and ILP. GA is used to produce different networks to find the best structural modifications. Genetic algorithms are typically suitable for structural optimization and are able to avoid being trapped in local optima as shown by Bochenek and Jezowski (2006), where they used GA to solve retrofit problem by considering the actual network and potential savings related to reusing exchanger units. Biyanto et al. (2016) developed a genetic algorithm to solve the NLP formulation of a HEN retrofit with an emphasis on the increase and optimization of the overall heat transfer coefficient using heat transfer enhancement. It was found that coiled wire inserts had the greatest improvement out of all examined enhancement devices.

Differential Evolution, first proposed by Storn (1996), Storn and Price (1997), is a population based algorithm designed to optimize continuous variables such as heat loads. To the authors best knowledge, DE has been applied mostly for HEN synthesis instead of retrofit processes. Yerramsetty and Murty (2008) applied DE to HEN synthesis, where the problem is not decomposed like GA but employs a simultaneous approach to optimize the structure of HEN, heat loads of HEXs, split streams, and minimum approach temperature. Zhang and Rangaiah (2013) applied DE to the case study used by Bochenek and Jezowski (2006), and found the solution to be better by preventing the algorithm from being trapped in a local optima and increase computational efficiency. Aguitoni et al. (2018) used both GA and DE, GA optimizes the variable related to topology and DE optimizes the heat loads and stream split fraction, and found that better or equal total annual cost (TAC) solutions were achieved for the six HEN synthesis case studies.

Most of the reviewed case studies focuses on single period operation. However, industrial processes might exhibit multiple periods over time. Methods to help optimize multi-period design for the retrofit case are needed. Jones (1991) mentioned that HEN design for multi-period processes have three fundamental design types, conventional design, re-sequence design, and re-piping design. Kang and Liu (2014) presented a two-step HEN retrofitting approach for multi-period operations to improve the operational flexibility of the HEN. They used a reverse order matching method, which simultaneously adjust the heat transfer area, re-matching stream, and adjusting the heat transfer area to result in the least increase. They further extended the method to minimize the investment costs by using different strategies to match the heat transfer areas (Kang and Liu, 2015). The strategies applied comprise maximum number of substituted HEXs after retrofit, minimum additional heat transfer areas in the retrofitted HEN, and minimum investment cost for retrofit. The results based on these strategies were reported to be better than other literature results and provide greater benefit for a large-scale HEN retrofit problem in practice. Kang and Liu (2017) also presented a systematic strategy to retrofit multi-period HEN using multi-objective optimization with multiple practical restrictions. The optimized objectives are minimizing TAC and total annual CO_2 emission by providing a Pareto front to represent a series of retrofit targets, and the most desirable option to be selected. Isafiade (2018) applied a reduced superstructure synthesis approach to retrofit of HENs for multi-period operations. Langner et al. (2020) proposed a framework that splits the retrofit process into five sub-steps to reduce the complexity of the problem. The framework derives different design configurations through Pinch based approaches and uses MP to efficiently derive flexible and cost-efficient structural feasible designs. Non-deterministic approaches, meta-heuristics are seldom used for multi-period HEN, the above studies mentioned for GA and DE are only applied to a single OP. Pavão et al. (2018) integrated a post-optimization (PO) strategy to their two-level meta-heuristic method based on Simulated Annealing and Rocket Fireworks Optimization (Pavão et al., 2017) to allow the method to handle multi-period HEN optimization. With the PO integrated, the solutions presented achieved lower TAC compared to other methods and significantly improve the results. Wang et al. (2021) carried out bi-level optimization strategy that combines binary particle swarm optimization and an Alopex-based evolutionary algorithm to establish a simultaneous flexible HEN model. The flexibility analysis adjusts the HEX areas if a critical point arises during a non-convex problem.

2. Problem statement

The current EnergieSchweiz program is to promote energy efficiency in Switzerland. In industry, one of the methods to improve energy efficiency of industrial processes is retrofit of existing plants. Multi-period operation is common in the Swiss industry and is thus, the focus of this paper. Feasible heat transfer in each OP can be achieved by integrating mixer into the HEN to increase flexibility. Thereby, two mixer configurations are distinguished: bypasses which modify the outlet temperature and admixers which modify the inlet temperature of the heat exchanger. The heat exchanger network optimization in the retrofit process is part of conceptual design and therefore the following assumptions are made: 1) detailed heat exchanger design is not considered in this step; 2) only counter-current heat transfer is possible; 3) all heat transfer coefficients are considered to be constant; and 4) fouling is neglected. These points are to be investigated in a detail design step after the optimization.

The introduction of mixer configurations into the network demand additional practical constraints. By reducing the mass flow, hazardous temperature levels might be point of concerns (e.g., phase change). Therefore, new constraints are introduced that limit the maximum or minimum temperature for each process stream. In industry, often more practical solutions are preferred over the global optimum solution. Therefore, one of the key challenges is to find a local optima which can be practically implemented instead of the global optimum. In addition to the required constraints, practical considerations such as a limited number of HEXs per split are to be considered.

Furman and Sahinidis (2001), showed that the formulation of MINLP HEN synthesis for single period processes is already $\mathcal{NP}$-hard *in the strong sense*. In addition, due to the initial HEN design in the retrofit problem, the complexity is increased. The additional constraints as well as the additional dimensions for the multi-period operation, with the possibility to integrate bypasses and admixers, increase the complexity of the solution space which might lead to not finding feasible solutions for large-scale problems at all. Accordingly, stochastic rather than deterministic algorithms are utilized.

In a previous work (Stampfli et al., 2020), a two-level genetic algorithm with differential evolution algorithm was introduced and applied to a small case study from literature. In this work, the algorithm is applied to a more complex case study from industry. Therefore, the algorithm needs to be adapted in order to be able to handle soft streams (non-process streams with no fixed target temperature, e.g., waste gas from a boiler which is emitted to the environment), and streams which are not active in every OP. With the aim to increase practicability of the solutions, integration of bypasses and admixer is analyzed in more detail. Hence, the mixing temperature need to be calculated based on the HEX areas. Further constraints such as extreme stream temperatures (e.g. phase change or equipment constraints) at any mixing point need to be considered. Finally, piping can have a large impact on the retrofit design and, therefore, must also be included.

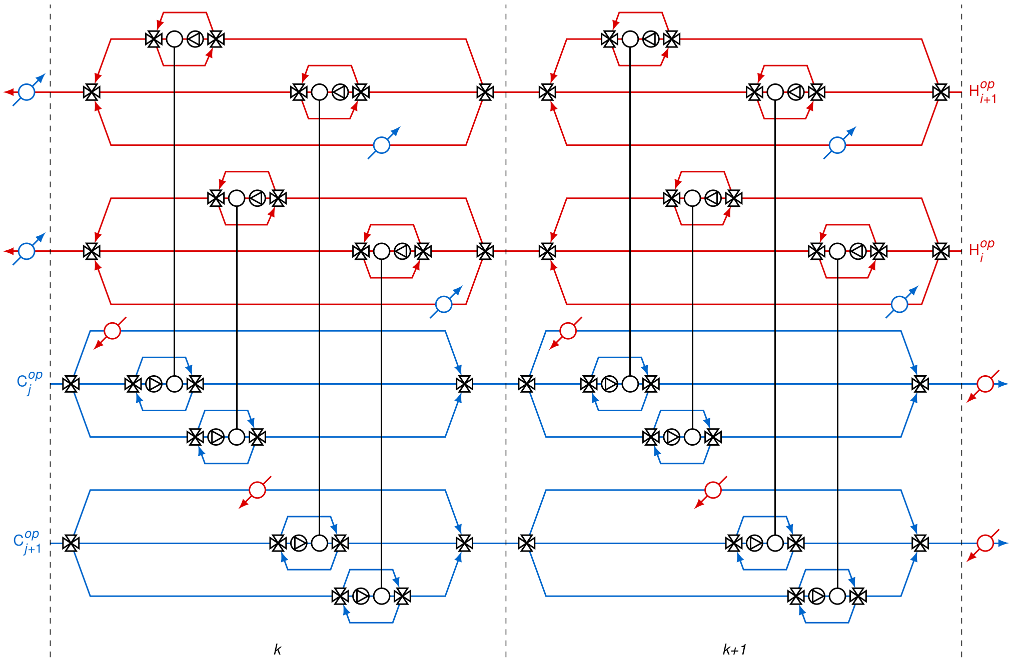

Fig. 1. Superstructure for retrofit of multi-period heat exchanger networks.

3. Heat exchanger network retrofit model

The retrofit model (see Fig. 1) is based on the stage-wise superstructure (SWS) from Yee and Grossmann (1990). In each enthalpy stage k, every hot stream H_i can be connected with every cold stream C_j. At the end of each stream, an utility re-balancing HEX can be placed to fulfill the energy balance. The mixing process in splits is considered to be isothermal. The SWS is extended with (1) an additional dimension of operating periods (OPs) (e.g., Verheyen and Zhang, 2006) with different process requirements (existence of a process stream, mass flows, specific heat capacities, film heat transfer coefficients) and operation parameter (temperatures, heat loads, mixing fractions), (2) possible utility HEX within each enthalpy stage, and (3) possible mixer (bypass and admixer) for each HEX. The latter increases the flexibility of the network and ensures to achieve the process requirements in each OP.

With a bypass, only a fraction of the mass flow passes through the HEX and is heated up, resulting in a change of the outlet temperature. The remaining partial mass flow and the outlet mass flow of the HEX are mixed together non-isothermally. With an admixer to a HEX, a partial fraction of the outlet mass flow of the HEX is non-isothermally mixed to the inlet mass flow of the HEX. Thereby, the mass flow in the HEX is increased resulting in a change of the inlet temperature.

In contrast to heat exchanger network synthesis (HENS), an initial network of the existing process is given for heat exchanger network retrofit (HENR). Therefore, the minimal number of required enthalpy stages k is given by the existing topology. In an enthalpy stage, each stream can only have one heat exchanger in series. Multiple heat exchangers in parallel are possible with splits. During the retrofit process, the following modifications on the network are possible: (1) re-piping of a HEX, (2) re-sequencing of a HEX, (3) adding area to a HEX, (4) adding a new HEX, and (5) removing an existing HEX.

3.1. Heat exchanger network without mixer

Hot streams H_i are cooled down from the last to the first enthalpy stage. With

$$T^{op}_{i,k} = \begin{cases} T^{op}_{i,S} & \text{if } k = NK \\ T^{op}_{i,k+1} - \dfrac{\sum_{e \in E_{i,k}} \dot{Q}^{op}_e}{cp^{op}_i \, \dot{m}^{op}_i} & \text{otherwise} \end{cases} \qquad \forall i, k, op, \tag{1}$$

the temperature of the last enthalpy stage $k = NK$ is equal to the supply temperature of the hot stream. For all other enthalpy stages, the temperatures are given by the enthalpy stage temperatures above and the heat loads within the stages. Thereby, $E_{i,k}$ represents the set of all heat exchangers connected to the hot stream H_i in enthalpy stage k, $\dot{Q}^{op}_e$ the heat load of a heat exchanger e in operating period op, cp^{oc}_i and $\dot{m}^{op}_i$, are the given specific heat capacity and mass flow of the process stream in operating period op. In contrast to this, cold streams C_j are heated up from the first to the last enthalpy stage. Therefore, with

$$T^{op}_{j,k} = \begin{cases} T^{op}_{j,S} & \text{if } k = 0 \\ T^{op}_{j,k-1} + \dfrac{\sum_{e \in E_{j,k}} \dot{Q}^{op}_e}{cp^{op}_j \, \dot{m}^{op}_j} & \text{otherwise} \end{cases} \qquad \forall j, k, oc, \tag{2}$$

the temperature of the first enthalpy stage $k = 0$ is equal to the supply temperature of the cold stream. For all other enthalpy stages, the temperatures are given by the previous enthalpy stage temperature and the heat loads within the stage.

Based on the enthalpy stage temperatures, the required area for each HEX can be determined by

$$A_e = \max_{op \in OP} \left(A^{op}_e \right) = \max_{op \in OP} \left(\frac{\dot{Q}^{op}_e}{U^{op}_e \, \Delta T^{op}_{m,e}} \right) \qquad \forall e \tag{3}$$

whereby, A_e is the minimum required area (largest area of all OPs) of a HEX over all operating periods to ensure feasible heat transfer.

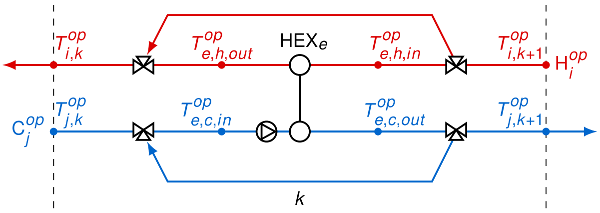

Fig. 2. Heat exchanger temperatures.

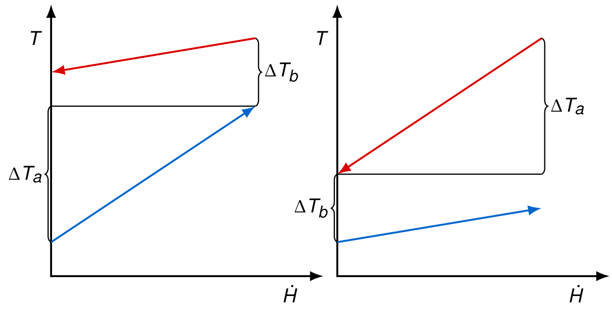

Fig. 3. Relevant temperature differences for mixer type selection.

U^{op}_e is the overall heat transfer coefficient computed by

$$U^{op}_e = \frac{1}{\frac{1}{h^{op}_i} + \frac{1}{h^{op}_j}} \qquad \forall e, op \tag{4}$$

where, h^{op}_i and h^{op}_j are the corresponding film heat transfer coefficients of the connected hot and cold stream. The mean temperature difference in the HEX $\Delta T^{op}_{m,e}$ is determined using the logarithmic mean temperature difference (LMTD) given by

$$\Delta T^{op}_{m,e} = \begin{cases} \dfrac{\Delta T^{op}_{e,1} - \Delta T^{op}_{e,2}}{\ln\left(\dfrac{\Delta T^{op}_{e,1}}{\Delta T^{op}_{e,2}}\right)} & \text{if } \Delta T^{op}_{e,1} \neq \Delta T^{op}_{e,2} \\ \Delta T^{op}_{e,1} & \text{otherwise.} \end{cases} \qquad \forall e, op \tag{5}$$

If the temperature differences on both sides of the heat exchanger are equal, there is no need to calculate the LMTD, as the temperature difference between the streams is constant in the whole HEX. The temperature differences on both sides of the HEX are given by

$$\Delta T^{op}_{e,1} = T^{op}_{i,k} - T^{op}_{j,k} \qquad \forall e, op \tag{6}$$

$$\Delta T^{op}_{e,2} = T^{op}_{i,k+1} - T^{op}_{j,k+1} \qquad \forall e, op \tag{7}$$

under consideration of counter-current operation.

3.2. Heat exchanger and mixer temperatures

Due to the inclusion of a mixer, HEXs can have four different temperatures on each side (see Fig. 2). Thereby, in this work the term mixer configuration, includes the splitter as well as the mixer before and after the HEX. The temperatures upstream and downstream of the mixer configuration are the corresponding enthalpy stage temperature ($T^{op}_{i,k}$, $T^{op}_{j,k}$, $T^{op}_{i,k+1}$, and $T^{op}_{j,k+1}$), which are determined using the energy balance over one enthalpy stage as described in Eqs. (1) and (2) respectively. With a mixer, one of the inlet or outlet temperatures of the HEX ($T^{op}_{e,h,in}$, $T^{op}_{e,h,out}$, $T^{op}_{e,c,in}$, or $T^{op}_{e,c,out}$) can be manipulated. Non-isothermal mixing is considered for the calculation of these manipulated temperatures.

For each operating period in which,

$$A^{op}_e \le A_e \quad \forall e, op \tag{8}$$

the area A^{op}_e is smaller than the minimal required area A_e, a mixer configuration is needed to achieve the targeted enthalpy stage temperatures. In each of these OPs, the mixer configuration is always chosen to be on the stream with the lower heat capacity flow CP (mass flow changes have a higher impact on the temperature (see Fig. 3)). To decide which mixer configuration is selected, their feasible temperature ranges are compared to each other and the mixer configuration with the larger feasible range is selected. For a bypass on the cold stream, the outlet temperature of the stream is increased by reducing the mass flow passing through the HEX. To ensure feasible heat transfer, the outlet temperature of the cold stream cannot be increased beyond the inlet temperature of the hot stream. The feasible range of the temperature change for a bypass ΔT_b is shown in the left diagram in Fig. 3. For an admixer on the cold stream, the inlet temperature is increased by increasing the mass flow passing through the HEX. The inlet temperature of the HEX for the cold stream cannot be increased above it's outlet temperature, therefore, the feasible range for the temperature change of an admixer ΔT_a is, in this case, the change in temperature of the cold stream in the HEX. The right diagram in Fig. 3 shows the same concept for a mixer on the hot stream. An exception to this concepts, are HEXs with zero heat load in an OP connected to an active stream. In this case, the stream needs to be fully bypassed.

In each operating period one mixer temperature ($T^{op}_{e,h,in}$, $T^{op}_{e,h,out}$, $T^{op}_{e,c,in}$, or $T^{op}_{e,c,out}$) has changed and needs to be determined. However, these new mixer temperatures cannot simply be calculated because the LMTD (Eq. (5)) cannot be solved explicit for one of the temperature differences ($\Delta T^{op}_{e,1}$ or $\Delta T^{op}_{e,2}$). These temperature differences are usually determined using an approximation (Chen, 1987). However, Chen (2019) has proposed an explicit solution approach using the Lambert W-function (Lambert, 1758; Euler, 1779). This work uses the explicit solution. The adapted derivation for the application of the Lambert W-function to the logarithmic mean can be found in Appendix A. The Lambert W-function is computed using the Python library Scipy (Virtanen et al., 2020). The procedure for bypass on a hot stream is shown below. Thereby, $T^{op}_{e,h,out} \neq T^{op}_{i,k}$ because of the reduced mass flow through the HEX. To determine the new value of $T^{op}_{e,h,out}$ the procedure is applied as follows:

1. Determine the new LMTD for the given operating period by

$$LMTD^{op} = \frac{\dot{Q}^{op}_e}{U^{op}_e A_e} \tag{9}$$

whereby, A_e is the needed minimum area which ensures feasible heat transfer for every OP.

2. Calculate the temperature difference ratio between the known temperature difference and the LMTD:

$$\psi_2 = \frac{\Delta T^{op}_{e,2}}{LMTD^{op}} \tag{10}$$

3. Thus, the Lambert W-function is ill-defined (the solution can be on two different branches W^-_0 and W_{-1} and the point between those), there are three different cases which need to be considered depending on ψ_2.
   (a) If the LMTD is equal to the known temperature difference ($LMTD^{op} = \Delta T^{op}_{e,2}$; $\psi_2 = 1$), the temperature difference is constant in the HEX. In this case the unknown temperature

difference is given by:

$$\Delta T^{op}_{e,1} = \Delta T^{op}_{e,2} \tag{11}$$

(b) If the LMTD is smaller than the known temperature difference ($LMTD^{op} < \Delta T^{op}_{e,2}$; $\psi_2 > 1$), the solution is on branch W_0^-:

$$\psi_1 = \frac{-W(-\psi_2\, e^{-\psi_2}, W_0^-)}{\psi_2} \tag{12}$$

$$\Delta T^{op}_{e,1} = \psi_1\, \Delta T^{op}_{e,2} \tag{13}$$

(c) If the LMTD is larger then the known temperature difference ($LMTD^{op} > \Delta T^{op}_{e,2}$; $\psi_2 < 1$) the solution is on branch W_{-1}:

$$\psi_1 = \frac{-W(-\psi_2\, e^{-\psi_2}, W_{-1})}{\psi_2} \tag{14}$$

$$\Delta T^{op}_{e,1} = \psi_1\, \Delta T^{op}_{e,2} \tag{15}$$

4. The new mixer temperature is determined by replacing $T^{op}_{i,k}$ with $T^{op}_{e,h,out}$ in Eq. (6):

$$T^{op}_{e,h,out} = T^{op}_{j,k} + \Delta T^{op}_{e,1} \tag{16}$$

3.3. Total annual cost

Total annual cost of the HEN is given by

$$TAC = \frac{i_r\,(1+i_r)^n}{(1+i_r)^n - 1}\, C_{cap} + C_{op,a}. \tag{17}$$

whereby, i_r is the interest rate and n the depreciation period. The capital costs C_{cap} are given by

$$C_{cap} = \sum_e \left(C_{HEX,e} + C_{mix,e} + C_{split,e} + C_{move,e} + C_{match,e}\right). \tag{18}$$

The HEX costs $C_{HEX,e}$ are given by

$$C_{HEX,e} = C_{0,e} + c_{A,e}\,(A_e - A_{e,init})^{f_{d,e}} \tag{19}$$

whereby, $C_{0,e}$ are the base costs, $c_{A,e}$ the specific costs per area, and $f_{d,e}$ the degression factor which decreases cost per area as area increases for a particular HEX. If an existing HEX is removed, the costs are given by

$$C_{HEX,e} = C_{0,e} + c_{R,e}\, A^{f_{d,e}}_{e,init} \tag{20}$$

whereby, $c_{R,e}$ is a specific removal cost per area of the HEX. Additional mixer costs $C_{mix,e}$, and split costs $C_{split,e}$ are fixed costs independent from the area. However, the cost for adding and removing can be different. Further costs for re-piping and re-sequencing $C_{move,e}$ are also constant coefficients per HEX. Each of these cost coefficients can be adapted for every HEX separately. Additional match costs $C_{match,e}$ are considered for HEX that are far apart. Due to the fact, that these costs are highly plant layout dependent (e.g. additional drilling), no equation is provided here. The cost for each match is a constant user input value. The annual operating costs $C_{op,a}$ are given by

$$C_{op,a} = \sum_{op \in OP} \left(c_{HU} \left(\sum_{e \in E_{HU}} \dot{Q}^{op}_e\, \Delta t^{op} \right) + c_{CU} \left(\sum_{e \in E_{CU}} \dot{Q}^{op}_e\, \Delta t^{op} \right) \right) \tag{21}$$

whereby, c_{HU} and c_{CU} are specific utility cost per energy, Δt^{op} the operating period duration. E_{HU} and E_{CU} are the sets of hot and cold utility HEXs.

4. Evolutionary optimization approach

The model formulated in Section 3 is a MINLP formulation which is at least $\mathcal{NP}$-hard *in the strong sense*. Therefore, a stochastic optimization algorithm with two levels is used (Stampfli et al., 2022). The algorithm is developed in Python and available under an open source license (Stampfli, 2021). The algorithm is based on evolutionary concepts using a GA for the topology optimization (discrete variables) on the top level and on the sub level a DE for the optimization of the heat loads. In Fig. 4, an overview of the algorithm is provided. The constraints used in both algorithms are described in Section 4.1. The procedure is as follows. First, a random population of topologies is initialized and checked for feasibility. Thereby, the topology is checked for exceeding the allowed number of HEXs in a split as well as for connections between utility streams. These constraints are evaluated previously in order to reduce unnecessary computation of infeasible solutions. Instead of applying the DE for heat load optimization and the evaluation using the HEN model, a penalty function, which results always in higher TAC than the initial solution, is applied to compute the objective.

In a next step, all feasible solutions are distributed to the available CPU cores, and for each topology, a random population of heat loads is initialized. Thereby, the maximal and minimal possible heat load of each heat exchanger is constrained by a stream dependent on the maximal heat load and a user defined minimum heat load. Next, all heat load populations are evaluated and checked for feasibility. Thereby, the objective is the TAC as described in Section 3.3. The constraints for the DE evaluation are the energy balances of each process stream in every OP and positive temperature differences for each HEX. Further, mixer temperatures, cannot exceed or fall below stream specific extreme temperatures (e.g., phase change or equipment constraints). Costs for infeasible solutions are evaluated with another penalty function. In the DE, the three evolutionary operators' mutation, crossover, and selection are performed to optimize the heat loads. The termination criteria for the DE are a maximal number of generations and a maximal number of generations without improvement. After the DE, the best solutions are stored in a Hall of Fame list, which is always updated as soon as a better solution is found. As long as the termination criterion of a maximal number of topology generations is not fulfilled, the evolutionary operators (selection, crossover, and mutation) are executed, and new modified topologies are evaluated by checking for feasibility and optimizing the heat loads with the DE.

4.1. Constraints

In order to provide feasible and practical solutions the use of some constraints is essential. To reduce the search space, the connection between utility streams is forbidden. The user has to set the maximal number of total possible HEXs. Splits in a HEN increase the complexity of the network and the controllability of the system. Therefore, an additional constraint limiting the number of possible HEX in a split is provided for the user to decide on the desired complexity of the system:

$$\sum \#E_{i,k} \leq \#E_{\max} \qquad \forall i, k \tag{22}$$

$$\sum \#E_{j,k} \leq \#E_{\max} \qquad \forall j, k, \tag{23}$$

whereby $\#E_{i,k}$, $\#E_{j,k}$ are cardinalities of the sets of HEXs on hot i or cold j stream in the enthalpy stage k. $\#E_{\max}$ is a user defined variable and represents the maximal possible number of HEX in a

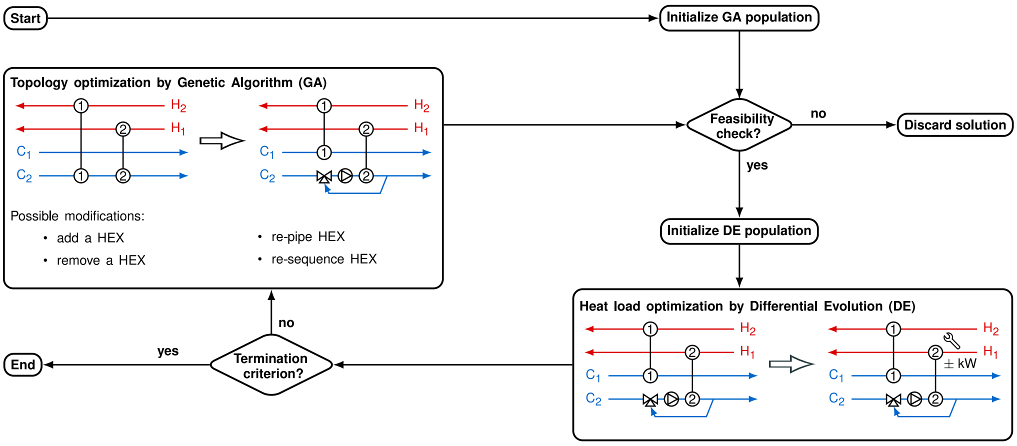

Fig. 4. Overview of the evolutionary algorithm.

split. The heat load of each HEX is limited to

$$\dot{Q}_{\min} \leq \dot{Q}_e^{op} \leq \dot{Q}_{e,max}^{op} \qquad \forall e, op \tag{24}$$

whereby, $\dot{Q}_{\min}$ is a user defined variable and $\dot{Q}_{e,max}$ is given by

$$\dot{Q}_{e,max}^{op} = \min\left(\Delta\dot{H}_i^{op}, \Delta\dot{H}_j^{op}\right) \qquad \forall e, op \tag{25}$$

whereby the enthalpy flows of the process streams are given by

$$\Delta\dot{H}_i^{op} = c_{p,i}^{op}\,\dot{m}_i^{op}\left(T_{i,S}^{op} - T_{i,T}^{op}\right) \qquad \forall i, op \tag{26}$$

$$\Delta\dot{H}_j^{op} = c_{p,j}^{op}\,\dot{m}_j^{op}\left(T_{j,T}^{op} - T_{j,S}^{op}\right) \qquad \forall j, op. \tag{27}$$

Non-negative re-balancing utilities at the end of the streams is ensured by the energy balance given by

$$\Delta\dot{H}_i^{op} - \sum_{\forall e \in E_i} \dot{Q}_e^{op} = \dot{Q}_{CU}^{op} \geq 0 \qquad \forall i, op \tag{28}$$

$$\Delta\dot{H}_j^{op} - \sum_{\forall e \in E_j} \dot{Q}_e^{op} = \dot{Q}_{HU}^{op} \geq 0 \qquad \forall j, op. \tag{29}$$

whereby, E_i and E_j are the sets of all HEXs on the hot i or cold j stream. In order to ensure feasible heat transfer in each HEX, the temperatures on both sides of the HEX need to be positive which is given by

$$T_{e,h,in}^{op} - T_{e,c,out}^{op} \geq \Delta T_{\min} \qquad \forall e, op \tag{30}$$

$$T_{e,h,out}^{op} - T_{e,c,in}^{op} \geq \Delta T_{\min} \qquad \forall e, op. \tag{31}$$

The minimal temperature difference $\Delta T_{\min}$ is a user defined variable. If there is a mixer additional temperature constraints need to be considered. For admixers a positive temperature difference within the stream needs to be ensured for hot streams by

$$T_{e,h,in}^{op} - T_{e,h,out}^{op} > 0 \qquad \forall e, op \tag{32}$$

and for cold streams by

$$T_{e,c,out}^{op} - T_{e,c,in}^{op} > 0 \qquad \forall e, op. \tag{33}$$

For bypasses, additional stream specific extreme temperatures, which cannot be exceeded, need to be considered, given by

$$T_{e,h,out}^{op} - T_{i,extr} > 0 \qquad \forall e, op \tag{34}$$

$$T_{j,extr} - T_{e,h,out}^{op} > 0 \qquad \forall e, op. \tag{35}$$

For evolutionary algorithms there are various constraint handling techniques such as penalizing or decoding strategy (Talbi, 2009). In this case, constraints on topology modifications (Eqs. (22) and (23)) are based on the penalizing strategy. The distance to the feasible solution is used to guide the algorithm to the feasible region. This is achieved by a penalty function which replaces the objective if the solution is infeasible. The quadratic penalty function

$$h = \Delta + \left(x_{feas} - x\right)^2 \tag{36}$$

is used. The value Δ is a penalty constants which ensure that every infeasible solution is more expensive than the worst feasible solution. The distance to the feasible solution $\left(x_{feas} - x\right)$ is squared, since the optimum of a quadratic function is easy to find. For constraining the heat loads (Eq. (24)) the decoding strategy is used. This means, that the algorithm cannot create solutions in the feasible region. This is achieved only by allowing to select a random value between $\dot{Q}_{\min}$ and $\dot{Q}_{e,\max}^{op}$. Equations (28) to (31) are constraints which are often violated. Therefore, the penalizing strategy is applied.

5. Industrial case study - potato chips production

The developed algorithm is applied to a straightforward and realistic industrial case study to guide the readers application of the optimization. A potato chips production plant from the Zweifel Pomy-Chips AG (ZPC) is analyzed (Fotsch, 2006). ZPC is a Swiss food company, producing snacks such as potato chips. The frying process (fritter line 1) for the potato chips has a heating demand of around 64% of their total heating demand.

5.1. Process description

The fritter line 1 (see Fig. 5), is used to fry two varieties of potato chips: (1) Regular chip (oil mass fraction $w_{oil} = 35\%$; 4'410 h/y) and (2) cractive chips (oil mass fraction $w_{oil} = 25\%$; 2'610 h/y). The HEN needs to be flexible to cover both OPs. The core operation of the process is the frying of the raw chips. The main heating demand is to maintain a constant temperature of the frying-oil. Therefore, a separate utility system consisting of a natural gas boiler is installed. Hence, this match is considered to be fixed and not a process requirement. With the fried chips, a fraction of the frying-oil is removed. Therefore, a make-up-oil feed is

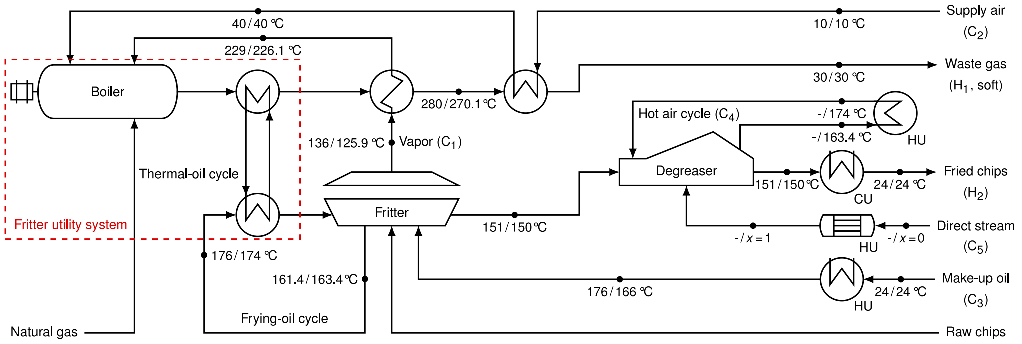

Fig. 5. Flow chart of the Fritter-line 1 plant for chips production at Zweifel. Stream temperatures correspond to the two OPs: regular chips / cractive chips.

needed which is pre-heated by hot utility to the frying temperature (C_3). The vapor (C_1) of the fritter is used as additional fuel for the boiler. In order to reduce the natural gas demand, the boiler waste gas (H_1) is used to heat the fritter vapor (C_1) and the boiler supply air (C_2). After frying, the chips are cooled down by cold utility to room temperature (H_2). For the production of the cractive chips, the degreaser is in operation to reduce the oil mass fraction of the fried chips. Hot air (C_4) and direct steam (C_5) are used to reduce the oil content. The heating of the air, as well as the evaporation of the direct steam is covered by hot utility. In the cractive chips production, the frying-oil temperature is reduced from 176 °C to 166 °C. Due to this, most temperatures of the cractive chips production are lower as in the regular chips production. The waste gas stream (H_1) from the natural gas boiler is a soft stream. After the heat recovery (vapor heating and boiler supply air heating), the waste gas can be optionally cooled down to 30 °C.

In Appendix B, the corresponding process requirements of the fritter line 1 for both OPs are shown in Table B.3. The utility data is shown in Table B.4 and the equipment modification cost is shown in Table B.5. Lang factors of 1.1 and 3.0 are assumed for the removal of existent and the installation of new equipment, respectively (Lang, 1948). Table B.6 shows the match cost between the streams. The existing HEN is shown in Fig. 6.

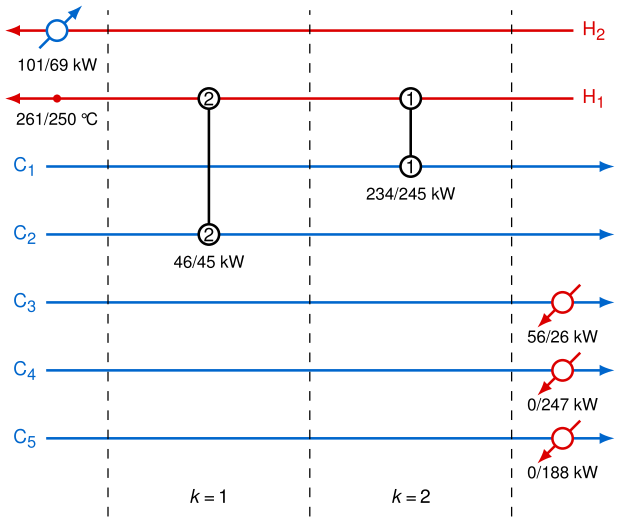

Fig. 6. Initial HEN design with two process internal HEXs. Heat loads are given below each HEX corresponding to the two OPs: regular chips / cractive chips. The outlet temperature of the soft stream H_1 is given as well.

5.2. Algorithm configuration

For the GA, a population of $NCT = 100$ chromosomes is initialized. During the tournament selection, the best of $NT = 5$ chromosomes is chosen. To monitor the best solutions, the $HoF = 10$ best solutions are stored in the Hall of Fame list. Crossover is performed with a probability of $CR = 90\%$ and mutation is performed with a probability of $MT = 10\%$. For the GA, $NGT = 50$ are performed before termination. For each feasible GA chromosome, a DE population of $NCH = 200$ chromosomes is initialized. With a probability of $CR = 90\%$ crossover is performed. The perturbation factor is set to $F_P = 0.5$. The DE is terminated after $NGH = 100$ generations or $NGHOP = 5$ generations without improvement.

The algorithm was executed on a Linux based server with 256 GB RAM, 128 threads distributed over 64 CPU cores. Thereby, the feasible GA chromosomes are distributed to all threads to run the DE and evaluate the solution.

6. Results

To evaluate the case study, the manual case study parameters where chosen as follows: minimal temperature difference $\Delta T_{min} = 2$ K, minimal heat load $\dot{Q}_{min} = 10$ kW, cost penalty $\Delta = 500{,}000$ CHF/y. First, in Section 6.1 the best found solution is analyzed by its comparison to the initial design. Thereby, the topology modifications, the heat load, area changes, and the resulting cost are analyzed.

Section 6.2, analyzes the performance of the algorithm as well as its sensitivity depending on the number of possible HEXs, enthalpy stages, and allowed HEXs per split.

6.1. Best found solution

The topology of the best found solution is shown in Fig. 7, whereby it cannot be guaranteed that this is the global optimum but rather a local optimum. The number of possible HEXs within the process was set to $NE = 7$, the number of enthalpy stages to $NK = 3$, and the number of possible HEX within one split to $\#E_{max} = 2$. The retrofitted design resulted in one HEX being removed (HEX 2) and six new are being added (HEX 3–6). The topology of HEX 1 is not modified (no re-piping, re-sequencing with only one existing HEX is not possible). The new HEX, number 5, is directly connected to hot utility. All the other HEXs require a mixer to ensure feasible heat transfer in each OP. The admixer for HEX 1 and 4 have a very low mixer fraction. Such admixers are unlikely to be implemented and the heat balance is rather fulfilled

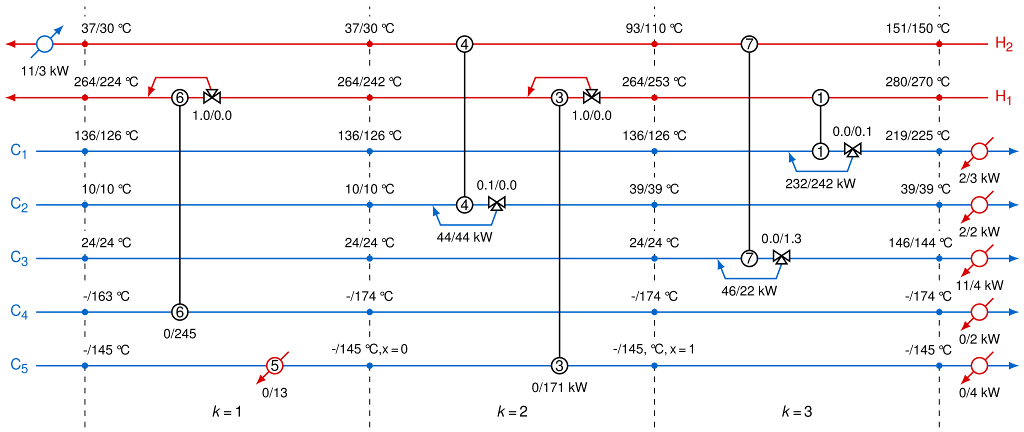

Fig. 7. Best found HEN design with six process internal HEXs. Heat loads are given below each HEX corresponding to the two OPs: regular chips / cractive chips. The mixing fractions for each mixer as well as the outlet temperature of the soft stream H_1 are shown. Stream C_5 is a steam evaporation (x is the vapor fraction).

Table 1
Comparison of heat loads and areas between the best found solution and the initial solution.

HEX	Initial design			Best found design		
	$\dot{Q}_e^1$ kW	$\dot{Q}_e^2$ kW	A_e m^2	$\dot{Q}_e^1$ kW	$\dot{Q}_e^2$ kW	A_e m^2
Process HEX						
1	234	245	16.0	232	242	15.2
2	46	45	2.5	–	–	–
3	–	–	–	0	171	8.3
4	–	–	–	44	44	5.7
5	–	–	–	0	13	0.4
6	–	–	–	0	245	19.1
7	–	–	–	46	22	10.3
Balance utility HEX*						
CU_1	–	–	–	–	–	–
CU_2	101	69	5.6	11	3	1.4
HU_1	–	–	–	2	3	0.1
HU_2	–	–	–	2	2	0.1
HU_3	56	26	0.8	11	4	0.2
HU_4	0	247	4.8	0	2	0.1
HU_5	0	188	0.5	0	4	0.1

Balance utility HEX number is corresponding to the connected process stream (e.g., CU_1 at the end of H_1).

by utility compensation. HEX 3 and HEX 6 need to have a bypass because they are connected to cold streams which are only active in one OP.

By comparing the topology to the initial design (see Fig. 6), it can be seen that in the new design, every stream (except soft stream H_1) is in need of a balancing utility HEXs. However, the heat loads of all utility HEXs are small, or even negligible. Furthermore, more waste heat from the soft stream is recovered. In the initial design 280 kW in OP1 and 290 kW in OP2 are reused, resulting in a total of 1990 MWh/y. In the retrofitted design, 232 kW in OP1 and 658 kW in OP2 are reused, resulting in a total of 2740 MWh/y. As a result, the outlet temperature is for OP1 slightly increased from 261 °C to 264 °C and for OP2 decreased from 250 °C to 224 °C.

The changes in heat loads and the resulting area are given in Table 1. HEX 1 is the only reused HEX. The area does not need to be extended. The heat loads of the balance utility HEXs are reduced significantly by increasing the heat loads of the process internal HEX. Also HEX 5, which is connected to hot utility, is rather small compared to the other process internal HEXs. Therefore, it can be said that the HR of the process is exploited quite well. The two new balance utility HEX HU_1 and HU_2 are rather small (heat load of 2 kW to 3 kW). By a manual post-optimization, analyzing loops and paths within the network, such HEXs are likely to be avoided. E.g., by reducing the outlet temperature of the waste gas (H_1) and the utility consumption at the end of the chips cooling (H_2), HEX HU_1 and HEX HU_2 are likely to be redundant.

For the comparison of TACs, it is assumed that the investment costs of the initial design are already depreciated (C_{Cap} = 0; reducing the TAC to the annual operating cost: TAC = $C_{Op,a}$). The HU demand is 1451 MWh/y and the CU demand 623 MWh/y. This results in annual operating costs of $C_{Op,a}$ = TAC = 141,080 CHF/y. By investing C_{cap} = 273,495 CHF, respectively $C_{cap,a}$ = 35,419 CHF/y with interest rate of i_r 5% over a depreciation lifetime of n = 10 y, HU and CU demand can be significantly reduced to 132 MWh/y and 55 MWh/y. This results in annual operating costs of $C_{Op,a}$ = 12,780 CHF/y, reducing TAC by around 66% to 48,198 CHF/y. Such result is quite common for existing plants in industry which were not optimized for heat recovery. HR in such plants is often limited to pre-heating supply air with waste gas.

6.2. Performance and sensitivity analysis

Figure 8 shows the evolution of the previously discussed best found solution. The diagram shows the lowest TAC for each topology generation (comparing all TAC of the current population).

TAC is observed falling sharply initially, although stagnates over time. After around 50 topology generations, no improvement is noted. The convergence is highly dependent on parameters such as the number of possible HEX *NE*, the number of enthalpy stages *NK*, and the number of allowed HEX per split $\#E_{\max}$. Therefore, in Table 2, the results of the sensitivity analysis on these parameters are shown. The experiments where performed under the Ockham's Razor principle, *plurality should not be posited without necessity*", meaning to keep the model as simple as necessary and not as accurate as possible. Hence, only reasonable parameter values are chosen to be investigated.

In the first experiment, the number of possible HEX *NE* is increased, starting with the two existing ones. It can be seen that the *TAC* are nearly similar to the initial design, meaning there is no room for improvement without adding additional HEX. By increasing *NE*, *TAC* can be reduced to a certain amount. However, the

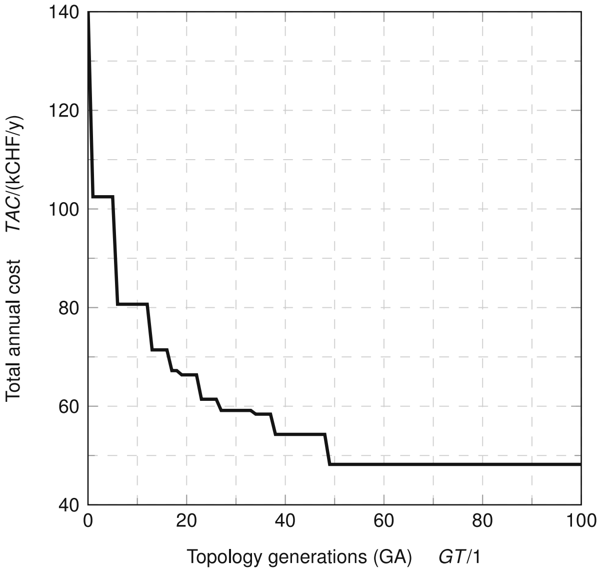

Fig. 8. Convergence of the best found solution ($NE = 7$, $NK = 3$, $\#E_{max} = 2$).

Table 2
Comparison of heat loads and areas between the best found solution and the initial solution.

Experiment	Parameter			Results	
	NE –	NK –	$\#E_{max}$ –	TAC CHF/y	Δt s
Amount of possible HEX					
1	2	2	2	140,867	18,922
2	3	2	2	108,648	26,195
3	4	2	2	85,287	24,787
4	5	2	2	75,281	26,573
5	6	2	2	68,276	27,030
6	7	2	2	62,280	25,852
7	8	2	2	71,322	28,141
Number of enthalpy stages					
8	7	3	2	48,198	27,207
9	7	4	2	62,982	27,621
10	7	5	2	60,380	29,842
11	7	6	2	55,450	30,683
Number of enthalpy stages (splits with three HEX possible)					
12	7	2	3	63,305	29,628
13	7	3	3	65,967	27,812
14	7	4	3	59,141	28,915
15	7	5	3	57,357	30,481
16	7	6	3	63,231	30,362

reduction stagnates after five to six HEX. As expected, the computation time increases with increasing number of HEX due to the increase of optimization parameters.

For the next experiment, the number of enthalpy stages NK is increased (additional empty enthalpy stages with no existing heat exchanger matches were added to the initial design). Thereby, $NE = 7$ is the best solution found solution in this configuration. By increasing the NK, a slight increase in TAC, as well as in computation time is observed, with its best solution at $NK = 3$. The same experiment was performed but with an increase in the maximal possible HEX number in a split to $\#E_{max} = 3$. The results are quite similar to $\#E_{max} = 2$, however the computation time is increased by 5 to 10%. The results of these experiments are to be taken with caution, as it is influenced by the randomness of the algorithm. However, the results are in a reasonable region.

Computation time is dependent on hardware and software. python was used for the software development which is an interpreted language. However, computation times could be improved by using a compiled language such as C++.

7. Conclusions

In this work, a two-level GA/DE algorithm for multi-period heat exchanger network retrofit was developed. For its application in industry, practical constraints are incorporated. The algorithm must handle soft streams, as well as streams which are only active in certain operating periods. Further practical constraints on the mixer temperatures to omit extreme temperatures (e.g.,phase change or equipment constraints), or a maximum number of possible HEX in a split are implemented. In order to calculate the mixer temperature an explicit approach using the Lambert W-function is implemented. Piping usually has a significant impact on retrofit investment costs. Therefore, additional match costs are considered in the optimization.

The algorithm was successfully applied to an industrial case study, a frying process of two different potato chip variants. Thereby its application on a process with soft streams and partially existing streams is demonstrated. To achieve the retrofitted design, one of the existing heat exchangers is reused, one is removed, and six new heat exchangers are incorporated. The heat loads of the utility heat exchangers is reduced significantly resulting in a reduction of approximately 66% in its total annual cost. By performing a sensitivity analysis on the constraint parameters, it was found that the number of possible heat exchangers has the highest influence on reducing cost. An optimum in the total annual cost was found to require 7 possible heat exchangers. Increasing the number of enthalpy stages or increasing the number of possible heat exchangers within one split had a minor influence on the resulting cost. This suggests that the number of possible heat exchangers is the most important parameter for the optimization and has to be chosen carefully. By increasing the constraint parameters, the number of decision variables increases, as well resulting in higher computation times.

A high number of modifications is needed to get from the existing to the retrofitted design. Therefore, future work should investigate methods to limit the number of modifications on the network to give more flexibility to the user. A promising approach would be to switch to a simulated annealing algorithm for the topology optimization.

Declaration of Competing Interest

The authors declare that they have no known competing financial interests or personal relationships that could have appeared to influence the work reported in this paper.

CRediT authorship contribution statement

Jan A. Stampfli: Conceptualization, Methodology, Software, Validation, Formal analysis, Investigation, Data curation, Writing – original draft, Visualization, Writing – review & editing. **Benjamin H.Y. Ong:** Writing – original draft, Writing – review & editing. **Donald G. Olsen:** Conceptualization, Data curation, Writing – review & editing, Supervision. **Beat Wellig:** Writing – review & editing, Supervision, Funding acquisition. **René Hofmann:** Resources, Writing – review & editing, Supervision.

Acknowledgments

This research project is financially supported by the Swiss Innovation Agency Innosuisse and is part of the Swiss Competence Center for Energy Research – Efficiency of Industrial Processes SCCER EIP. Further financial support is provided by the Lucerne University of Applied Sciences and Arts, Switzerland. This research is part of a collaboration between the Lucerne University of Applied Sciences and Arts and TU-Wien.

Appendix A. Application of the Lambert W-function to the logarithmic mean

The derivation for the application of the Lambert W-function, by Chen (2019) is slightly modified and updated to the here used variables below. The Lambert W-function is evaluated using Scipy Virtanen et al. (2020).

$$LMTD^{oc} = \frac{\Delta T^{oc}_{e,1} - \Delta T^{oc}_{e,2}}{\ln\left(\frac{\Delta T^{oc}_{e,1}}{\Delta T^{oc}_{e,2}}\right)} \Bigg| \cdot \frac{1}{\Delta T^{oc}_{e,2}} \tag{A.1}$$

$$\frac{LMTD^{oc}}{\Delta T^{oc}_{e,2}} = \frac{\frac{\Delta T^{oc}_{e,1}}{\Delta T^{oc}_{e,2}} - 1}{\ln\left(\frac{\Delta T^{oc}_{e,1}}{\Delta T^{oc}_{e,2}}\right)} \tag{A.2}$$

$$\frac{\Delta T^{oc}_{e,1}}{\Delta T^{oc}_{e,2}} = \exp\left(\left[\frac{\Delta T^{oc}_{e,1}}{\Delta T^{oc}_{e,2}} - 1\right] \underbrace{\frac{\Delta T^{oc}_{e,2}}{LMTD^{oc}}}_{\psi_2}\right) \tag{A.3}$$

$$\frac{\Delta T^{oc}_{e,1}}{\Delta T^{oc}_{e,2}} \exp\left(-\frac{\Delta T^{oc}_{e,1}}{\Delta T^{oc}_{e,2}}\psi_2\right) = \exp(-\psi_2) \qquad |\cdot(-\psi_2) \tag{A.4}$$

$$\underbrace{-\frac{\Delta T^{oc}_{e,1}}{\Delta T^{oc}_{e,2}}\psi_2}_{x} \exp\left(\underbrace{-\frac{\Delta T^{oc}_{e,1}}{\Delta T^{oc}_{e,2}}\psi_2}_{x}\right) = \underbrace{-\psi_2 \exp(-\psi_2)}_{y} \tag{A.5}$$

which can be substituted into the form of

$$x \exp(x) = y. \tag{A.6}$$

Thereby, the variable y is known and x unknown. By the use of the Lambert W-function x can be defined by

$$x = \mathrm{W}(y) = \mathrm{W}(x \exp(x)). \tag{A.7}$$

The application of Eq. (A.7) to right hand side Eq. (A.5) results in

$$-\frac{\Delta T^{oc}_{e,1}}{\Delta T^{oc}_{e,2}}\psi_2 = \mathrm{W}(-\psi_2 \exp(-\psi_2)). \tag{A.8}$$

The temperature difference can be determined by

$$\Delta T^{oc}_{e,1} = -\frac{\mathrm{W}(-\psi_2 \exp(-\psi_2))}{\psi_2}\Delta T^{oc}_{e,2} = \psi_1 \Delta T^{oc}_{e,2}. \tag{A.9}$$

Due to the fact, that W is ill-defined, the Lambert W-function has three possible branches (W_0^+, W_0^-, and W_{-1}) which are depending on $y = -\psi_2 \exp(-\psi_2)$ respectively ψ_2. The minimal value of y function is $y(\psi_2 = 1) = -\frac{1}{e}$ and thus, ψ_2 is always positive, the maximal value 0. Branch W_0^+ is only defined for $y > 1$. Therefore, the only decision on which branch the solution is, is depending on which side of the minimum in $y(\psi_2 = 1) = -\frac{1}{e}$ the solution is:

- W_0^- branch if $\psi_2 > 1$
- W_{-1} branch if $\psi_2 < 1$

For the case where $\psi_2 = 1 = \frac{\Delta T^{oc}_{e,2}}{LMTD^{oc}}$, the temperature difference over the whole heat exchanger is constant and therefore, $\Delta T^{oc}_{e,1} = \Delta T^{oc}_{e,2}$. Hence, the Lambert W-function is not needed.

Appendix B. Process requirements and cost data for the potato chips production case study

Table B.4
Utility data.

Utility	T_S °C	T_T °C	h W/(m² K)	c_U CHF/MWh
Heating steam (HU)	300	299	5,000	80
Cooling water (CU)	0	1	2,000	40

Table B.3
Process requirements of the fritter line 1 for the regular chips and cractive chips OC.

Stream	# –	T_S °C	T_T °C	$T_{extr.}$ °C	CP kW/K	h W/(m² K)
Regular chips (4'410 h/y)						
Vapor heating	C_1	136	229	500	2.51	400
Boiler air pre-heating	C_2	10	40	300	1.52	100
Make-up oil pre-heating	C_3	24	176	210	0.37	400
Degreaser air heating	C_4	–	–	–	–	–
Degreaser direct steam evaporation	C_5	–	–	–	–	–
Waste gas cooling*	H_1	280	30	30	14.81	400
Chips cooling	H_2	151	24	24	0.79	300
Cractive chips (2'610 h/y)						
Vapor heating	C_1	125.9	226.1	500	2.45	400
Boiler air pre-heating	C_2	10	40	300	1.48	100
Make-up oil pre-heating	C_3	24	166	210	0.18	400
Degreaser air heating	C_4	163.4	174	500	23.31	100
Degreaser direct steam evaporation	C_5	144.9	145.1	145.1	940.00	5,000
Waste gas cooling*	H_1	270.1	30	30	14.3	400
Chips cooling	H_2	150	24	24	0.55	300

* Soft streams.

Table B.5
Modification cost factors (including Lang factors (Lang, 1948): 3 for adding equipment; 1.1 for removing equipment). Only cost for the removal of an equipment is listed, if it is existing (HEX, and admixer).

Equipment	C_0 CHF	Q [Q]	c_A CHF/Q	c_R CHF/Q	d_f –
HEX	0	A (m^2)	1,731	635	0.61
Split	0	–	40,000	–	1.00
Bypass	0	–	40,000	–	1.00
Admixer	0	–	40,000	14,666	1.00
Re-pipe	0	–	68,000	–	1.00
Re-sequence	0	–	68,000	–	1.00

Deprecation lifetime $n = 10$ y; interest rate $i_r = 5\%$.

Table B.6
Match cost matrix (including utility streams) in CHF.

H \ C	C_1	C_2	C_3	C_4	C_5	CU
H_1	0	1,500	2,100	2,100	2,100	0
H_2	900	3,000	600	300	300	0
HU	0	0	0	0	0	0

References

Aguitoni, M.C., Pavão, L.V., Siqueira, P.H., Jiménez, L., Ravagnani, M.A.d.S.S., 2018. Heat exchanger network synthesis using genetic algorithm and differential evolution. Comput. Chem. Eng. 117, 82–96. doi:10.1016/j.compchemeng.2018.06.005.

Akpomiemie, M.O., Smith, R., 2015. Retrofit of heat exchanger networks without topology modifications and additional heat transfer area. Appl. Energy 159, 381–390. doi:10.1016/j.apenergy.2015.09.017.

Asante, N.D., Zhu, X.X., 1996. An automated approach for heat exchanger network retrofit featuring minimal topology modifications. Comput. Chem. Eng. 20 (SUPPL.1). doi:10.1016/0098-1354(96)00013-0.

Biyanto, T.R., Gonawan, E.K., Nugroho, G., Hantoro, R., Cordova, H., Indrawati, K., 2016. Heat exchanger network retrofit throughout overall heat transfer coefficient by using genetic algorithm. Appl. Therm. Eng. 94, 274–281. doi:10.1016/j.applthermaleng.2015.10.146.

Björk, K.M., Nordman, R., 2005. Solving large-scale retrofit heat exchanger network synthesis problems with mathematical optimization methods. Chem. Eng. Process. 44 (8), 869–876. doi:10.1016/j.cep.2004.09.005.

Bochenek, R., Jezowski, J.M., 2006. Genetic algorithms approach for retrofitting heat exchanger network with standard heat exchangers. Comput. Aided Chem. Eng. 21 (C), 871–876. doi:10.1016/S1570-7946(06)80155-0.

Bonhivers, J.C., Moussavi, A., Alva-Argaez, A., Stuart, P.R., 2016. Linking pinch analysis and bridge analysis to save energy by heat-exchanger network retrofit. Appl. Therm. Eng. 106, 443–472. doi:10.1016/j.applthermaleng.2016.05.174.

Chen, J.J., 2019. Logarithmic mean: Chen's approximation or explicit solution? Comput. Chem. Eng. 120, 1–3. doi:10.1016/j.compchemeng.2018.10.002.

Chen, J.J.J., 1987. Comments on improvements on a replacement for the logarithmic mean. Chem. Eng. Sci. 42 (10), 2488–2489. doi:10.1016/0009-2509(87)80128-8.

Chin, H.H., Wang, B., Varbanov, P.S., Klemeš, J.J., Zeng, M., Wang, Q.W., 2020. Long-term investment and maintenance planning for heat exchanger network retrofit. Appl. Energy 279 (August). doi:10.1016/j.apenergy.2020.115713.

Euler, L., 1779. De serie Lambertina plurismique eius insignibus propretatibus. Acta Academiae scientiarum imperialis petropolitanae 6, 29–51.

European Commission, 2020. Energy efficiency directive. https://ec.europa.eu/energy/topics/energy-efficiency/targets-directive-and-rules/energy-efficiency-directive_en#content-heading-0.

Fotsch, P., 2006. Pilotpahse Pinch-Methodik 2006/07: Zweifel Pomy-Chips AG. Technical Report. Swiss Federal Office of Energy SFOE, Zurich.

Furman, K.C., Sahinidis, N.V., 2001. Computational complexity of heat exchanger network synthesis. Comput. Chem. Eng. 25 (9–10), 1371–1390. doi:10.1016/S0098-1354(01)00681-0.

Gadalla, M.A., 2015. A new graphical method for Pinch Analysis applications: heat exchanger network retrofit and energy integration. Energy 81, 159–174. doi:10.1016/j.energy.2014.12.011.

Holland, J.H., 1975. Adaptation in Natural and Artificial Systems. University Michigan Press, Ann Arbor, MI.

Isafiade, A.J., 2018. Retrofitting multi-period heat exchanger networks using the reduced superstructure synthesis approach. Chem. Eng. Trans. 70, 133–138. doi:10.3303/CET1870023.

Jiang, N., Shelley, J.D., Doyle, S., Smith, R., 2014. Heat exchanger network retrofit with a fixed network structure. Appl. Energy 127, 25–33. doi:10.1016/j.apenergy.2014.04.028.

Jones, P.S., 1991. Targeting and design of heat exchanger networks under multiple base case operation. University of Manchester Institute of Science and Technology (UMIST) Ph.D. thesis..

Kamel, D.A., Gadalla, M.A., Abdelaziz, O.Y., Labib, M.A., Ashour, F.H., 2017. Temperature driving force (TDF) curves for heat exchanger network retrofit – a case study and implications. Energy 123, 283–295. doi:10.1016/j.energy.2017.02.013.

Kang, L., Liu, Y., 2014. Retrofit of heat exchanger networks for multiperiod operations by matching heat transfer areas in reverse order. Ind. Eng. Chem. Res. 53 (12), 4792–4804. doi:10.1021/ie4041143.

Kang, L., Liu, Y., 2015. Minimizing investment cost for multi-period heat exchanger network retrofit by matching heat transfer areas with different strategies. Chin. J. Chem. Eng. 23 (7), 1153–1160. doi:10.1016/j.cjche.2015.03.003.

Kang, L., Liu, Y., 2017. A systematic strategy for multi-period heat exchanger network retrofit under multiple practical restrictions. Chin. J. Chem. Eng. 25 (8), 1043–1051. doi:10.1016/j.cjche.2017.01.002.

Kemmler, A., Spillmann, T., 2020. Analyse des schweizerischen Energieverbrauchs 2000 - 2019 nach Verwendungszwecken. Technical Report. Swiss Federal Office of Energy SFOE.

Klemeš, J.J., 2013. Handbook of process integration (PI).

Lai, Y.Q., Manan, Z.A., Wan Alwi, S.R., 2018. Simultaneous diagnosis and retrofit of heat exchanger network via individual process stream mapping. Energy 155, 1113–1128. doi:10.1016/j.energy.2018.05.021.

Lai, Y.Q., Wan Alwi, S.R., Manan, Z.A., 2019. Customised retrofit of heat exchanger network combining area distribution and targeted investment. Energy 179, 1054–1066. doi:10.1016/j.energy.2019.05.047.

Lakshmanan, R., Bañares-Alcántara, R., 1996. A novel visualization tool for heat exchanger network retrofit. Ind. Eng. Chem. Res. 35 (12), 4507–4522. doi:10.1021/ie960372+.

Lal, N.S., Walmsley, T.G., Walmsley, M.R., Atkins, M.J., Neale, J.R., 2018. A novel heat exchanger network bridge retrofit method using the modified energy transfer diagram. Energy 155, 190–204. doi:10.1016/j.energy.2018.05.019.

Lambert, J.H., 1758. Observationes variae in mathesin puram. Acta Helvetica 3 (1), 128–168.

Lang, H.J., 1948. Simplified approach to preliminary cost estimates. Chem. Eng. 55 (6), 112–113.

Langner, C., Svensson, E., Harvey, S., 2020. A framework for flexible and cost-efficient retrofit measures of heat exchanger networks. Energies 13 (6), 1–24. doi:10.3390/en13061472.

Lewin, D.R., 1998. A generalized method for HEN synthesis using stochastic optimization - II. The synthesis of cost-optimal networks. Comput. Chem. Eng. 22 (10), 1387–1405. doi:10.1016/S0098-1354(98)00221-X.

Lewin, D.R., Wang, H., Shalev, O., 1998. A generalized method for HEN synthesis using stochastic optimization – I. general framework and MER optimal synthesis. Comput. Chem. Eng. 22 (10), 1503–1513. doi:10.1016/S0098-1354(98)00220-8.

Liu, X.W., Luo, X., Kabelac, S., 2016. Optimal retrofit strategy of heat exchanger networks applied in crude oil distillation units. Ind. Eng. Chem. Res. 55 (43), 11283–11290. doi:10.1021/acs.iecr.6b01931.

Liu, X.W., Luo, X., Ma, H.G., 2014. Studies on the retrofit of heat exchanger network based on the hybrid genetic algorithm. Appl. Therm. Eng. 61 (2), 785–790. doi:10.1016/j.applthermaleng.2013.10.036.

Maus, K., Faust, A.-K., Wirz, M., Nowak, S., Alles, C., 2020. Energy Research Masterplan of the Federal Government 2021–2024. Technical Report. Federal Energy Research Commission CORE, Berne.

Pavão, L.V., Costa, C.B.B., Ravagnani, M.A.d.S.S., Jiménez, L., 2017. Large-scale heat exchanger networks synthesis using simulated annealing and the novel rocket fireworks optimization. Am. Inst. Chem. Eng. 63 (5), 1582–1600. doi:10.1002/aic.15524.

Pavão, L.V., Miranda, C.B., Costa, C.B., Ravagnani, M.A., 2018. Efficient multiperiod heat exchanger network synthesis using a meta-heuristic approach. Energy 142, 356–372. doi:10.1016/j.energy.2017.09.147.

Rezaei, E., Shafiei, S., 2009. Heat exchanger networks retrofit by coupling genetic algorithm with NLP and ILP methods. Comput. Chem. Eng. 33 (9), 1451–1459. doi:10.1016/j.compchemeng.2009.03.009.

Sreepathi, B.K., Rangaiah, G.P., 2014. Review of heat exchanger network retrofitting methodologies and their applications. Ind. Eng. Chem. Res. 53 (28), 11205–11220. doi:10.1021/ie403075c.

Stampfli, J.A., Olsen, D.G., Wellig, B., Hofmann, R., 2020. Heat exchanger network retrofit for processes with multiple operating cases : a metaheuristic approach. In: Proceedings of the 30th European Symposium on Computer Aided Process Engineering, vol. 48. Elsevier B.V., Amsterdam, pp. 781–786. doi:10.1016/B978-0-12-823377-1.50131-2.

Stampfli, J. A., 2021. J-A-St/moc_retrofit_ga_de: v1.0 (Version v1.0). doi:10.5281/zenodo.4441140.

Stampfli, J.A., Olsen, D.G., Wellig, B., Hofmann, R., 2022. A parallelized hybrid genetic algorithm with differential evolution for heat exchanger network retrofit. MethodsX, MEX-D-22-00113 Submitted for publication doi:10.1016/j.mex.2022.101711.

Storn, R., 1996. On the usage of differential evolution for function optimization. In: Biennial Conference of the North American Fuzzy Information Processing Society - NAFIPS, pp. 519–523. doi:10.1109/nafips.1996.534789.

Storn, R., Price, K., 1997. Differential evolution – a simple and efficient heuristic for global optimization over continuous spaces. J. Global Optim. 11, 341–359. doi:10.1023/A:1008202821328.

Talbi, E.-G., 2009. Methaheuristics From Design to Implementation. John Wiley & Sons Inc, Hoboken, New Jersey.

Toimil, D., Gómez, A., 2017. Review of metaheuristics applied to heat exchanger network design. Int. Trans. Oper. Res. 24 (1–2), 7–26. doi:10.1111/itor.12296.

Verheyen, W., Zhang, N., 2006. Design of flexible heat exchanger network for multi-period operation. Chem. Eng. Sci. 61 (23), 7730–7753. doi:10.1016/j.ces.2006.09.028.

Virtanen, P., Gommers, R., Oliphant, T.E., Haberland, M., Reddy, T., Van der Walt, S.J., Brett, M., Wilson, J., Millman, K.J., Mayorov, N., Nelson, A.R.J., Jones, E., Robert, K., Larson, E., Carey, C.J., Polat, I., Feng, Y., Moore, E.W., Van der Plas, J., Laxalde, D., Perktold, J., Cimrman, R., Henriksen, I., Quintero, E.A., Harris, C.R., Archibald, A.M., Ribeiro, A.H., Pedregosa, F., van Mulbregt, P., 2020. SciPy 1.0: fundamental algorithms for scientific computing in Python. Nat. Methods 17, 261–272. doi:10.1038/s41592-019-0686-2.

Wan Alwi, S.R., Manan, Z.A., 2010. STEP-A new graphical tool for simultaneous targeting and design of a heat exchanger network. Chem. Eng. J. 162 (1), 106–121. doi:10.1016/j.cej.2010.05.009.

Wang, S., Tian, Y., Li, S., 2021. A simultaneous optimization of a flexible heat exchanger network under uncertain conditions. Appl. Therm. Eng. 183 (P2), 116230. doi:10.1016/j.applthermaleng.2020.116230.

Yee, T.F., Grossmann, I.E., 1990. Simultaneous optimization models for heat integration - II. Heat exchanger network synthesis. Comput. Chem. Eng. 14 (10), 1165–1184. doi:10.1016/0098-1354(90)85010-8.

Yerramsetty, K.M., Murty, C.V., 2008. Synthesis of cost-optimal heat exchanger networks using differential evolution. Comput. Chem. Eng. 32 (8), 1861–1876. doi:10.1016/j.compchemeng.2007.10.005.

Yong, J.Y., Varbanov, P.S., Klemeš, J.J., 2014. Shifted retrofit thermodynamic diagram: a modified tool for retrofitting heat exchanger networks. Chem. Eng. Trans. 39 (Special Issue), 97–102. doi:10.3303/CET1439017.

Yong, J.Y., Varbanov, P.S., Klemeš, J.J., 2015. Heat exchanger network retrofit supported by extended grid diagram and heat path development. Appl. Therm. Eng. 89, 1033–1045. doi:10.1016/j.applthermaleng.2015.04.025.

Zhang, H., Rangaiah, G.P., 2013. One-step approach for heat exchanger network retrofitting using integrated differential evolution. Comput. Chem. Eng. 50, 92–104. doi:10.1016/j.compchemeng.2012.10.018.

Zore, Ž., Čuček, L., Kravanja, Z., 2017. Syntheses of sustainable supply networks with a new composite criterion – sustainability profit. Comput. Chem. Eng. 102, 139–155. doi:10.1016/j.compchemeng.2016.12.003.

Article 3

A Parallelized Hybrid Genetic Algorithm with Differential Evolution for Heat Exchanger Network Retrofit

published in MethodsX in collaboration with Donald G. Olsen, Beat Wellig and, René Hofmann

This journal article is an extension of Article 2 describing the evolutionary optimization algorithm. It contains explanations of the two-stage GA/DE algorithm including the needed data structures for the optimization, the evolutionary operators, and the parallelization of the algorithm.

My contribution: Conceptualization, Methodology, Software, Validation, Formal analysis, Investigation, Data curation, Writing –original draft, Visualization, Writing –review & editing.

Stampfli, J. A., Olsen, D. G., Wellig, B., and Hofmann, R. (2022a). A parallelized hybrid genetic algorithm with differential evolution for heat exchanger network retrofit. MethodsX *9, p. 101711.*

DOI: 10.1016/j.mex.2022.101711

MethodsX 9 (2022) 101711

Contents lists available at ScienceDirect

MethodsX

journal homepage: www.elsevier.com/locate/mex

Method Article

A parallelized hybrid genetic algorithm with differential evolution for heat exchanger network retrofit

Jan A. Stampfli[a,b,*], Donald G. Olsen[a], Beat Wellig[a], René Hofmann[b]

[a] *Lucerne University of Applied Sciences and Arts, Competence Center Thermal Energy Systems and Process Engineering, Technikumstrasse 21, Horw 6048, Switzerland*
[b] *TU-Wien, Institute of Energy Systems and Thermodynamics, Getreidemarkt 9/BA, Vienna 1060, Austria*

A B S T R A C T

The challenge of heat exchanger network retrofit is often addressed using deterministic algorithms. However, the complexity of the retrofit problems, combined with multi-period operation, makes it very difficult to find any feasible solution. In contrast, stochastic algorithms are more likely to find feasible solutions in complex solution spaces. This work presents a customized evolutionary based optimization algorithm to address this challenge. The algorithm has two levels, whereby, a genetic algorithm optimizes the topology of the heat exchanger network on the top level. Based on the resulting topology, a differential evolution algorithm optimizes the heat loads of the heat exchangers in each operating period. The following bullet points highlight the customization of the algorithm:

- The advantage of using both algorithms: the genetic algorithm is used for the topology optimization (discrete variables) and the differential evolution for the heat load optimization (continuous variables).
- Penalizing and preserving strategies are used for constraint handling
- The evaluation of the genetic algorithm is parallelized, meaning the differential evolution algorithm is performed on each chromosome parallel on multiple cores.

A R T I C L E   I N F O

Method name: Evolutionary based heat exchanger network retrofit for multi-period processes
Keywords: Heat exchanger network (HEN), Retrofit, Multi-period, Meta-heuristics, Genetic algorithm, Differential evolution, Parallel processing
Article history: Received 15 March 2022; Accepted 19 April 2022; Available online 26 April 2022

DOI of original article: 10.1016/j.compchemeng.2022.107771

* Corresponding author at: Lucerne University of Applied Sciences and Arts, Competence Center Thermal Energy Systems and Process Engineering, Technikumstrasse 21, 6048 Horw, Switzerland.

E-mail addresses: jan.stampfli@hslu.ch (J.A. Stampfli), donald.olsen@hslu.ch (D.G. Olsen), beat.wellig@hslu.ch (B. Wellig), rene.hofmann@tuwien.ac.at (R. Hofmann).

https://doi.org/10.1016/j.mex.2022.101711

Specification table

Subject area:	Chemical Engineering, Computer Science
More specific subject area:	Process Integration, Heat exchanger network retrofit
Method name:	Evolutionary based heat exchanger network retrofit for multi-period processes
Name and reference of original method:	n/a
Resource availability:	doi:10.5281/zenodo.4441140

Sets	
$C = \{1 \ldots j \ldots NC\}$	Set of cold streams
$CH = \{1 \ldots ch \ldots NCH\}$	Set of heat load chromosomes
$CT = \{1 \ldots ct \ldots NCT\}$	Set of topology chromosomes
$E = \{1 \ldots e \ldots NE\}$	Set of heat exchangers
$H = \{1 \ldots i \ldots NH\}$	Set of hot streams
$K = \{1 \ldots k \ldots NK\}$	Set of enthalpy stages
$GH = \{1 \ldots gh \ldots NGH\}$	Set of heat loads generations
$GT = \{1 \ldots gt \ldots NGT\}$	Set of topology generations
$OP = \{1 \ldots op \ldots NOP\}$	Set of operating periods
Parameter	
a	Admixer existence (boolean)
b	Bypass existence (boolean)
CR	Crossover probability
$\mathbf{EAM}$	Exchanger address matrix / GA chromosome
ex	Heat exchanger existence (boolean)
F_p	Perturbation factor
f	Fitness function
h	Penalty function
MT	Mutation probability
n	number of infeasible solutions
P	Population
$\mathbf{U}$	trial chromosome
$\mathbf{V}$	donor chromosome
$\mathbf{X}$	Heat load matrix / DE chromosome
Δ	Ineasibility penalty
Subscripts	
best	best found solution
init	Initial solution
viol	constraint violations
Abbreviations	
DE	Differential evolution
EAM	Exchanger address matrix
GA	Genetic algorithm
HEN	Heat exchanger network
HENS	Heat exchanger network synthesis
HEX	Heat exchanger
HoF	Hall of Fame
TAC	Total annual cost

Method details

Heat exchanger network synthesis (HENS) is an important tool to design energy efficient production plants in process industry. Furman and Sahinidis [1] showed, that HENS is $\mathcal{NP}$-hard *in the strong sense*. The heat exchanger network retrofit formulation, is an extension of HENS with increased complexity. Complexity is further increased by the additional dimension of operating periods, the possibility to integrate bypasses or admixers, and practical constraints. It is unlikely that deterministic algorithms can provide a feasible solution for such problems on a large-scale. Stochastic algorithms are able to handle such problems. Therefore, a hybrid two-level evolutionary algorithm based on genetic algorithm (GA) and differential evolution (DE) is developed. The concept of GA was first introduced by Holland [2] and further extended by Goldberg [3]. DE was introduced by Storn [4],

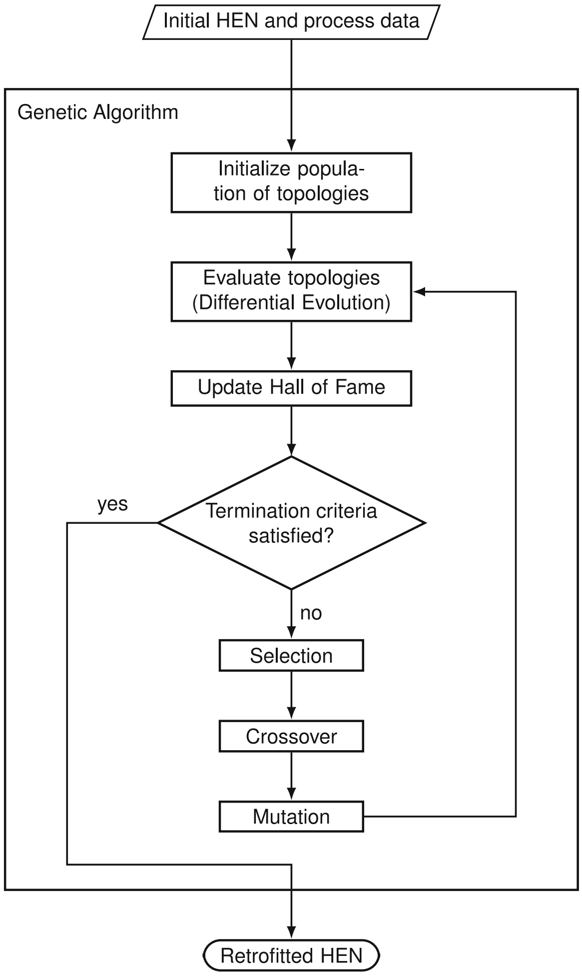

Fig. 1. Flowchart of Genetic Algorithm for topology optimization.

Storn and Price [5]. In the developed algorithm, a GA handles the topology optimization in the top level and a DE in the sub level is used to optimize the operation parameter.

Topology optimization using genetic algorithm

In order to define the topology of a HEN, integer values are used to address the position of each heat exchanger (HEX). Genetic algorithms, which are based on the evolution process in nature, are suitable to handle such discrete variables. Thereby, individuals within a population are compared and only the fittest of them survive. During the process, new individuals are generated through the mating of the fittest individuals. Coping errors (mutations) may occur during mating. An overview of the algorithm is shown in Fig. 1. The following sections describe the evolutionary operators in detail.

Genetic algorithm - initialization

In a first step, a population $P_t = \{\mathbf{EAM}_0 \ldots \mathbf{EAM}_{NCT}\}$ with NCT random individual topologies, hereafter called chromosomes, is initialized. Each of these chromosomes represents a HEN topology and is described using an exchanger address matrix (EAM). An EAM of an example topology is shown in Fig. 2. A chromosome contains the following genes (configurations of a HEX): (e) HEX number, (i) hot stream number, (j) cold stream number, (k) enthalpy stage number, (b_h) bypass on hot stream, (a_h) admixer on hot stream, (b_c) bypass on cold stream, (a_c) admixer on cold stream, and (ex) existence

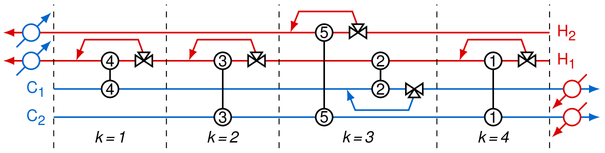

$$
\mathbf{EAM} = \begin{array}{c} \begin{array}{ccccccccc} \mathrm{e} & \mathrm{i} & \mathrm{j} & \mathrm{k} & \mathrm{b_h} & \mathrm{a_h} & \mathrm{b_c} & \mathrm{a_c} & \mathrm{ex} \end{array} \\ \begin{bmatrix} 1 & 1 & 2 & 4 & 1 & 0 & 0 & 0 & 1 \\ 2 & 1 & 1 & 3 & 0 & 0 & 0 & 1 & 1 \\ 3 & 1 & 2 & 2 & 1 & 0 & 0 & 0 & 1 \\ 4 & 1 & 1 & 1 & 1 & 0 & 0 & 0 & 1 \\ 5 & 2 & 2 & 3 & 1 & 0 & 0 & 0 & 1 \end{bmatrix} \end{array}
$$

Fig. 2. Example heat exchanger network with corresponding exchanger address matrix (bypasses on hot side of HEX 1, 3, 4, and 5; admixer on cold side of HEX 2).

of the HEX. During the initialization, for heach HEX it is first randomly decided if the HEX exists. For all existing HEXs, a random hot stream, cold stream, and enthalpy stage is defined. To ensure only feasible solution, the preserving constraint handling technique is used (e.g., for the stream number a random value between zero and the number of hot streams *NH* is selected). Bypass and admixer are not initialized, thus their existence depends on the heat loads. Hence, the need of a mixer and its configuration is determined in the DE.

Genetic algorithm - evaluation

After the initialization, each chromosome needs to be evaluated. In order to define the required areas and thus, the resulting cost, the heat loads need to be defined first. The optimal heat loads are found by the DE. To reduce computation time, the penalizing constraint handling technique is used. Thereby, only feasible topologies are optimized using DE. Infeasible solutions are evaluated by a penalty function which is less computationally expensive. The fitness $f^{gt}_{\mathrm{GA},ct}$ of the topology chromosome ct in the topology generation gt is given by

$$
f^{gt}_{\mathrm{GA,ct}}(\mathbf{EAM^{gt}_{ct}}) = \begin{cases} f^{gt}_{\mathrm{DE,best}}(\mathbf{EAM^{gt}_{ct}}, \mathbf{X^{gt}_{ct,best}}) & \text{if} \quad \mathrm{n^{gt}_{GA,viol}} = 0 \\ \dfrac{1}{h^{gt}_{\mathrm{GA}}(n^{gt}_{\mathrm{GA,viol}})} & \text{otherwise} \end{cases} \tag{1}
$$

whereby, $f^{gt}_{\mathrm{DE,best}}$ is the fitness of the DE in function of the EAM and the heat loads of the best DE solution $\mathbf{X}^{gt}_{ct,best}$. The distance of each violated constraint c is given by $n^{gt}_{\mathrm{GA,viol},c}$. For infeasible topologies, the fitness is defined by reciprocal value of the penalty function, given by

$$
h^{gt}_{\mathrm{GA}}\left(n^{gt}_{\mathrm{GA,viol}}\right) = \Delta + \underbrace{\sum_{c \in C_{\mathrm{GA}}} \left(0 - n^{gt}_{viol,c}\right)^2}_{n^{gt}_{\mathrm{GA,viol}}} \quad \text{with } \Delta >> \mathrm{TAC_{init}} \tag{2}
$$

whereby C_{GA} is the set of all GA constraints. A constant value Δ, which is larger than the initial total annual cost of the existing process, is added to the sum of the squared distances to the feasible region.

Genetic algorithm - selection

To choose the parent chromosomes for mating, tournament selection is performed. This means that the fittest out of a given number of randomly selected chromosomes is chosen.

Genetic algorithm - crossover

With a crossover probability of CR_{GA}, the parents mate. Thereby, a one-point crossover is performed. Both parent chromosomes are cut below a random selected HEX number. The HEXs above the cut are swapped between the two chromosomes. The two resulting children chromosomes replace the parent chromosomes and are evaluated.

Genetic algorithm - mutation

In nature, during the mating process in the crossover, coping errors (mutations) may occur. In the algorithm, with a mutation probability of MT_{GA}, for each allele (a single scalar value within a gene), a mutation occurs. For the mutation in the existence of a HEX gene (ex), a random bit flip is performed.

In the genes (i), (j), and (k), the value is changed within the upper and lower boundary (e.g., for (i) the number of existent hot streams) of the gene using an uniform distribution. It is ensured by using the preserving strategy, none of these values exceed their boundaries.

Genetic algorithm - next generation

After the application of the evolutionary operators (selection, crossover, and mutation), the new generated topologies are evaluated and the population is updated by replacing the parent chromosome with the new children chromosomes for the next generation. In order to keep track of the best solutions, a Hall of Fame (HoF) list is created. This list contains the current best solutions. If in the evaluation step a fitter solution is found, the HoF list is updated. With this additional feature, the flexibility of the algorithm in use is increased as the engineer is now able to choose between the most promising solutions. The algorithm is terminated as soon the maximal number of topology generations *NGT* is reached.

Heat load optimization using differential evolution

In contrast to the topology optimization, the heat loads are continuous variables with upper and lower bounds. Differential evolution algorithms are best to deal with the continuous variables. Compared to deterministic algorithms such as gradient descent, DE does not require the model to be differentiable. DE algorithms use the same concepts of evolution as GAs. However, the order of the evolutionary operators is reversed. There are different options for the DE configuration. In this case, the standard configuration *DE/rand/1/bin* is used. This means that the individuals for mutation are selected randomly, only one difference for perturbation (F_P: perturbation factor) is considered, and a binomial crossover is performed. In Fig. 3, an overview of the algorithm is shown. The following sections describe the algorithm in detail.

Differential evolution - initialization

For each feasible topology from the GA, a population $P_h = \{\mathbf{X}_0 \ldots \mathbf{X}_{NCH}\}$ with NCH random heat load chromosomes is initialized. Each of these chromosomes consists of all the heat loads of each heat exchanger in every OP, resulting in a two-dimensional array. Chromosome ch is given by

$$\mathbf{X_{ch}} = \left(\dot{Q}_e^{op}\right) \tag{3}$$

whereby the heat load is an array of the size $NE \times NOP$. The initialization of the heat loads of existing HEXs $\dot{Q}_{ch,e}^{op}$ is constraint by a minimal user defined value and a maximal value given by the enthalpy differences of the connected streams (case study dependent value).

Differential evolution - evaluation

For the evaluation of the population of heat loads, the fitness of each chromosome needs to be determined. Infeasible solutions are evaluated by a penalty function. In each generation gh the fitness $f_{\mathrm{DE},ch}^{gh}$ is given by

$$f_{\mathrm{DE},ch}^{gh}\left(\mathbf{EAM}_{ct}^{gt}, \mathbf{X}_{ch}^{gh}\right) = \begin{cases} \dfrac{1}{TAC\left(\mathbf{EAM}_{ct}^{gt}, \mathbf{X}_{ch}^{gh}\right)} & \text{if} \quad n_{\mathrm{DE},viol}^{gh} = 0 \qquad (4) \\ \dfrac{1}{h_{\mathrm{DE}}^{gh}\left(n_{\mathrm{DE},viol}^{gh}\right)} & \text{otherwise.} \qquad (5) \end{cases}$$

whereby, the *TAC* is the total annual cost of the current topology and heat loads. TAC consists the yearly operating cost and the investment cost for the retrofit. The detailed model for calculating the TAC is formulated in the corresponding research paper [6]. In order to minimize the TAC, the reciprocal value represents the fitness of a chromosome. Each distance of a heat load constraint violation is given by $n_{\mathrm{DE},viol,c}^{gh}$. For infeasible operation parameter, the fitness is defined by reciprocal

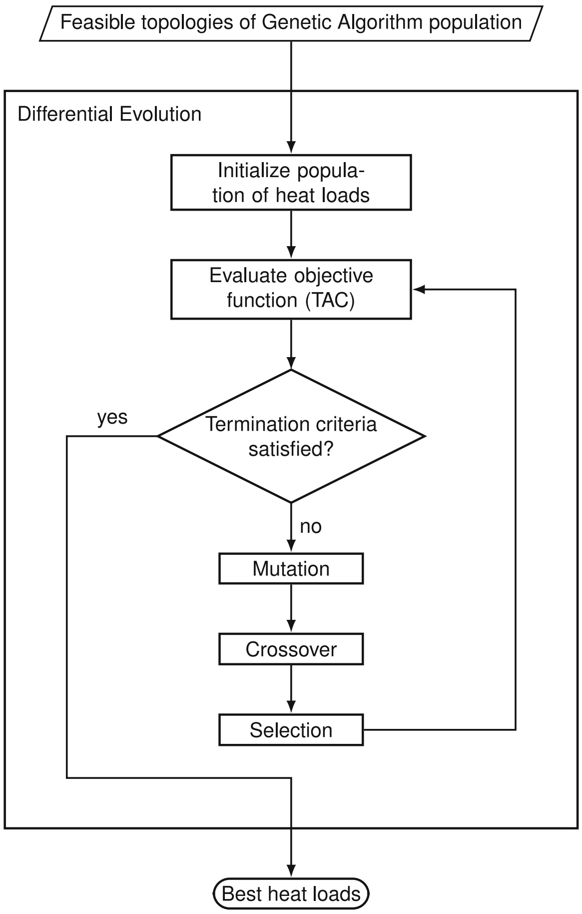

Fig. 3. Flowchart of Differential Evolution for operation parameter optimization.

value of the penalty function, given by

$$h_{\mathrm{DE}}^{gh}(n_{\mathrm{DE},viol}^{gh}) = \Delta + \underbrace{\sum_{c \in C_{\mathrm{DE}}} \left(0 - n_{viol,c}\right)^2}_{n_{\mathrm{DE},viol}^{gh}} \text{ with } \Delta >> TAC_{init} \tag{6}$$

whereby C_{DE} is the set of all DE constraints. A constant value Δ which is larger than the initial TAC is added to the sum of the squared distances to the feasible region.

Differential evolution - mutation

The first evolutionary operation in a DE is mutation. Thereby, a three non-equal chromosomes $\mathbf{X}_{r1}^{gh}, \mathbf{X}_{r2}^{gh}, \mathbf{X}_{r3}^{gh}$ $(r_1 \neq r_2 \neq r_3)$ of the current generation gh are selected randomly. A new donor chromosome is generated by

$$\mathbf{V}_{ch}^{gh} = \mathbf{X}_{r1}^{gh} + F_P\left(\mathbf{X}_{r2}^{gh} - \mathbf{X}_{r3}^{gh}\right) \tag{7}$$

whereby one difference for perturbation is used and weighted with the perturbation factor $F_P \in [0, 2]$. After the mutation, for all infeasible heat loads a new random value within the boundaries is assigned.

Differential evolution - crossover

In the crossover operator, a trial chromosome $\mathbf{U}_{ch}^{gh}$ is generated by

$$u_{ch,e}^{gh,oc} = \begin{cases} v_{ch,e}^{gh,oc}, & r^{gh} < CR_{\mathrm{DE}} \vee p = r \\ x_{ch,e}^{gh,oc}, & \text{otherwise} \end{cases} \tag{8}$$

whereby, $r^{gh} \sim U(0, 1)$ has a uniform distribution. With a probability of CR_{DE} a crossover is performed. To ensure at least one crossover per operating parameter, a random index within the chromosome is chosen for which crossover is always performed.

Differential evolution - selection

In the selection operator, the new created trial chromosome is evaluated. To determine the new target chromosome for the next generation $gh + 1$ with

$$\mathbf{X}_{ch}^{gh+1} = \begin{cases} \mathbf{U}_{ch}^{gh}, & \text{if} \quad f(\mathbf{U}_{ch}^{gh}) > f(\mathbf{X}_{ch}^{gh}) \\ \mathbf{X}_{ch}^{gh}, & \text{otherwise,} \end{cases} \tag{9}$$

a simple greedy selection is performed.

Differential evolution - next generation

For each generation, the evolutionary operators (mutation, crossover, and selection) are executed till one of the termination criteria is fulfilled. The first termination criterion is satisfied when the maximal number of heat load generations *NGH* is reached. The second termination criterion is reached when the number of consecutive generations without improvement of the fitness exceeds its limit.

Implementation and parallelization

The algorithm is implemented in Python 3.8.2 using the library *DEAP - Distributed Evolutionary Algorithms in Python* [7]. Evolutionary algorithms are predestined for parallel computing as they work with populations of chromosomes which can be evaluated separately by distributing them among multiple processors. Therefore, all feasible GA chromosomes are distributed to multiple processors on which the heat loads are optimized using DE. The source code of the algorithm is published under an open-source license [8].

Conflict of Interest

The Authors confirm that there are no conflicts of interest.

Acknowledgments

This research project is financially supported by the Swiss Innovation Agency Innosuisse and is part of the Swiss Competence Center for Energy Research – Efficiency of Industrial Processes SCCER EIP. Further financial support is provided by the Lucerne University of Applied Sciences and Arts, Switzerland. This research is part of a collaboration between the Lucerne University of Applied Sciences and Arts and TU-Wien.

References

[1] K.C. Furman, N.V. Sahinidis, Computational complexity of heat exchanger network synthesis, Comput. Chem. Eng. 25 (9-10) (2001) 1371–1390, doi:10.1016/S0098-1354(01)00681-0.
[2] J.H. Holland, Adaptation in Natural and Artificial Systems, University Michigan press, Ann Arbor, MI, 1975.
[3] D.E. Goldberg, Genetic Algorithms in Search, Optimization and Machine Learning, Addison-Wesley Publish Company, Inc., 1989.
[4] R. Storn, On the usage of differential evolution for function optimization, in: Biennial Conference of the North American Fuzzy Information Processing Society - NAFIPS, 1996, pp. 519–523, doi:10.1109/nafips.1996.534789.

[5] R. Storn, K. Price, Differential evolution – a simple and efficient heuristic for global optimization over continuous spaces, J. Global Optim. 11 (1997) 341–359, doi:10.1023/A:1008202821328.
[6] J.A. Stampfli, B.H. Ong, D.G. Olsen, B. Wellig, R. Hofmann, Applied heat exchanger network retrofit for multi-period processes in industry: A hybrid evolutionary algorithm, Computers and Chemical Engineering 161 (2022) 107771, doi:10.1016/j.compchemeng.2022.107771.
[7] F.-A. Fortin, F.-M. De Rainville, U. Marc-André Gardner, M. Parizeau, C. Gagné, et al., DEAP: evolutionary algorithms made easy, J. Mach. Learn. Res. 13 (2012) 2171–2175.
[8] Stampfli, J. A. (2021). J-A-St/moc_retrofit_ga_de: v1.0 (Version v1.0). 10.5281/zenodo.4441140

Article 4

A Hybrid Evolutionary Algorithm for Heat Exchanger Network Retrofit for Processes with Multiple Operating Cases

published in Proceedings of the 16th Conference on Sustainable Development of Energy, Water and Environment Systems in collaboration with Benjamin H.Y. Ong, Donald G. Olsen, Beat Wellig, and René Hofmann

The research in this conference proceeding was presented in the form of a talk by Jan A. Stampfli at the 16th Conference on Sustainable Development of Energy, Water and Environment Systems, in Dubrovnik, Croatia. The research published in this article focuses on the calculation of the mixer temperatures using the Lambert W-function.

My contribution: Conceptualization, Methodology, Software, Validation, Formal analysis, Investigation, Data curation, Writing –original draft, Visualization, Writing –review & editing.

Stampfli, J. A., Ong, B. H. Y., Olsen, D. G., Wellig, B., and Hofmann, R. (2021). A hybrid evolutionary algorithm for heat exchanger network retrofit for processes with multiple operating cases. In: Proceedings of the 16th Conference on Sustainable Development of Energy, Water and Environment Systems*, p. 116.*

0116-1

A hybrid evolutionary algorithm for heat exchanger network retrofit for processes with multiple operating cases

Jan A. Stampfli, Benjamin H.Y. Ong, Donald G. Olsen, Beat Wellig
Competence Center Thermal Energy Systems and Process Engineering
Lucerne University of Applied Sciences and Arts, Horw, Switzerland
e–mail: jan.stampfli@hslu.ch

René Hofmann
Institute of Energy Systems and Thermodynamics
Technische Universität Wien, Vienna, Austria
e–mail: rene.hofmann@tuwien.ac.at

ABSTRACT

Heat exchanger network retrofit is a useful strategy to increase energy efficiency in process industry. In Switzerland, processes often have multiple operating cases caused by environmental or multi-product production. In order to consider such variations over time, additional mixers are included in the heat exchanger network retrofit. To ensure practicability in industrial application, additional practical constraints, such as a maximal number of heat exchangers in a split, are considered. These additions increase the complexity of optimization. Therefore, in this work, a two-level hybrid evolutionary algorithm is proposed. The network topology is optimized in a top-level genetic algorithm, and the heat loads are optimized using a differential evolution at a sub-level. The algorithm was successfully applied to a chips production plant from the industry. As a result, the total annual cost was reduced by around 66%.

KEYWORDS

Heat exchanger network (HEN), Retrofit, Multi-period, Meta-heuristics, Genetic algorithm, Differential evolution, Parallel processing, Lambert W-function

INTRODUCTION

The current EnergieSchweiz program is to promote energy efficiency in Switzerland. In industry, one of the methods to improve energy efficiency of industrial processes. Multiple operating cases (MOCs) are common in the Swiss industry and thus are the focus of this paper. Feasible heat transfer in each operating case (OC) can be achieved by integrating bypasses and admixer into the heat exchanger network (HEN) to increase flexibility.

In industry, often more practical solutions are preferred over the global optimum solution. Therefore, one of the key challenges is to find a local optima which can be practically implemented instead of the global optimum. In addition to the required constraints, practical considerations such as a limited number of heat exchangers (HEXs) per split are to be considered.

Most the reviewed studies focus on a single OC. However, industrial processes might exhibit MOCs over time. Methods to help optimize MOCs design for the retrofit case are needed.

Jones mentioned that HEN design for processes that have MOCs have three fundamental design types, conventional design, re-sequence design, and re-piping design [1]. Kang and Liu presented a two-step HEN retrofitting approach for multi-period operations to improve the operational flexibility of the HEN [2]. They used a reverse order matching method, which simultaneously adjust the heat transfer area, re-matching stream, and adjusting the heat transfer area to result in the least increase. They further extended the method to minimize the investment costs by using different strategies to match the heat transfer areas [3]. The strategies applied comprise maximum number of substituted HEXs after retrofit, minimum additional heat transfer areas in the retrofitted HEN, and minimum investment cost for retrofit. The results based on these strategies were reported to be better than other literature results and provide greater benefit for a large-scale HEN retrofit problem in practice. Kang and Liu also presented a systematic strategy to retrofit multi-period HEN using multi-objective optimization with multiple practical restrictions [4]. The optimized objectives are minimizing total annual cost (TAC) and total annual carbon dioxide emission by providing a Pareto front to represent a series of retrofit targets, and the most desirable option to be selected. Isafiade applied a reduced superstructure synthesis approach to retrofit of HENs for multi-period operations [5].

Furmann and Sahinidis, showed that the formulation of mixed-integer nonlinear programming (MINLP) HEN synthesis for single OC processes is already *NP*-hard *in~the~strong~sense* [6]. In addition, due to the initial HEN design in the retrofit problem, the complexity is increased. The additional constraints as well as the additional dimensions for the MOCs, with the possibility to integrate bypasses and admixers, increase the complexity of the solution space which might lead to not finding feasible solutions for large-scale problems at all. Accordingly, stochastic rather than deterministic algorithms are utilized.

In a previous work [7], a two-level genetic algorithm (GA) with differential evolution (DE) was introduced and applied to a small case study from literature. In this work, the algorithm is applied to a more complex case study from industry. Therefore, the algorithm needs to be adapted in order to be able to handle soft streams, and streams which are not active in every OC. With the aim to increase practicability of the solutions, integration of bypasses and admixer is analyzed in more detail. Hence, the mixing temperature need to be calculated based on the HEX areas. Further constraints such as extreme stream temperatures (e.g. phase change or equipment constraints) at any mixing point need to be considered. Finally, piping can have a large impact on the retrofit design and, therefore, must also be included.

HEAT EXCHANGER NETWORK RETROFIT MODEL

The retrofit model (Figure 1) is based on the stage-wise superstructure (SWS) developed by Yee and Grossmann [8]. In each enthalpy stage k, every hot stream H_i can be connected with every cold stream C_j. At the end of each stream, an utility re-balancing HEX can be placed to fulfill the energy balance. The mixing process in splits is considered to be isothermal. The SWS is extended with (1) an additional dimension of OCs (e.g., [9]) with different process requirements (existence of a process stream, mass flows, specific heat capacities, film heat transfer coefficients) and operation parameter (temperatures, heat loads, mixing fractions), (2) possible utility HEX within each enthalpy stage, and (3) possible mixer (bypass and admixer) for each HEX. The latter increases the flexibility of the network and ensures to achieve the process requirements in each OC. With a bypass, only a fraction of the mass flow is heated up by passing through the HEX.

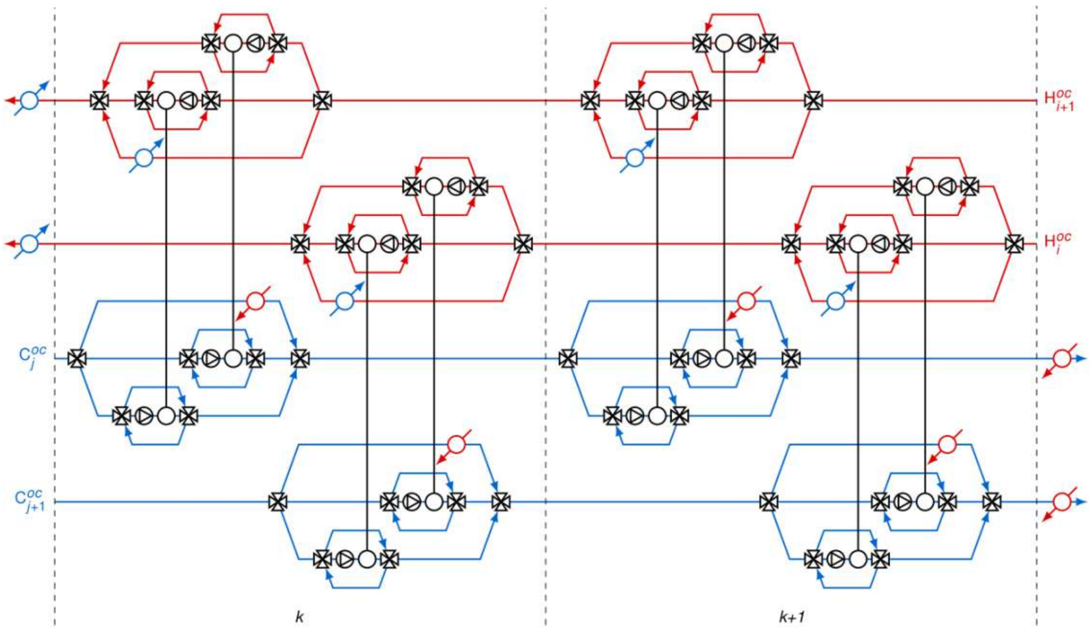

Figure 1. Superstructure for retrofit of HEN with multiple OCs

The remaining partial mass flow and the outlet mass flow of the HEX are mixed non-isothermally. By adding an admixer to a HEX, a partial fraction of the outlet mass flow of the HEX is non-isothermally mixed to the inlet mass flow of the HEX. Thereby, the mass flow through the HEX is increased. In contrast to heat exchanger network synthesis, in heat exchanger network retrofit an initial network of the existing process is given. The number of enthalpy stages depends on the topology of the existing network. During the retrofit process, the following modifications on the network are possible: (1) re-piping of a HEX, (2) re-sequencing of a HEX, (3) adding area to a HEX, (4) adding a new HEX, and (5) removing an existing HEX.

Temperature calculations

The temperatures for all the enthalpy stages ($T_{i,k}^{oc}$, $T_{j,k}^{oc}$). are calculated using the energy balance of each enthalpy stage. Thereby mass flows, specific heat capacity as well as heat loads can be different in every OC. By calculating the area using the enthalpy stage temperatures, the maximal needed area can be determined. For each OC in which, the calculated area is smaller than the maximal needed area, a mixer is needed to achieve the targeted enthalpy stage temperatures.

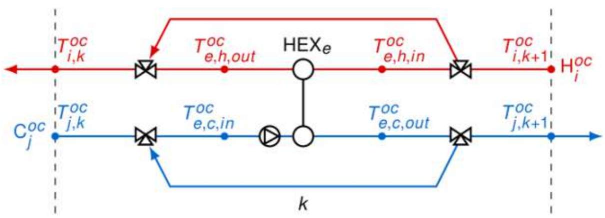

Figure 2. HEX temperatures (example of a bypass mixer on the hot stream and an admixer on the cold stream)

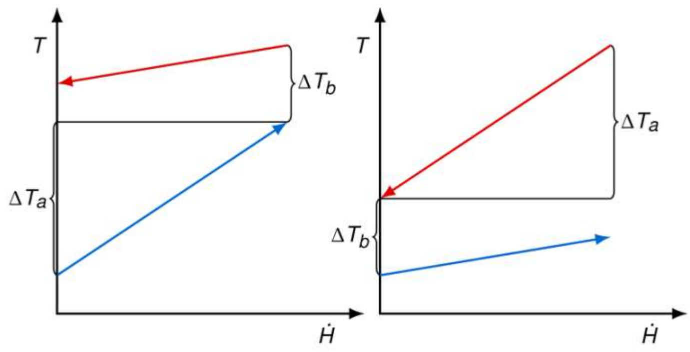

Figure 3. Relevant temperature differences for mixer type selection

Due to the inclusion of a mixer, HEXs can have four different temperatures on each side (see Figure 2). Thereby, the temperatures upstream and downstream the mixer are the enthalpy stage temperature ($T_{i,k}^{oc}$, $T_{j,k}^{oc}$). The HEX inlet and outlet temperatures ($T_{e,h,in}^{oc}$, $T_{e,h,out}^{oc}$, $T_{e,c,in}^{oc}$, $T_{e,c,out}^{oc}$) change depending on the mixer type and its mass flow. In each of the OC, the mixer is always chosen on the stream with the lower heat capacity flow *CP* (mass flow changes have a higher impact on the temperature (see Figure 3)). The mixer type with the larger feasible range is always selected. For a bypass on the cold stream, the outlet temperature of the stream ($T_{e,c,out}^{oc}$) is increased by reducing the mass flow passing the HEX. The maximum outlet temperature of the cold stream is limited by the heat transfer and thus equal to the inlet temperature of the hot stream resulting in a feasible temperature difference ΔT_b shown in the left diagram in Figure 3. For an admixer on the cold stream, the inlet temperature can be increased. The feasible temperature difference ΔT_a is in this case the change in temperature of the cold stream (the inlet temperature of stream which needs to be heated up cannot be higher than its outlet temperature). The right diagram in Figure. 3 shows the same concept for a mixer on the hot stream. An exception to this concept, are HEXs with zero heat load in an OC connected to an active stream. In this case, the stream needs to be fully bypassed. In each OC, the corresponding mixer temperature needs to be back calculated using the area difference between the calculated and the maximal area. As a result, a new logarithmic mean temperature can be determined by

$$\Delta T_{m,new} = \frac{\dot{Q}_e^{oc}}{U_e^{oc} A_{e,\max}} \tag{1}$$

Thereby, $\dot{Q}_e^{oc}$ represents the heat load, U_e^{oc} the overall heat transfer coefficient, and $A_{e,\max}$ the maximal area of HEX *e* in *oc*. In the next step, the unknown mixer temperature needs to be determined. However, the logarithmic mean temperature (see Equation 1; the temperature differences ΔT_1 and ΔT_2 are the temperature differences for a counter-current HEX) cannot be solved explicit for one of the temperature differences.

$$\Delta T_{m,new} = \frac{\Delta T_1 - \Delta T_2}{\ln\left(\frac{\Delta T_1}{\Delta T_2}\right)} \tag{2}$$

Therefore the Lambert W-function is used as an explicit solution, as proposed by Chen [10] is used to solve the logarithmic mean temperature. The Lambert W-function is computed using the Python library Scipy [11].

Total annual cost

The TAC for the HEN is given by the annualized capital costs and the operating costs. As capital costs adding or removing of HEX, mixers, and splits are considered. Further re-piping or re-sequencing costs as well as match (e.g., cost for distance) costs are included as well. The annual operating cost are given by the utility consumption.

EVOLUTIONARY OPTIMIZATION APPROACH

The HEN retrofit model formulated is a MINLP formulation which is at least *NP*-hard *in~the~strong~sense*. Therefore, a stochastic optimization algorithm with two levels is used. The algorithm is developed in Python and available under an open source license [12]. The algorithm is based on evolutionary concepts using a GA for the topology optimization (discrete variables) on the top-level and on the sub-level a DE for the optimization of the heat loads. In Figure 4, an overview of the algorithm is provided. The procedure is as follow: First, a random population of topologies is initialized and checked for feasibility. Thereby, the topology is checked for exceeding the allowed number of HEXs in a split as well as for connections between utility streams. These constraints are evaluated previously in order to reduce unnecessary computation of infeasible solutions. Instead of applying the DE for heat load optimization and the evaluation using the HEN model, a penalty function, which results always in higher TAC than the initial solution, is applied to compute the objective.

In a next step, all feasible solutions are distributed to the available central processing unit (CPU) cores, and for each topology, a random population of heat loads is initialized. Thereby, the maximal and minimal possible heat load of each HEX is constrained by a stream dependent on the maximal heat load and a user defined minimum heat load. Next, all heat load populations are evaluated and checked for feasibility. Thereby, the objective is to minimize the TAC. The constraints for the DE evaluation are the energy balances of each process stream in every OC and positive temperature differences for each HEX. Further, mixer temperatures, cannot exceed or fall below stream specific extreme temperatures (e.g., phase change or equipment constraints).

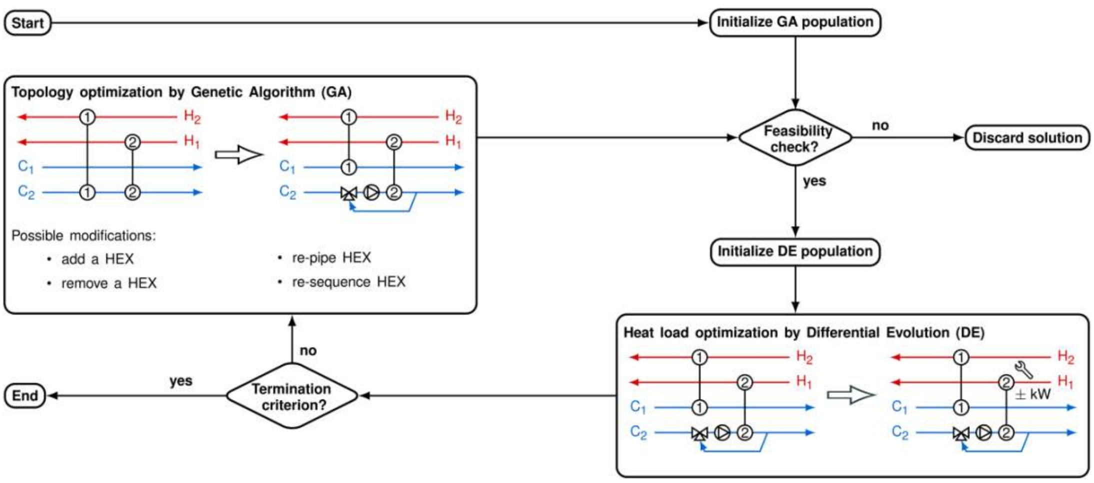

Figure 4. Overview of the evolutionary algorithm

Costs for infeasible solutions are evaluated with another penalty function. In the DE, the three evolutionary operators' mutation, crossover, and selection are performed to optimize the heat loads. The termination criteria for the DE are a maximal number of generations and a maximal number of generations without improvement. After the DE, the best solutions are stored in a Hall of Fame list, which is always updated as soon as a better solution is found. As long as the termination criterion of a maximal number of topology generations is not fulfilled, the evolutionary operators (selection, crossover, and mutation) are executed, and new modified topologies are evaluated by checking for feasibility and optimizing the heat loads with the DE. The evolutionary operators are explained in more detail in a previous paper [7].

POTATO CHIPS PPRODUCTION CASE STUDY

The developed algorithm is applied to an industrial case study. A potato chips production plant from the Zweifel Pomy-Chips AG (ZPC) is analyzed [13]. ZPC is a Swiss food company, producing snacks such as potato chips. The frying process for the potato chips has a heating demand of around 64% of their total heating demand and is used to produce two different chips types. The process requirements for both OCs are listed in Table 1. The Utility data is shown in Table 2 and the equipment modification costs are shown in Table 3. Lang factors of 1.1 and 3.0 are assumed for the removal of existent and the installation of new equipment, respectively [14]. Table 4 shows the match costs (e.g., piping) between the streams. The initial HEN is shown in Figure 5.

For the GA, a population of 100 topologies is initialized. During the selection, the best of 5 random selected topologies is chosen. To monitor the best solutions, the 10 best solutions over all generations are stored in a list. Crossover is performed with a probability of 90% and mutation is performed with a probability of 10%. For the GA, 50 generation are performed before termination. For each feasible GA chromosome, a DE population of 200 heat load configurations is initialized.

Table 1. Process requirements of the fritter line 1 for the regular chips and the cractive chips OCs (*soft streams)

Stream	Supply temperature (°C)	Target temperature (°C)	Extreme temperature (°C)	Heat capacity flow (kW/K)	Heat transfer coefficient (W/(m²K))
Regular chips (4,410 h/y)					
C_1	136	229	500	2.51	400
C_2	10	40	300	1.52	100
C_3	24	176	210	0.37	400
C_4					
C_5					
H_1^*	280	30	30	14.81	400
H_2	151	24	24	0.79	300
Cractive chips (2,610 h/y)					
C_1	125.9	226.1	500	2.45	400
C_2	10	40	300	1.48	100
C_3	24	166	210	0.18	400
C_4	163.4	174	500	23.31	100
C_5	144.9	145.1	145.1	940.00	5,000
H_1^*	270.1	30	30	14.3	400
H_2	150	24	24	0.55	300

0116-7

Table 2. Utility data

Utility	Supply temperature (°C)	Target temperature (°C)	Heat transfer coefficient (W/(m^{2}K))	Specific utility cost (CHF/MWh)
Steam (HU)	300	290	5,000	80
Cooling water (CU)	0	1	2,000	40

Table 3. Capital costs for HEX, split, mixer (bypass or admixer), and moves (re-pipe or re-sequence)

Equipment	Quantity ([Q])	Specific addition costs (CHF/[Q])	Specific removal costs (CHF/[Q])	Degression factor ()
HEX	A (m^2)	1,731	635	0.61
Split / Mixer	1 ()	40,000	0	1.00
Move	1 ()	68,000	0	1.00

Table 4. Match costs matrix in CHF

H \ C	C_1	C_2	C_3	C_4	C_5
H_1	0	1,500	2,100	2,100	2,100
H_2	900	3,000	600	300	300

With a probability of 90% crossover is performed. The perturbation factor is set to 0.5. The DE is terminated after 100 generations or 5 generations without improvement.

The algorithm was executed on a Linux based server with 256 GB Random-access memory (RAM), 128 threads distributed over 64 CPU cores. Thereby, the feasible GA topologies are distributed to all threads to run the DE and evaluate the solution.

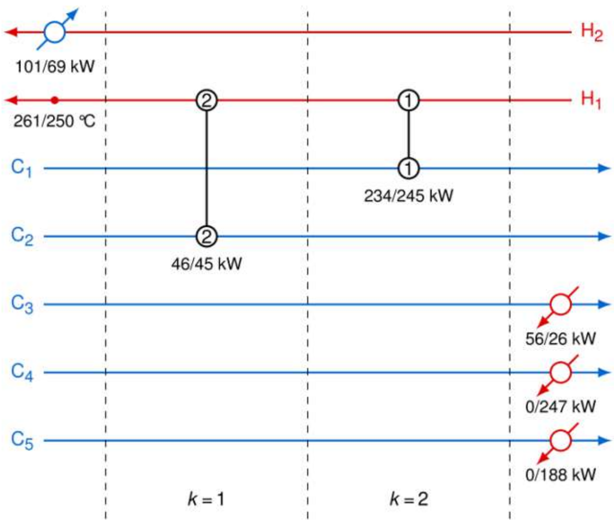

Figure 5. Initial HEN design with two process internal HEXs. The heat loads for both OCs are noted as: regular chips / cractive chips.

RESULTS

The topology of the best found solution is shown in Figure 6. The number of possible HEXs within the process was set to 7, the number of enthalpy stages to 3, and the number of possible HEX within one split to 2. The retrofitted design resulted in one HEX being removed (HEX 2) and six new are being added (HEX 3-6). The topology of HEX 1 is not modified (no re-piping, re-sequencing with only one existing HEX is not possible at all). The new HEX, number 5, is directly connected to hot utility. All the other HEXs require a mixer to ensure feasible heat transfer in each OC. The admixers for HEX 1 and 4 have very low mixer fraction. Such admixers are unlikely to be implemented and the heat balance is rather fulfilled by utility compensation. HEX 3 and HEX 6 need to have a bypass because they are connected to cold streams which are only active in one OC.

By comparing the topology to the initial design (see Figure 5), it can be seen that in the new design, every stream (except soft stream H_1) is in need of a balancing utility HEXs. However, the heat loads of all utility HEXs are small, or even negligible. Furthermore, more waste heat from the soft stream is recovered. In the initial design 280 kW in OC1 and 290 kW in OC2 are reused, resulting in a total of 1,990 MWh/y. In the retrofitted design, 232 kW in OC1 and 658 kW in OC2 are reused, resulting in a total of 2,740 MWh/y. As a result, the outlet temperature is for OC1 slightly increased from 261°C to 264°C and for OC2 decreased from 250°C to 224°C. The changes in heat loads and the resulting area are given in Table 5. HEX 1 is the only reused HEX. The area does not need to be extended. The heat loads of the balance utility HEXs are reduced significantly by increasing the heat loads of the process internal HEX. Also HEX 5, which is connected to hot utility, is rather small compared to the other process internal HEXs. Therefore, it can be said that the HR of the process is exploited quite well. The two new balance utility HEXs HU_1 and HU_2 are rather small (heat load of 2 kW to 3 kW). By a manual post-optimization, analyzing loops and paths within the network, such HEXs are likely to be avoided. E.g., by reducing the outlet temperature of the waste gas (H_1 and the utility consumption at the end of the chips cooling (H_2), HEX HU_1 and HEX HU_2 are likely to be redundant.

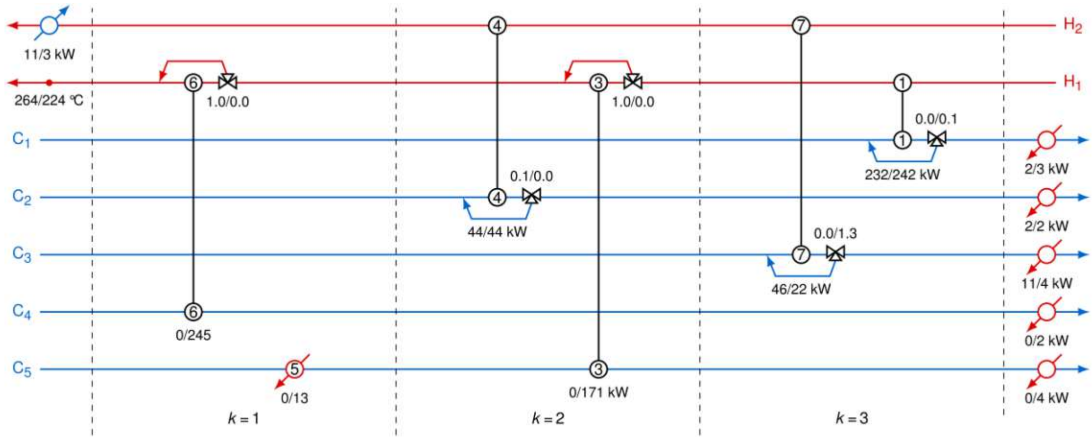

Figure 6. Best found HEN design with six process internal HEXs. The heat loads for both OCs are noted as: regular chips / cractive chips. The mixing fractions as well as the outlet temperature of the soft stream H_1 are shown.

Table 5. Comparison of heat loads and areas between the best found solution and the initial solution. (balance utility HEX number is corresponding to the connected process stream: e.g., CU_1 at the end of H_1)

HEX	Initial design			Best found design		
	Heat load OC1(kW)	Heat load OC2 (kW)	Area (m^2)	Heat load OC1 (kW)	Heat load OC2 (kW)	Area (m^2)
Process HEX						
1	234	245	16.0	232	242	15.2
2	46	45	2.5			
3				0	171	8.3
4				44	44	5.7
5				0	13	0.4
6				0	245	19.1
7				46	22	10.3
Balance utility HEX						
CU_1						
CU_2	101	69	5.6	11	3	1.4
HU_1				2	3	0.1
HU_2				2	2	0.1
HU_3	56	26	0.8	11	4	0.2
HU_4	0	247	4.8	0	2	0.1
HU_5	0	188	0.5	0	4	0.1

For the comparison of TACs, it is assumed that the investment costs of the initial design are already depreciated. The HU demand is 1,451 MWh/y and the CU demand 623 MWh/y. This results in annual operating costs of 141,080 CHF/y, which is equal to its TAC. By investing 273,495 CHF, respectively 35,419 CHF/y with interest rate of 5% over a depreciation lifetime of 10 y, HU and CU demand can be significantly reduced to 132 MWh/y and 55 MWh/y. This results in annual operating costs of 12,780 CHF/y, reducing TAC by around 66% to 48,198 CHF/y. Such result is quite common for existing industrial which were not optimized for heat recovery. HR in such plants is often limited to pre-heating supply air with waste gas.

CONCLUSIONS

In this work, a two-level GA-DE algorithm was developed. For its application in industry, practical constraints are incorporated. The algorithm must handle soft streams, as well as streams which are only active in certain OCs. Further practical constraints on the mixer temperatures to omit extreme temperatures (e.g.,phase change or equipment constraints), or a maximum number of possible HEX in a split are implemented. In order to calculate the mixer temperature an explicit approach using the Lambert W-function is implemented. Piping usually has a significant impact on retrofit investment costs. Therefore, additional match costs are considered in the optimization.

The algorithm was successfully applied to an industrial case study, a frying process of two different potato chip variants. Thereby its application on a process with soft streams and partially existing streams is demonstrated. The best found solutions proposes a reduction of approximately 66% in TAC.

To achieve the retrofitted design, one existing HEX is removed, and six new HEXs are incorporated. Future work should investigate methods to limit the number of modifications on the network to give more flexibility to the user. A promising approach would be to switch to a simulated annealing algorithm for the topology optimization.

ACKNOWLEDGMENTS

This research project is financially supported by the Swiss Innovation Agency Innosuisse and is part of the Swiss Competence Center for Energy Research Efficiency of Industrial Processes SCCER EIP. Further support is provided by the Lucerne University of Applied Sciences and Arts, Switzerland. This research is part of a collaboration between the Lucerne University of Applied Sciences and Arts and TU-Wien.

NOMENCLATURE

Symbols	
A (m^2)	Area
C ()	Cold stream
H ()	Hot stream
$\dot{Q}$ (kW)	Heat load
Q ([Q])	Quantity
T (°C)	Temperature
ΔT (K)	Temperature difference
Subscripts/superscripts	
i	Hot stream number
in	Inlet
j	Cold stream number
k	Enthalpy stage number
m	Logarithmic mean difference
oc	Operating case number
out	Outlet
Acronyms/abbreviations	
CPU	Central Processing Unit
CU	Cooling water (CU)
DE	Differential evolution
GA	Genetic algorithm
HEN	Heat exchanger network
HEX	Heat exchanger
HU	Steam (Hot utility)
MOCs	Multi operating cases
MINLP	Mixed-integer nonlinear programming
NP-hard	Non-deterministic polynomial-time hardness
OC	Operating case
RAM	Random-access memory
SWS	Stage-wise superstructure
TAC	Total annual cost
ZPC	Zweifel Pomy-Chips AG

0116-11

REFERENCES

[1] Jones PS. Targeting and design of heat exchanger networks under multiple base case operation. University of Manchester Institute of Science and Technology (UMIST), 1991.

[2] Kang L, Liu Y. Retrofit of heat exchanger networks for multiperiod operations by matching heat transfer areas in reverse order. Ind Eng Chem Res 2014;53:4792–804. doi:10.1021/ie4041143.

[3] Kang L, Liu Y. Minimizing investment cost for multi-period heat exchanger network retrofit by matching heat transfer areas with different strategies. Chinese J Chem Eng 2015;23:1153–60. doi:10.1016/j.cjche.2015.03.003.

[4] Kang L, Liu Y. A systematic strategy for multi-period heat exchanger network retrofit under multiple practical restrictions. Chinese J Chem Eng 2017;25:1043–51. doi:10.1016/j.cjche.2017.01.002.

[5] Isafiade AJ. Retrofitting multi-period heat exchanger networks using the reduced superstructure synthesis approach. Chem Eng Trans 2018;70:133–8. doi:10.3303/CET1870023.

[6] Furman KC, Sahinidis N V. Computational complexity of heat exchanger network synthesis. Comput Chem Eng 2001;25:1371–90. doi:10.1016/S0098-1354(01)00681-0.

[7] Stampfli JA, Olsen DG, Wellig B, Hofmann R. Heat Exchanger Network Retrofit for Processes with Multiple Operating Cases : a Metaheuristic Approach. Proc. 30th Eur. Symp. Comput. Aided Process Eng., vol. 48, Amsterdam: Elsevier B.V.; 2020, p. 781–6. doi:10.1016/B978-0-12-823377-1.50131-2.

[8] Yee TF, Grossmann IE. Simultaneous optimization models for heat integration - II. Heat exchanger network synthesis. Comput Chem Eng 1990;14:1165–84. doi:10.1016/0098-1354(90)85010-8.

[9] Verheyen W, Zhang N. Design of flexible heat exchanger network for multi-period operation. Chem Eng Sci 2006;61:7730–53. doi:10.1016/j.ces.2006.09.028.

[10] Chen JJJ. Logarithmic mean: Chen's approximation or explicit solution? Comput Chem Eng 2019;120:1–3. doi:10.1016/j.compchemeng.2018.10.002.

[11] Virtanen P, Gommers R, Oliphant TE, Haberland M, Reddy T, Van der Walt SJ, et al. SciPy 1.0: fundamental algorithms for scientific computing in Python. Nat Methods 2020;17:261–72. doi:10.1038/s41592-019-0686-2.

[12] Stampfli JA. J-A-St/moc_retrofit_ga_de: v1.0 (Version v1.0) 2021. doi:10.5281/zenodo.4441140.

[13] Fotsch P. Pilotpahse Pinch-Methodik 2006/07: Zweifel Pomy-Chips AG. Zurich: 2006.

[14] Lang HJ. Simplified approach to preliminary cost estimates. Chem Eng 1948;55:112–3.

Article 5

A Hybrid Evolutionary Algorithm for Multi-Objective Heat Exchanger Network Retrofit for Multi-Period Processes

published in Proceedings of the 25th Conference on Process Integration, Modelling and Optimisation for Energy Saving and Pollution Reduction in collaboration with Benjamin H.Y. Ong, Donald G. Olsen, Beat Wellig, and René Hofmann

The research in this conference proceeding was presented in the form of a talk by Jan A. Stampfli at the 25th Conference on Process Integration, Modelling and Optimisation for Energy Saving and Pollution Reduction in Split and Bol, Croatia. In this conference proceeding, the GA/DE algorithm is extended for multi-objective optimization. Therefore, the selection process of the DE algorithm is extended using an NSGA-II algorithm and the fitness of the GA is adapted using hypervolume indicators to handle Pareto fronts. The algorithm is applied to the potato chips production case study from industry (Fotsch, 2006) and compared with the single-objective optimization form Article 2.

My contribution: Conceptualization, Methodology, Software, Validation, Formal analysis, Investigation, Data curation, Writing –original draft, Visualization, Writing –review & editing.

Stampfli, J. A., Ong, B. H. Y., Olsen, D. G., Wellig, B., and Hofmann, R. (2022b). A hybrid evolutionary algorithm for multi-objective heat exchanger network retrofit for multi-period processes. In: Proceedings of the 25th Conference on Process Integration, Modelling and Optimisation for Energy Saving and Pollution Reduction*, pp. 1–8.*

PRES'22
Proceedings of the 25th Conference on Process Integration, Modelling and Optimisation for Energy Saving and Pollution Reduction, 5 – 8 September 2022, Split and Bol, Croatia

Editors: Jiří J. Klemeš, Sandro Nižetić, Petar S. Varbanov
Copyediting and Composition: Xuexiu Jia, Xuechao Wang, Hon Huin Chin

A Hybrid Evolutionary Algorithm for Multi-Objective Heat Exchanger Network Retrofit for Multi-Period Processes

Jan A. Stampfli[a,b,*], Benjamin H.Y. Ong[a], Donald G. Olsen[a], Beat Wellig[a], René Hofmann[b]

[a]Lucerne University of Applied Sciences and Arts, Competence Center Thermal Energy Systems and Process Engineering, Technikumstrasse 21, 6048 Horw, Switzerland
[b]TU-Wien, Institute of Energy Systems and Thermodynamics, Getreidemarkt 9/BA, 1060 Vienna, Austria
jan.stampfli@hslu.ch

With the growing awareness of the need to mitigate greenhouse gas (GHG) emissions, the world is transitioning towards more sustainable and energy-efficient alternatives. A large share of the Swiss process industry relies on multi-period production. Retrofitting such plants often has a high potential to improve energy efficiency and thus reducing the GHG emissions. To analyze such processes, in this work, an existing two-level algorithm using a genetic algorithm for topology optimization and a differential evolution for heat load optimization is extended to a multi-objective algorithm to consider GHG emissions besides total annual cost (TAC). The algorithm is applied to a chips production plant from industry. Comparing the results to the single-objective algorithm, GHG emissions can be further reduced by 50 %, causing an increase in TAC by 27 %. With the introduction of GHG emissions as the second objective, utility demand is included in both objectives leading to having a larger impact on the results than capital costs. However, it has been shown beneficial compared to solutions omitting this higher impact.

1. Introduction

In view of the policy objective of net zero carbon emissions, the deepest possible level of decarbonization must be achieved in all sectors. However, decarbonization of the industry sector is challenging due to the high complexity of the systems, heterogeneity, and high temperature levels. The systematic overall optimization of processes, in terms of their energy, is referred to as Process Integration (PI; Linnhoff and Flower, 1978), with Heat Exchanger Networks (HEN) representing a key strategy (Klemeš, 2013). Methods and tools are required for retrofitting pre-existing processes (brownfield), particularly multi-period processes, considering the overwhelming share of high value-added industries present in Switzerland (e.g., fine chemicals, pharma, food, beverages). Furthermore, in many Swiss companies, one single processing line is used to manufacture a portfolio of products, resulting in multi-period problems and representing additional challenges for PI.

To reach higher levels of rigor, reproducibility, and comparability, optimization based on Mathematical Programming (MP) needs to be developed. Some research on HEN retrofit has already been conducted with MP-based optimization, which can be divided into stochastic and deterministic methods. Deterministic approaches are very challenging for HEN retrofit being a more complex sub-problem of HEN synthesis. The latter is already hard to solve without metaheuristic solvers due to the high complexity of mixed-integer nonlinear programming (MINLP). Considering, among other things, the increased availability of computational power, Toimil and Gómez (2016) explained why there is a trend toward stochastic optimization methods, in particular towards metaheuristics. Metaheuristics combine local search methods (heuristics) with an algorithm to explore the search space to find an optimal or near-optimal solution. A subgroup of metaheuristics is population-based algorithms such as Genetic Algorithms (GA) and Differential Evolution (DE). GA is a stochastic method based on the concept of survival of the fittest by comparing a population of solutions and selecting the best for further exploration. DE is similar to GA but designed to optimize continuous variables such as heat loads. Application of both GA/DE has been conducted by Stampfli et al. (2020).

HEN problems can be divided into two classifications, single objective optimization (SOO), focusing on reducing total annual cost (TAC), and multi-objective optimization (MOO). MOO adds a layer of complexity to the optimization for the retrofit of existing HEN. Sreepathi and Rangaiah (2014) developed a MOO to retrofit HEN, where the objective functions are utility and investment costs. The authors used a program based on the non-dominated sorting genetic algorithm (NSGA-II), resulting in better MOO solutions. The authors then extended the work to retrofit HEN involving streams with variable heat capacity (Sreepathi and Ranagaiah, 2015). Their continuous approach to handling the variable heat capacity provided better and more practical solutions for the retrofit of HEN. Kang and Liu (2017) developed a three-stage MOO procedure to retrofit multi-period HENs. Their optimization model aims have two objective functions, total annual CO_2 emissions with capital cost for retrofit, number of substituted heat exchangers (HEXs), modification to the existing HEN structure, or additional heat transfer areas. With the current focus on reducing the GHG emissions of the industrial sector, this paper extends the work carried out in Stampfli et al. (2022a) to include GHG emissions in the MOO for multi-period HEN retrofit.

2. Methods

For the MOO, the single-objective hybrid evolutionary algorithm for HEN retrofit for multi-period processes (Stampfli et al., 2020) was later extended to consider detailed mixer configurations (Stampfli et al. 2022a) and has been further developed to optimize GHG emissions besides TAC. An overview of the algorithm is shown in Figure 1. A detailed explanation of the algorithm, including its application, is provided by Stampfli et al. (2022a), and details on the implementation in Python 3.8.2 using the library DEAP - Distributed Evolutionary Algorithms in Python (Fortin et al., 2012) is provided by Stampfli et al. (2022b).

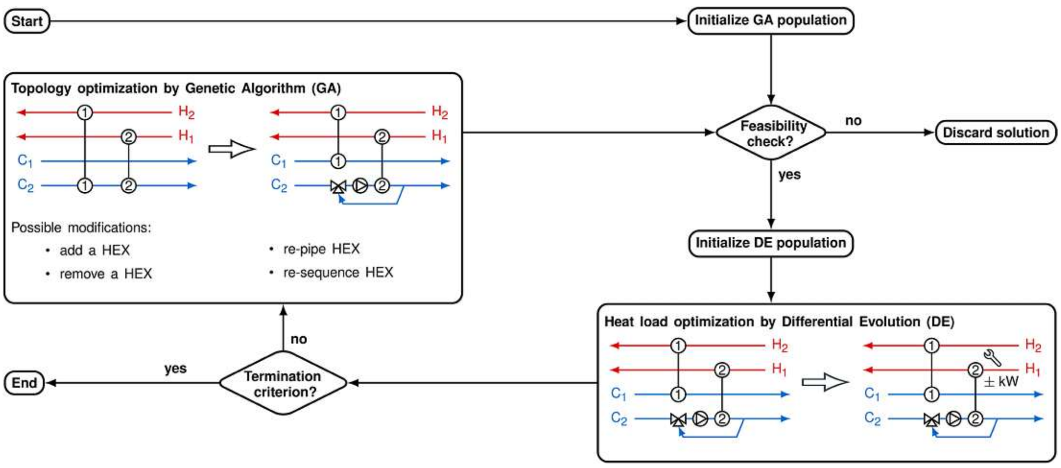

Figure 1: Algorithm overview (Stampfli et al., 2022a)

The hybrid evolutionary algorithm has two stages whereby in the top-stage, the topology of the HEN (discrete variables) is optimized using a GA. For every feasible HEN design, the DE in the sub-stage optimizes to find the best heat load distribution on the network (continuous variables). Thereby, a population of potential solutions is evaluated using a HEN model. To determine the fitness of the solutions, the TAC is used. To ensure feasible solutions, constraints which are violated often, are handled using penalizing strategies. For other constraints, decoding strategies are used. In this work, GHG emissions are introduced as a second fitness function. The functions needed to extend the existing algorithm are provided in Section 2.1. For the selection of the multi-objective fitness in the DE, the NSGA-II is used to produce a Pareto front in which every solution has a fixed HEN topology but different heat loads. The concepts of the NSGA-II selection and the integration into the DE are explained in Section 2.2. In the GA, topologies are evaluated. Therefore, the hypervolume for every Pareto front is calculated and used as its fitness. The hypervolume calculation and its integration in the GA are explained in Section 2.2.

2.1 Heat exchanger network model

The HEN model is based on Yee and Grossmann's (1990) stage-wise superstructure (SWS). It is extended with (1) an additional dimension of operating periods (OPs), (2) utility heat exchanger within the enthalpy stages, and (3) selection and calculation of detailed mixer configuration using Chen's (2019) explicit solution of the logarithmic mean. Therefore, (3) uses the Lambert W-function (Lambert, 1758) to ensure feasible heat transfer

in every OP, extreme temperatures. (4) In industry, non-process streams such as exhaust gas are often soft streams (they can but do not have to be cooled down). Thus, the SWS model is extended to handle such streams, which have no fixed target temperature and no need for utility.
To ensure practical results, additional constraints are added to the SWS: (1) The number of splits per stream and enthalpy stage can be limited to prevent Spaghetti design (Ahmad and Smith, 1989), and (2) extreme temperatures (e.g., phase change) for every stream which cannot be exceeded or fallen short of, respectively. This constraint ensures feasible temperatures in the mixer configurations.
The fitness of the retrofitted network is determined using the TAC as the objective function (OF), which is composed of capital and operating costs. Thereby, capital costs for adding or removing area, new HEXs, and new mixer configurations are considered. Further, capital costs include modification costs for re-piping and re-sequencing HEXs and resulting piping costs (depending on the plant layout). Finally, the utility costs are considered as the operating costs. A detailed description of the model, including all the equations, is published by Stampfli et al. (2022a) and Stampfli et al. (2022b).

2.2 Extension to multi-objective optimization

The model described in Section 2.1 is extended for MOO by adding GHG emissions as a second OF. GHG emissions are based on utility consumption and can be determined by

$$\mathrm{GHG} = \sum_{\forall op} \left(\dot{Q}_{HU,op}\, \xi_{HU,op} + \dot{Q}_{CU,op}\, \xi_{CU,op} \right) \Delta t_{op} \tag{1}$$

Thereby, $\dot{Q}_{HU,op}$ and $\dot{Q}_{CU,op}$ describe the hot and cold utility demands, respectively, in an operating period (OP). $\xi_{HU,op}$ and $\xi_{CU,op}$ are specific CO_2 emissions per MWh and Δt_{op} is the duration of the associated OP. The objective for the SOO is the TAC determined by

$$\mathrm{TAC} = C_{cap,a} + C_{op,a} = C_{cap,a} + \sum_{\forall op} \left(\dot{Q}_{HU,op}\, c_{HU,op} + \dot{Q}_{CU,op}\, c_{CU,op} \right) \Delta t_{op} \tag{2}$$

whereby $C_{cap,a}$ are the annualized capital costs. The operating costs $C_{op,a}$ depend on the utility demand $\dot{Q}_{HU,op}$ and $\dot{Q}_{CU,op}$ in the same way as the GHG but using specific cost coefficients $c_{HU,op}$ and $c_{CU,op}$ instead of specific emission coefficients $\xi_{HU,op}$ and $\xi_{CU,op}$. This similarity of both functions creates a dependency between both objectives. Therefore, its effect on the results must be analyzed and compared to alternative objectives by omitting the operating costs $C_{op,a}$ in Eq(2). To omit distorting the solutions due to different order of magnitudes of objectives, both are referenced to the existing HEN:

$$\mathrm{OF}_{\mathrm{TAC}} = \frac{\mathrm{TAC}_{ex}}{\mathrm{TAC}} \tag{3}$$

$$\mathrm{OF}_{\mathrm{GHG}} = \frac{\mathrm{GHG}_{ex}}{\mathrm{GHG}} \tag{4}$$

2.3 Differential evolution with NSGA-II selection for Pareto optimization

For the extension to a MOO, the selection in the DE needs to be adapted because there are two objectives that counteract each other. Therefore, the selection is performed using NSGA-II (Deb et al., 2002). For a given HEN topology, non-dominated solutions (no other solution exists that is better in an objective without worsening another objective) with different heat load distributions are selected in a Pareto front (see points marked with an x in Figure 2 on the left). The NSGA-II algorithm stores multiple fronts. By ignoring the non-dominated solutions stored in the 1st front, a 2nd front (see points marked with an o on the diagram in Figure 2 on the left) can be generated, which is only dominated by solutions in the first front. The solutions are sorted using the generalized reduced run-time complexity non-dominated sorting algorithm (Fortin et al., 2013).
During the optimization of the heat loads in the DE, the whole list with all the Pareto fronts is considered, but only the non-dominated Pareto front is returned to the genetic algorithm.

2.4 Genetic algorithm with hypervolume indicator for Pareto selection

The DE returns a Pareto front of non-dominated solutions for every HEN topology. To compare the Pareto fronts between different topologies, the fitness of each front is quantified using hypervolume indicators (Zitzler et al., 2003). Thereby a reference point p_{ref} worse than every point in all the Pareto front is set. To avoid distorting the results, both TAC and GHG emissions are relativized with Eq(3) and Eq(4). Calculating the area between the reference point and the Pareto front determines the quality of the Pareto front (see Figure 2 on the right). The areas (hypervolume indicator) are used as the topologies' fitness for the GA selection process (the larger the area, the higher the fitness).

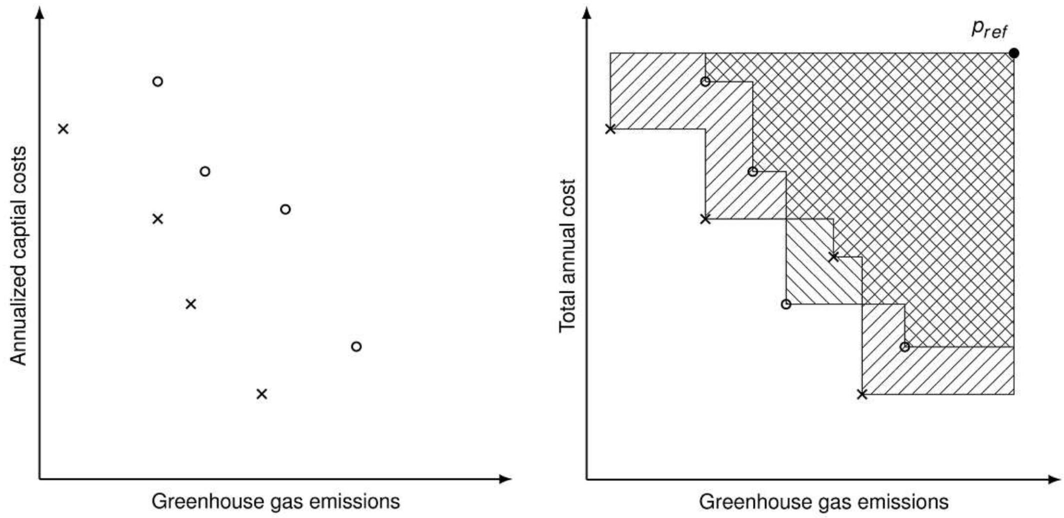

Figure 2: On the left, the 1st Pareto front (points marked with an x) and 2nd Pareto front (points marked with an o) created with the NSGA-II algorithm are shown. On the right, an exemplary hypervolume indicator for two different Pareto fronts is shown. In this case, the front, including points marked with an x, has a higher area resulting in a higher hypervolume indicator and thus a higher fitness.

3. Industrial case study: potato chips production

To illustrate the application of the algorithm, a potato chips production plant (fritter line 1) from the Zweifel Pomy-Chips AG is analyzed (Fotsch, 2006). It produced two types of chips: regular chips (w_{oil} = 0.35) and Cractive chips (w_{oil} = 0.25). A flow chart of the process is shown in Figure 3, the process requirements and the utility data are listed in Tables 1 and 2. The GHG emission coefficients in Table 2 are determined using data from BAFU (2022) for emissions caused by natural gas and (Krebs and Frischknecht, 2021) for emissions caused by the consumer electricity mix. A natural gas boiler supplies hot utility (HU) with an efficiency of 90% (0.22 t_{CO2eq}/MWh), and a refrigeration unit provides cold utility (CU) with a COP of 5.90 (0.02 t_{CO2eq}/MWh). A 10 y depreciation lifetime and 5 % interest rate are given for the cost evaluation. Further, cost data for equipment, modifications, and match costs are available by Stampfli et al. (2022a).

For the optimization, the practical constraints are limited as follows: the minimum temperature difference is set to $\Delta T_{min} = 2$ K, the minimal possible heat load to $\dot{Q}_{min} = 10$ kW, the maximum number of possible HEX is limited to $NE = 7$, the number of enthalpy stages is set to $NK = 3$, and the number of possible HEX within one split is limited to $\#E_{max} = 2$.

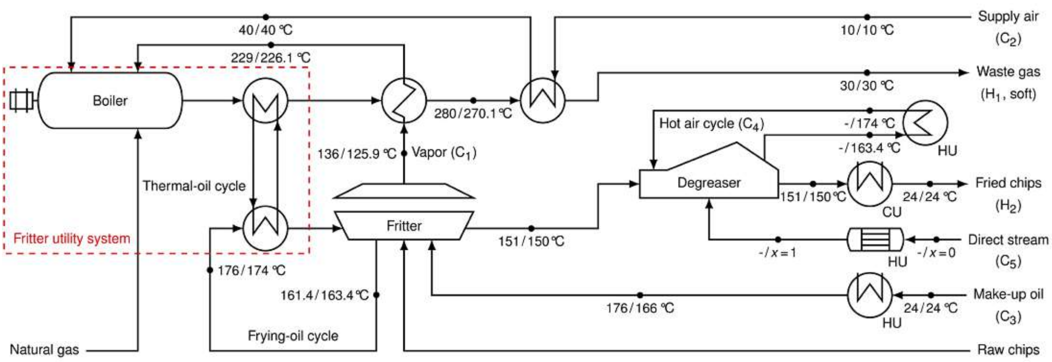

Figure 3: Flow chart of the fritter-line 1 plant for chips production at Zweifel. Stream temperatures correspond to the two OPs: regular chips / Cractive chips (Stampfli et al., 2022a).

Table 1: Process requirements of the fritter line 1 for both OPs

Stream	# (-)	T_S (°C)	T_T (°C)	$T_{extr.}$ (°C)	CP (kW/K)	h (W/(m^{2}K))
Regular chips (4,410 h/y)						
Vapor heating	C_1	136	229	500	2.51	400
Boiler air pre-heating	C_2	10	40	300	1.52	100
Make-up oil pre-heating	C_3	24	176	210	0.37	400
Degreaser air heating	C_4	-	-	-	-	-
Degreaser dir. steam evap.	C_5	-	-	-	-	-
Waste gas cooling*	H_1	280	30	30	14.81	400
Chips cooling	H_2	151	24	24	0.79	300
Cractive chips (2,610 h/y)						
Vapor heating	C_1	125.9	226.1	500	2.45	400
Boiler air pre-heating	C_2	10	40	300	1.48	100
Make-up oil pre-heating	C_3	24	166	210	0.18	400
Degreaser air heating	C_4	163.4	174	500	23.31	100
Degreaser dir. steam evap.	C_5	144.9	145.1	145.1	940.00	5,000
Waste gas cooling*	H_1	270.1	30	30	14.3	400
Chips cooling	H_2	150	24	24	0.55	300

*Soft streams.

Table 2: Utility data

Utility	# (-)	T_S (°C)	T_T (°C)	h (W/(m^{2}K))	c_U (CHF/MWh)	ξ_U (t_{CO2eq}/MWh)
Heating steam	HU	300	299	5,000	80	0.22*
Cooling water	CU	0	1	2,000	40	0.02**

*Natural gas boiler (η = 0.9)/ ** Refrigeration unit (COP = 5.90)

To ensure comparability with the published results (Stampfli et al., 2022a), the algorithm parameters are chosen to be similar. Only populations sizes are increased since with the additional objective function a larger solutions space is to be explored. For the GA, the population size is set to $NCT = 150$, for the tournament selection, the best of $NT = 5$ solutions is selected, the Hall of Fame size is set to $HoF = 100$, the crossover probability is set to $CR = 90\,\%$, the mutation probability is set to $MT = 10\,\%$, and the number of generations is set to $NGT = 75$. For the DE, the population size is set to $NCH = 200$, the Pareto front size is set to $NP = 20$, the crossover probability is set to $CR = 90\,\%$, the perturbation factor is set to $F_P = 0.5$, the number of generations is set to $NGH = 100$, and the number of generations without improvement is set to $NGHOP = 5$. The optimization was performed on a Linux-based server with 256 GB RAM, using 50 of the 128 available threads distributed over 64 CPU cores for parallel computing of the DE algorithm.

4. Results

The linear dependency between operating costs and GHG emissions is visible in the results by comparing TAC and GHG emissions (see Figure 4 on the left). Rather than a Pareto front, a single solution is found. By comparing the annualized capital costs and the GHG emissions in Figure 4 on the right, the linear dependency is omitted, and a Pareto front can be identified (red curve). Comparing the SOO_{TAC} result from Stampfli et al. (2022a) to the $MOO_{TAC,GHG}$ results shows that it is on the Pareto front. However, with the $MOO_{TAC,GHG}$ no results in this region with similar TAC are found (see Figure 4 on the left). This can be explained by the fact that the $MOO_{TAC,GHG}$ has a higher weight on the utilities. Besides considering the operating costs in the TAC objective, caused GHG emissions from the utilities represent the second objective. In Table 3, the result from the SOO_{TAC} is 12,780 CHF/y and 30.14 t_{CO2e}/y, almost double the operating costs and GHG emissions, compared to 6,888 CHF/y and 15.04 t_{CO2e}/y of the solution from the $MOO_{TAC,GHG}$. As a result of the lower utility demand, annualized capital costs for the $MOO_{TAC,GHG}$ are with 54,453 CHF/y higher than the 35,419 CHF/y of the SOO_{TAC}, which results in 61,341 CHF/y TAC compared to 48,198 CHF/y.

In Figure 4, on the right, grouped points represent a DE Pareto front. These fronts have all the same HEN topology but different heat load distributions. The range in annualized capital costs is relatively small compared to the range of GHG emissions. This indicates that changing the heat load distribution has a small effect on the

HEX areas, in contrast to the utility consumption, concluding that GHG emissions can be reduced without extensive topology modification.

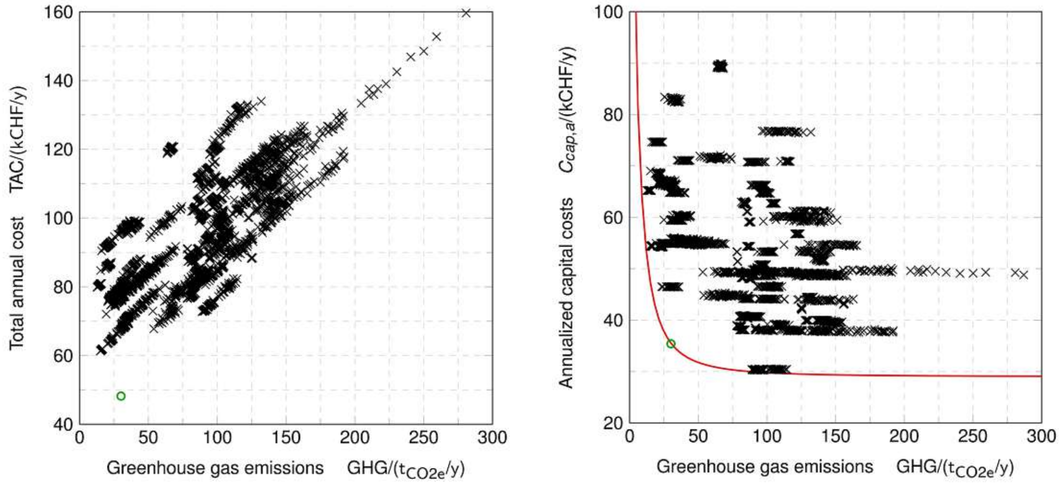

Figure 4: Optimization results using total annual cost and greenhouse gas emissions as objectives (MOO$_{TAC, GHG}$). The green circle indicates the solution of the SOO$_{TAC}$ from Stampfli et al. (2022a). On the left, the linear dependency between TAC and GHG emissions is visible. On the right, the Pareto front (red curve) between annualized capital costs and GHG emissions can be identified.

Table 3: Comparison of results for different objectives.

Optimization	TAC (CHF/y)	$C_{cap,a}$ (CHF/y)	$C_{op,a}$ (CHF/y)	GHG (t_{CO2e}/y)	Q_{HU} (MWh/y)	Q_{CU} (MWh/y)	OF$_{TAC}$ (-)	OF$_{cap,a}$ (-)	OF$_{GHG}$ (-)
Existing design	141,080	0	141,080	331.68	1451	623	1	-	1
SOO$_{TAC}$*	48,198	35,419	12,780	30.14	132	55	2.927	3.983	11.004
MOO$_{TAC,GHG}$	61,341	54,453	6,888	15.04	62	48	2.300	2.591	22.053
MOO$_{CAP,GHG}$	67,726	28,737	38,989	81.09	330	314	2.083	4.909	4.090

*Results from Stampfli et al. (2022a)

To analyze the influence, the weighting of the utility has, the operating costs $C_{cap,a}$ are excluded from the TAC objective. The results are visualized in Figure 5. Since utilities have a lower weight in this optimization, operating costs are a higher portion of the TAC. Therefore, on the left in Figure 5, the linear dependency between TAC and GHG emissions is more evident. On the right, it can be seen that the Pareto front is shifted down from the blue dashed curve (MOO$_{TAC,GHG}$) to the red curve (MOO$_{CAP,GHG}$). Thereby, no results in the region of the SOO$_{TAC}$ result (green circle) are found. In contrast to the TAC and GHG emission optimization, the SOO$_{TAC}$ result is not part of the Pareto front but dominates a large portion of the results. This indicates that by neglecting operating costs in the TAC objective, the weighting for the utilities is too low.
The results for MOO$_{TAC,GHG}$ and MOO$_{CAP,GHG}$ suggest that cost and emission coefficients strongly impact the weighting between costs and GHG emissions. By analyzing the ratio of the impact of 1 MWh utility reduction on the TAC and GHG emissions, using the existing plant as a reference, it can be shown that utility has around 18 % more impact on the cost than on the GHG emissions:

$$\frac{\mathrm{GHG}_{ex}\left(c_{HU,op} + c_{CU,op}\right)}{\mathrm{TAC}_{ex}\left(\xi_{HU,op} + \xi_{CU,op}\right)} = \frac{331.68\ \mathrm{t_{CO2eq}}/y\ (80\ \mathrm{CHF/MWh} + 40\ \mathrm{CHF/MWh})}{141{,}080\ \mathrm{CHF/y}\ \left(0.22\ \mathrm{t_{CO2eq}/MWh} + 0.02\ \mathrm{t_{CO2eq}/MWh}\right)} = 1.176 \quad (5)$$

This confirms the results in Table 3, where the utility is reduced less by the MOO$_{CAP,GHG}$ than by the SOO$_{TAC}$. By comparing all the objective values for the best-found solutions, the results suggest the SOO$_{TAC}$ had the highest impact on minimizing TAC, the MOO$_{TAC,GHG}$ had the highest impact on GHG emission minimization, and the MOO$_{CAP,GHG}$ has the highest impact on minimizing annualized capital costs.

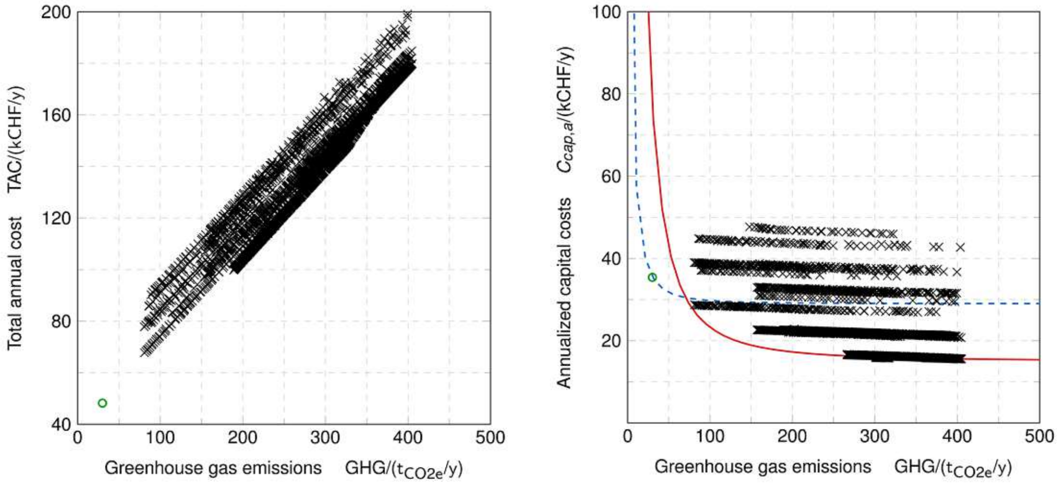

Figure 5: The optimization results using annualized capital costs and greenhouse gas emissions as objectives ($MOO_{CAP,GHG}$). The green circle indicates the solution of the SOO_{TAC} from Stampfli et al. (2022a). On the right, the new Pareto front between annualized capital costs and GHG emissions (red curve) and the Pareto front from $MOO_{TAC,GHG}$ (blue dashed curve), are visualized.

5. Conclusions

The hybrid two-level evolutionary-based algorithm for heat exchanger network (HEN) retrofit for multi-period processes using genetic algorithm (GA) for topology optimization and differential evolution (DE) for heat load optimization (Stampfli et al. 2022a) has been extended from single-objective optimization (SOO) to multi-objective optimization (MOO) to consider greenhouse gas (GHG) emissions as well. The selection process for both algorithms is modified to consider multiple objective functions. Using the non-dominated sorting genetic algorithm (NSGA-II), the DE algorithm returns a list of Pareto-optimal solutions for every HEN topology with respect to total annual cost (TAC) and GHG emissions. In the GA, the fitness of the Pareto fronts is quantified using hypervolume indicators.

The MOO introduces a linear dependency between operating costs (part of the TAC) and GHG emissions. The difference between GHG emissions and operating costs is using GHG emission coefficients instead of cost coefficients. Therefore, regarding TAC and GHG emissions, instead of a Pareto front, a single Pareto-optimal solution is found. However, with regard to annualized capital costs and GHG emissions, a Pareto front is identified. Comparing the result of the SOO from Stampfli et al. (2022a) to the MOO, it can be seen that it is part of the found Pareto front. However, with the MOO, no solutions in this region are found. This is because the MOO has a higher weight on the utility demand (operating costs and GHG emissions) compared to the SOO (only operating costs). As a result, the best-found solution of the MOO has 27 % higher TAC but 50 % lower GHG emissions than the SOO result.

The Pareto front analysis of a single topology (DE results) shows that changing the heat load distribution across the heat exchangers significantly impacts operating costs and GHG emissions but only a small impact on annualized capital costs.

To analyze the impact of the utility demand, another MOO is performed, which uses only annualized capital costs as the TAC (excluding operating costs). As a result, TAC's share of operating costs outweighs the annualized capital costs. Therefore, a large part of the Pareto front is dominated by the SOO solution, and the best-found MOO solution has higher TAC and GHG emissions.

Both results of the MOOs (with and without operating costs in the TAC objective) show that the introduction of GHG emission as a second objective shifts the optimum depending on the impact of utility reduction on the objective functions. The direction of the shift highly depends on the cost and emission coefficients. For the analyzed case study, the reduction of utility has an 18 % higher impact on operating costs than GHG emissions. Therefore, omitting operating costs in the TAC objective shifts the solution towards lower annualized capital costs but higher operating costs and GHG emissions. In contrast, considering operating costs in the TAC objective, the solution is shifted towards higher annualized capital costs but lower operating costs and GHG emissions.

In conclusion, the SOO is already considering GHG indirectly with the operating costs. By introducing GHG emissions as a second objective, operating costs should still be considered in the TAC. The MOO weights utility demand higher than the SOO, and thus results with lower GHG emissions can be expected. However, the awareness of the higher weight on utility demand is essential. Comparing the different objectives highlights the importance of cost and emission coefficients in the optimization. In future work, alternative objective combinations such as minimal operating costs and minimal annualized capital costs or minimal utility consumption and equipment sizes should be analyzed.

Acknowledgments

This research project is financially supported by the Swiss Innovation Agency Innosuisse and is part of the Swiss Competence Center for Energy Research – Efficiency of Industrial Processes SCCER EIP. Further financial support is provided by the Lucerne University of Applied Sciences and Arts, Switzerland. This research is part of a collaboration between the Lucerne University of Applied Sciences and Arts and TU-Wien.

References

Ahmad S., Smith R., 1989, Targets and design for minimum numbers of shells in heat exchanger networks. Chemical Engineering Research and Design, 67(5), 481-494.

Bundesamt für Umwelt (BAFU), 2022, CO2-Emissionsfaktoren des Treibhausgasinventars der Schweiz, Technical Report, Bundesamt für Umwelt (BAFU), Berne, Switzerland.

Chen J.J.J., 2019, Logarithmic mean: Chen's approximation or explicit solution? Computers and Chemical Engineering, 120, 1-3.

Deb, Pratab, Agarwal, Meyarivan, 2000, A fast elitist non-dominated sorting genetic algorithm for multi-objective optimization: NSGA-II. Lecture notes in computer science, 849-858.

Fortin F.-A., De Rainville, F.-M., Gardner M.-A., Parizeau, M., Gagné C., 2012, Deap: evolutionary algorithms made easy. Journal of Machine Learning Research, 13, 2171–2175.

Fortin F.-A., Grenier S., Parizeau M., 2013, Generalizing the improved run-time complexity algorithm for non-dominated sorting. GECCO '13: Proceedings of the 15th annual conference on Genetic and evolutionary computation, 615-622.

Fotsch P., 2006, Pilotpahse Pinch-Methodik 2006/07: Zweifel Pomy-Chips AG. Technical Report, Swiss Federal Office of Energy SFOE, Zurich, Switzerland.

Kang L., Yongzhong L., 2017, A systematic strategy for multi-period heat exchanger network retrofit under multiple practical restrictions. Chinese Journal of Chemical Engineering, 25(8), 1043-1051.

Klemeš J.J. (Ed), 2013, Handbook of Process Integration (PI): Minimisation of Energy and Water Use, Waste and Emissions, Woodhead Publishing Limited/Elsevier, Cambridge, UK.

Krebs L., Frischknecht R., 2021, Umweltbilanz Strommixe Schweiz 2018. Technical Report, Bundesamt für Umwelt (BAFU), Berne, Switzerland.

Linnhoff B., Flower J.R., 1978, Synthesis of Heat Exchanger Networks I: Systematic Generation of Energy Optimal Networks. AIChE Journal, 24, 633-642.

Sreepathi B.K., Rangaiah G.P., 2014, Improved heat exchanger network retrofitting using exchanger reassignment strategies and multi-objective optimization., Energy, 67(1), 584-594.

Sreepathi B.K., Rangaiah G.P., 2015, Retrofitting of heat exchanger networks involving streams with variable heat capacity: Application of single and multi-objective optimization. Applied Thermal Engineering, 75(22), 677-684.

Stampfli J.A., Ong B.H.Y. Olsen D.G., Wellig B., Hofmann R., 2022a, Applied heat exchanger network retrofit for multi-period processes in industry: a hybrid evolutionary algorithm. Computers and Chemical Engineering, 161, 107771.

Stampfli J.A., Olsen D.G., Wellig B. Hofmann R., 2022b, A parallelized hybrid genetic algorithm with differential evolution for heat exchanger network retrofit. MethodsX, 9, 101711.

Stampfli J.A., Olsen D.G., Wellig B. Hofmann R., 2020, Heat exchanger network retrofit for processes with multiple operating cases: a metaheuristic approach. In: Proceedings of the 30th European Symposium on Computer Aided Process Engineering, 48:781 – 786.

Toimil, D., Gómez, A., 2016, Review of metaheuristics applied to heat exchanger network design. International Transactions in Operational Research, 24(1-2), 7-26.

Yee T.F., Grossmann I.E., 1990, Simultaneous optimization models for heat integration - II. Heat exchanger network synthesis. Computers and Chemical Engineering, 14(10), 1165-1184.

Zitzler E., Thiele L. Laumanns M., Fonseca C.M., Da Fonseca V.G., 2003, Performance assessment of multi-objective optimizers: An analysis and review. IEEE Transactions on Evolutionary Computation, 7(2),117–132.

Article 6

Multi-Objective Evolutionary Optimization for Multi-Period Heat Exchanger Network Retrofit

published in Energy in collaboration with Benjamin H.Y. Ong, Donald G. Olsen, Beat Wellig, and René Hofmann

This journal article is an invited contribution to the special issue of the 25th Conference on Process Integration, Modelling and Optimisation for Energy Saving and Pollution Reduction of the Energy journal. The article explains the multi-objective approach from Article 5 in more detail. The results analyze how well the area of all HEXs are utilized over each operating period. Further, the influence of the selection of the objective functions on the final design is analyzed.

My contribution: Conceptualization, Methodology, Software, Validation, Formal analysis, Investigation, Data curation, Writing –original draft, Visualization, Writing –review & editing.

Stampfli, J. A., Ong, B. H., Olsen, D. G., Wellig, B., and Hofmann, R. (2023). Multi-objective evolutionary optimization for multi-period heat exchanger network retrofit. Energy *281, p. 128175.*

DOI: 10.1016/j.energy.2023.128175

Energy 281 (2023) 128175

Contents lists available at ScienceDirect

Energy

journal homepage: www.elsevier.com/locate/energy

Multi-objective evolutionary optimization for multi-period heat exchanger network retrofit

Jan A. Stampfli [a,b,*], Benjamin H.Y. Ong [a], Donald G. Olsen [a], Beat Wellig [a], René Hofmann [b]

[a] Lucerne University of Applied Sciences and Arts, Competence Center Thermal Energy Systems and Process Engineering, Technikumstrasse 21, 6048 Horw, Switzerland

[b] TU-Wien, Institute of Energy Systems and Thermodynamics, Getreidemarkt 9/BA, 1060 Vienna, Austria

ARTICLE INFO

Keywords:
Heat exchanger network (HEN)
Retrofit
Multi-period
Greenhouse gas emissions
Pareto optimization
NSGA-II
Hypervolume indicator

ABSTRACT

Increase in energy efficiency and reduction in greenhouse gas (GHG) emissions in industry are important steps towards a more sustainable economy. Due to the growing share of high value-added industries multi-period operation becomes more common in process industry. Therefore, retrofit of existing multi-period production plants is a key aspect towards more sustainable production processes. Hence, in this work, an existing two-level evolutionary algorithm using a genetic algorithm and a differential evolution for multi-period heat exchanger network retrofit is extended to consider GHG emissions as a second objective to the total annual cost (TAC). The multi-objective problem is addressed by incorporating a non-dominated sorting genetic algorithm (NSGA-II) and hypervolume indicators into the algorithm. By analyzing an industrial case study of a potato chips production, the results of the multi-objective optimization shows that GHG emissions can be reduced by 50%. However, compared to the single-objective optimization, TAC is increased by 27%. By selecting capital costs and operating costs as objectives instead, similar results to the single-objective optimization are achieved showing that the results are highly dependent on the selection of the objectives. Further, changes in utility costs and caused emissions have a high impact on the results.

1. Introduction

In view of the policy objective of net-zero carbon emissions, the deepest possible level of decarbonization must be achieved in all sectors. However, decarbonization of the industry sector is challenging due to the high complexity of the systems, heterogeneity, and high temperature levels. The systematic overall optimization of processes, in terms of their energy consumption, is referred to as Process Integration (PI) [1], with Heat Exchanger Networks (HEN) representing a key strategy [2]. Methods and tools are required for retrofitting pre-existing processes (brownfield), particularly multi-period processes, considering the overwhelming share of high value-added industries present in Switzerland (e.g., fine chemicals, pharma, food, beverages). Furthermore, in many Swiss companies, one single processing line is used to manufacture a portfolio of products, resulting in multi-period problems and representing additional challenges for PI. Methods are available for greenfield process design, e.g., Aguitoni et al. [3] used a bi-level optimization approach of Simulated Annealing and Differential Evolution (DE) to synthesize HEN. Pavão et al. [4] used metaheuristic approach, based on Simulated Annealing and Rocket Fireworks Optimization, to synthesize and efficient multi-period HEN. The approach was coupled with post-optimization strategy to further improve the total annual cost. The challenges and research conducted to optimize multi-period processes have been reviewed by Stampfli et al. [5].

To reach higher levels of rigor, reproducibility, and comparability, HEN retrofit for multi-period processes based on mathematical optimization needs to be developed. Some research has already been conducted with mathematical-based optimization, which can be divided into stochastic and deterministic methods. Deterministic approaches are very challenging for HEN retrofit being a more complex subproblem of HEN synthesis. The latter is already hard to solve without metaheuristic solvers due to the high complexity of mixed-integer nonlinear characteristics of the problem. Considering, among other things, the increased availability of computational power, Toimil and Gómez [6] explained why there is a trend towards stochastic optimization methods, in particular towards metaheuristics. Metaheuristics combine simple local search methods (heuristics) with an algorithm to explore the search space to find an optimal or near-optimal solution.

* Corresponding author at: Lucerne University of Applied Sciences and Arts, Competence Center Thermal Energy Systems and Process Engineering, Technikumstrasse 21, 6048 Horw, Switzerland.

E-mail addresses: jan.stampfli@hslu.ch (J.A. Stampfli), benjamin.ong@hslu.ch (B.H.Y. Ong), donald.olsen@hslu.ch (D.G. Olsen), beat.wellig@hslu.ch (B. Wellig), rene.hofmann@tuwien.ac.at (R. Hofmann).

https://doi.org/10.1016/j.energy.2023.128175
Received 26 January 2023; Received in revised form 1 June 2023; Accepted 18 June 2023
Available online 21 June 2023

Nomenclature

Sets

$C = \{0 \ldots j \ldots NC\}$	Set of cold streams
$E = \{0 \ldots e \ldots NE\}$	Set of heat exchangers
$H = \{0 \ldots i \ldots NH\}$	Set of hot streams
$K = \{0 \ldots k \ldots NK\}$	Set of enthalpy stages
$OP = \{0 \ldots op \ldots NOP\}$	Set of operating periods

Parameter

A	Heat exchanger area (m^2)
C	Cost factor (CHF)
c	Specific cost factor (e.g., CHF/m^2)
CP	Heat capacity flow rate (kW/K)
f_d	Degression exponent (–)
h	Film heat transfer coefficient (W/(m^2 K))
i_r	Interest rate (–)
n	Depreciation period (y)
Q	Thermal energy (kWh)/ Quantity ([Q])
$\dot{Q}$	Heat flow (kW)
T	Temperatures (°C)
w	Mass fraction (–)

Greek letters

ΔT	Temperature difference (K)
Δt	Time duration (h)
η	Efficiency coefficient (–)
ξ	Emission factor ($t_{CO2/MWh}$)

Subscripts

a	Annualized
0	Base
cap	Capital
op	Operating
c	Cold side
h	Hot side
$init$	Initial
in	Inlet
out	Outlet
R	Removal
S	Supply
T	Target
U	Utility

Abbreviations

CAP	Annualized capital costs
COP	Operating costs/Coefficient of performance
CU	Cold utility
DE	Differential evolution
FOEN	Federal Office for the Environment
GA	Genetic algorithm
GHG	Greenhouse gas
HEN	Heat exchanger network
HEX	Heat exchanger
HU	Hot utility
MOO	Multi-objective optimization
NSGA-II	non-dominant sorting genetic algorithm
OF	Objective function
SOO	Single-objective optimization
SWS	Stage-wise superstructure
TAC	Total annual cost

A subgroup of metaheuristics is population-based algorithms such as Genetic Algorithms (GA) and DE. GA is a stochastic method based on the concept of survival of the fittest by comparing a population of solutions and selecting the best for further exploration. DE is similar to GA but designed to optimize continuous variables such as heat loads. Application of both GA/DE has been conducted by Stampfli et al. [7]. HEN problems can be divided into two classifications, single objective optimization (SOO), focusing on reducing total annual cost (TAC), and multi-objective optimization (MOO). MOO adds a layer of complexity to the optimization for the retrofit of existing HEN. Only limited research has been conducted on MOO of HEN retrofit, which is the focus of this paper. Sreepathi and Rangaiah [8] developed a MOO to retrofit HEN, where the objective functions are utility and investment costs. The authors used a program based on the non-dominated sorting genetic algorithm (NSGA-II), resulting in better MOO solutions. The authors then extended the work to retrofit HEN involving streams with variable heat capacity [9]. Their continuous approach to handling the variable heat capacity provided better and more practical solutions for the retrofit of HEN. Kang and Liu [10] developed a three-stage MOO procedure to retrofit multi-period HENs. The model has two objective functions, either total annual CO_2 emissions with capital costs for retrofit, number of substituted heat exchangers (HEXs), modification to the existing HEN structure, or additional heat transfer areas. With the current focus on reducing the GHG emissions of the industrial sector, this paper extends the work carried out by Stampfli et al. [5] to include GHG emissions in the MOO for multi-period HEN retrofit.

2. Problem statement

In previous work a two-stage genetic algorithm with differential evolution was developed to solve HEN retrofit for multi-period problems with minimal TAC [5]. A large focus of this work was on the practicality and implementation of the new designs. Therefore, additional practical constraints such as limiting the complexity by restricting stream splitting or considering additional costs for piping and control systems are considered in the optimization. As a result, the method aims to find practical implementable designs rather than global optimum designs.

An important factor for the environment in retrofit projects is the emitted GHG. The main cause of GHG emissions is the utility which is usually provided using natural gas boilers (Scope-2 emissions). Gray GHG emissions (Scope-3 emissions) are not considered as they usually account for a negligible share of the total emissions in HEN design [11]. Hence, this work extends the previous developed SOO to a MOO by considering GHG emissions as a second objective. By introducing a second objective, instead of having one single best solution, a Pareto front of non-dominated solutions will be generated. Therefore, the following research questions need to be addressed: (1) How can the existing evolutionary algorithm be extended to handle multi-objective problems and generate a Pareto front? and (2) What are the influences on the solution by considering GHG emissions as a second objective?

To address the research question (1), the algorithm will be extended by integrating an NSGA-II in the differential evolution to generate Pareto fronts of the heat load distributions for a given HEN topology. In the topology optimization, these fronts need to be compared with each other. Therefore, the concept of hypervolume indicators is used to create a fitness value for each Pareto front. To answer research question (2), the impact of the utility demand on the two objectives is to be analyzed as it is considered in both. Therefore, experiments are performed using different objectives (e.g. excluding operating costs (utility demand) in TAC).

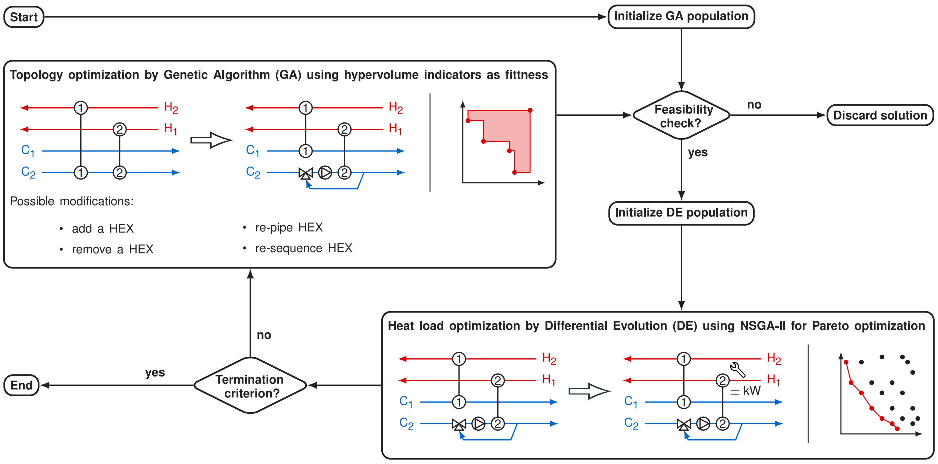

Fig. 1. Overview of the two-stage evolutionary algorithm for multi-objective optimization.

3. Methods

For the MOO, the single-objective hybrid evolutionary algorithm for HEN retrofit for multi-period processes [7] was later extended to consider detailed mixer configurations [5]. In this work, it has been further developed to include GHG emissions as a second objective in the optimization. An overview of the algorithm is shown in Fig. 1 and summarized in Section 3.1. A detailed explanation of the algorithm, including its application, is provided by Stampfli et al. [5], and details on the implementation in Python 3.8.2 using the library DEAP - Distributed Evolutionary Algorithms in Python [12] is provided by Stampfli et al. [13].

The hybrid evolutionary algorithm has two stages whereby in the top-stage, the topology of the HEN (discrete variables) is optimized using a GA. For every feasible HEN design, the DE in the sub-stage optimizes for the best heat load distribution over the network (continuous variables). Thereby, a population of potential solutions is evaluated using a HEN model. To determine the fitness of the solutions, the TAC is used. Constraints are implemented as following: (1) often violated constraints such as energy balances are handled using penalizing strategies, and (2) constraints which would create impossible solutions such as maximal possible heat load of a HEX are handled with decoding strategies. In this work, GHG emissions are introduced as a second fitness function. The functions needed to extend the existing algorithm are provided in Section 3.2. For the selection of the multi-objective fitness in the DE, the NSGA-II is used to produce a Pareto front in which every solution has a fixed HEN topology but different heat loads. The concepts of the NSGA-II selection and the integration into the DE are explained in Section 3.3. In the GA, topologies are evaluated. Therefore, the hypervolume for every Pareto front is calculated and used as its fitness. The hypervolume calculation and its integration in the GA are explained in Section 3.4. The SOO as well as the MOO version of the algorithm are available online and published under an open source licence [15,16].

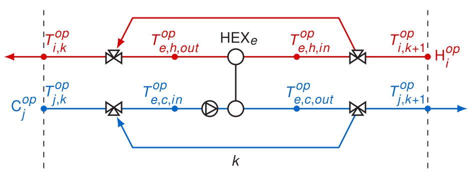

Fig. 2. Superstructure for the mixer configurations whereas $T^{op}_{i,k}$ and $T^{op}_{j,k}$ are the enthalpy stage temperatures, and $T^{op}_{e,h,in}$, $T^{op}_{e,c,in}$, $T^{op}_{e,h,out}$, and $T^{op}_{e,c,out}$ are the inlet and outlet temperatures of the HEX which are manipulated by the selected mixer configuration and determined using the Chen's explicit solution approach [5,14].

3.1. Heat exchanger network model

The HEN model introduced by Stampfli et al. [5,13] is reused in this work and summarized in this section. Yee and Grossmann [17] stage-wise superstructure (SWS) is used as a base of the model. It is extended with (1) an additional dimension of operating periods (OPs), (2) utility heat exchanger within the enthalpy stages, and (3) selection and calculation of detailed mixer configuration (superstructure for the mixer configurations is shown in Fig. 2) using the explicit solution of the logarithmic mean [14]. Therefore, (3) uses the Lambert W-function [18] to ensure feasible heat transfer in every OP. (4) In industry, non-process streams such as exhaust gas are often so-called soft streams which can, but do not have to be cooled down. Thus, the SWS model is extended to handle such streams, which have no fixed target temperature and no need for utility. To ensure practical results, additional constraints are added to the SWS: (1) the number of splits per stream and enthalpy stage can be limited to prevent an unnecessary number of splits (Spaghetti design) [19], and (2) to set limits on extreme temperatures (e.g., phase change) for every stream which cannot be exceeded or fallen short of, respectively. This constraint ensures feasible temperatures in the mixer configurations. The fitness of the retrofitted network is determined using the TAC as the objective function (OF), which is composed of capital and operating costs. Thereby, capital costs for adding or removing area, new HEXs, and new mixer configurations are considered. Further, the capital costs include modification costs for re-piping and re-sequencing of HEXs and resulting piping costs (depending on the plant layout). Finally, the utility costs are considered as the operating costs.

3.2. Extension to multi-objective optimization

The model described in Section 3.1 is extended for MOO by adding GHG emissions as a second OF. GHG emissions are based on utility consumption and can be determined by

$$\mathrm{GHG} = \sum_{\forall op} \left(\dot{Q}_{HU,op}\, \xi_{HU,op} + \dot{Q}_{CU,op}\, \xi_{CU,op} \right) \Delta t^{op} \tag{1}$$

Thereby, $\dot{Q}^{op}_{HU}$ and $\dot{Q}^{op}_{CU}$ describe the hot and cold utility (HU and CU) demands, respectively, in an operating period (OP). ξ^{op}_{HU} and ξ^{op}_{CU} are

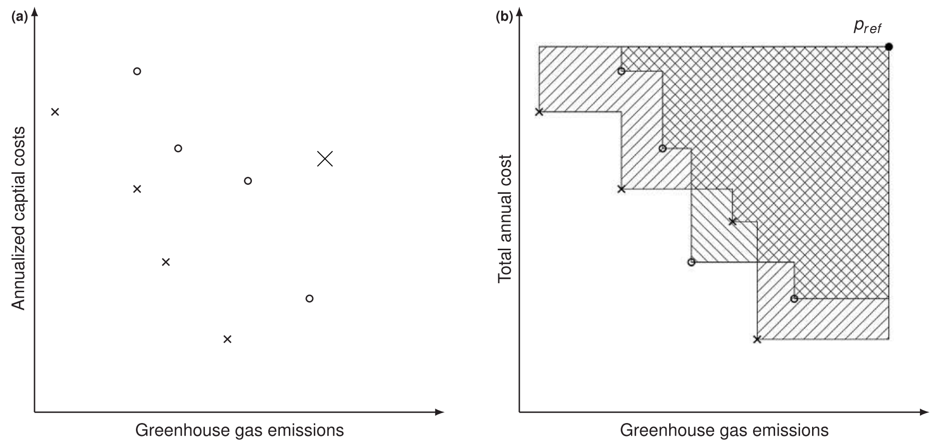

Fig. 3. (a) Exemplary Pareto fronts created by the NSGA-II selection. Multiple ranks of non-dominated Pareto fronts are created by ignoring the higher ranked fronts before. The 1st Pareto front points are marked with an "x" and 2nd Pareto front points are marked with an "o". (b) Exemplary hypervolume indicator for two different Pareto fronts is shown. In this case, the front, including points marked with an "x", has a higher area, resulting in a higher hypervolume indicator and thus a higher fitness.

CO_2 emission factors and Δt^{op} is the duration of the associated OP. The objective for the SOO is the TAC determined by

$$\mathrm{TAC} = C_{cap,a} + C_{op,a} = C_{cap,a} + \sum_{\forall op} \left(\dot{Q}_{HU,op}\, c_{HU,op} + \dot{Q}_{CU,op}\, c_{CU,op} \right) \Delta t^{op} \tag{2}$$

whereby $C_{cap,a}$ is the annualized capital costs. The operating costs $C_{op,a}$ depend on the utility demands $\dot{Q}^{op}_{HU}$ and $\dot{Q}^{op}_{CU}$ in the same way as the GHG but using specific cost factor c^{op}_{HU} and c^{op}_{CU} instead of specific emission factor ξ^{op}_{HU} and ξ^{op}_{CU}. This similarity of both functions creates a dependency between both objectives. Therefore, its effect on the results must be analyzed and compared to alternative objectives. To omit distorting of the solutions due to the different order of magnitudes in objectives, both are referenced to the initial HEN:

$$\mathrm{OF}_{\mathrm{TAC}} = \frac{\mathrm{TAC}_{init}}{\mathrm{TAC}} \tag{3}$$

$$\mathrm{OF}_{\mathrm{GHG}} = \frac{\mathrm{GHG}_{init}}{\mathrm{GHG}} \tag{4}$$

3.3. Differential evolution with NSGA-II selection for Pareto optimization

For the extension to a MOO, the selection in the DE needs to be adapted so that the algorithm can select solutions based on two instead of only one objective using NSGA-II [20]. For a given HEN topology, non-dominated solutions (there is no solution that is fitter in one objective without being less fit in another objective) with different heat load distributions are selected in a Pareto front (see points marked with an "x" in Fig. 3(a)). The NSGA-II algorithm stores multiple fronts. By ignoring the non-dominated solutions stored in the 1st front, a 2nd front (see points marked with an "o" on the diagram in Fig. 3(a)) can be generated, which is only dominated by solutions in the 1st front. The solutions are sorted using the generalized reduced run-time complexity non-dominated sorting algorithm [21]. During the optimization of the heat loads in the DE, the whole list with all the Pareto fronts is considered, but only the non-dominated Pareto front is returned to the GA.

3.4. Genetic algorithm with hypervolume indicator for Pareto selection

The DE returns a Pareto front of non-dominated solutions for every HEN topology. To compare the Pareto fronts between different topologies, the fitness of each front is quantified using hypervolume indicators [22]. Thereby a reference point, p_{ref}, that is worse than every point in all the Pareto fronts is set. To avoid distorting the results, both TAC and GHG emissions are relativized with Eqs. (3) and (4). The area between the reference point and each Pareto front is the hypervolume and thus indicates the quality of the Pareto front (see Fig. 3(b)). These hypervolumes are used as the topologies' fitness for the GA selection process (the larger the area, the higher the fitness).

4. Industrial case study: potato chips production

To illustrate the application of the algorithm, a potato chips production plant (fritter line 1) from the Zweifel Pomy-Chips AG is analyzed by Fotsch [23]. It produces two types of chips: regular chips (w_{oil} =

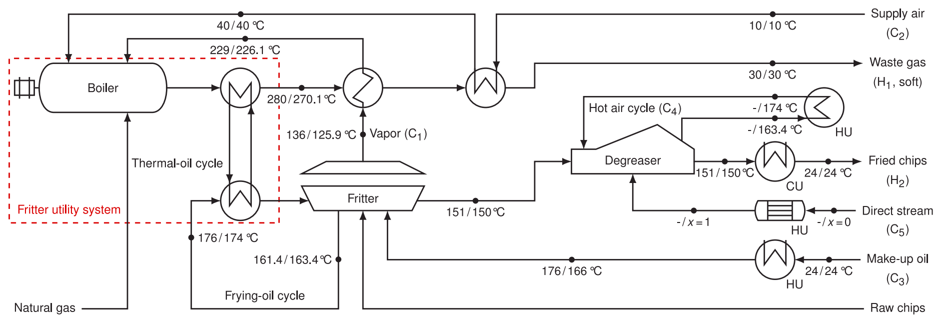

Fig. 4. Flow chart of the fritter-line 1 plant for chips production. Stream temperatures correspond to the two OPs: regular chips/Cractive chips [5].

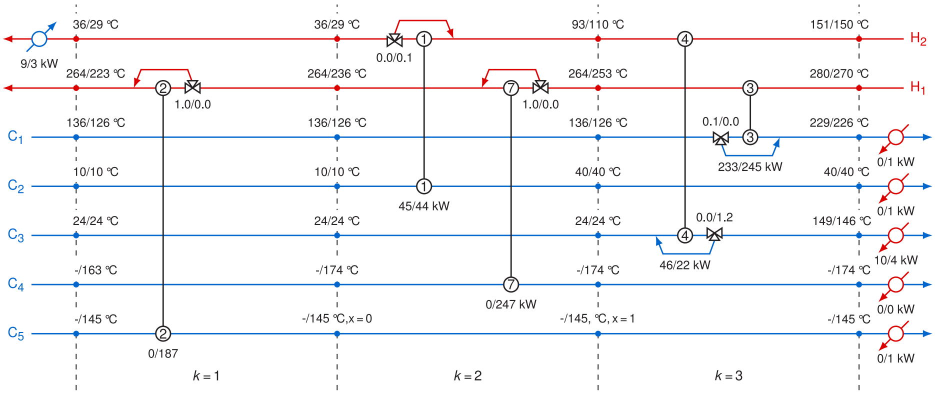

Fig. 5. Retrofitted HEN optimized by the $MOO_{TAC,GHG}$ algorithm configuration.

0.35) and Cractive chips (w_{oil} = 0.25). A flow chart of the process is shown in Fig. 4, the process requirements and the utility data are listed in Tables A.1 and A.2. The GHG emission factors in Table A.2 are determined using data published by the Federal Office for the Environment [24] for emissions caused by natural gas, and by Krebs and Frischknecht [25] for emissions caused by the consumer electricity mix. A natural gas boiler supplies hot utility with an efficiency of 90% (0.22 $t_{CO2e/MWh}$), and a refrigeration unit provides cold utility with a COP of 5.90 (0.02 $t_{CO2e/MWh}$). It is important to note, that the published data by Fotsch [23] uses pseudo-utilities which are not updated with realistic utilities in order to produce comparable results. Related investement costs and match costs for retrofit are listed in Tables A.3 and A.4. A 10 y depreciation period and 5% interest rate are given for the cost evaluation. For the optimization, the practical constraints are limited as follows: the minimum temperature difference is set to ΔT_{min} = 2 K, the minimal possible heat load to $\dot{Q}_{min}$ = 10 kW, the maximum number of possible HEX is limited to NE = 7, the number of enthalpy stages is set to NK = 3, and the number of possible HEX within one split is limited to $\#E_{max}$ = 2. To ensure comparability with the published results [5], the algorithm parameters are chosen to be similar. Only populations sizes are increased since with the additional objective function, a larger solutions space is to be explored. For the GA, the population size is set to 150, for the tournament selection, the best of 5 solutions is selected, the Hall of Fame size is set to 100, the crossover probability is set to 90%, the mutation probability is set to 10%, and the number of generations is set to 75. For the DE, the population size is set to 200, the Pareto front size is set to 20, the crossover probability is set to 90%, the perturbation factor is set to 0.5, the number of generations is set to 100, and the number of generations without improvement is set to 5. The optimization was performed on a Linux-based server with 256 GB RAM, using 50 of the 128 available threads distributed over 64 CPU cores for parallel computing of the DE algorithm.

5. Results

The results are split in three sections. First, in Section 5.1 the MOO solution is compared to the SOO solution published by Stampfli et al. [5], then in Section 5.2, the influences of the different objectives on the results is analyzed, and finally, in Section 5.3, the performance of the algorithm is analyzed and compared to the SOO algorithm configuration.

5.1. Comparison of the multi-objective to single-objective optimization

The resulting topology of the MOO, as shown in Fig. 5, is similar to the SOO result (shown in Fig. 6). It is important to notice that HEXs 3-7 are new, and therefore interchangeable without causing additional cost. For the MOO design, there is no process internal utility HEX. Although, the stream matches are identical, on process stream H_1, the order of the two last HEX (in declining temperature direction) is exchanged. In contrast to the SOO design, the MOO design re-uses HEX 2 from the initial design. Therefore, its HEX area needs to be increased by 8.6 m^2. Further, the placement of HEX 1 has changed and therefore, needs to be re-piped. In the SOO design, HEX 1 was not modified at all. In Table 1, the needed area to ensure feasible heat transfer in

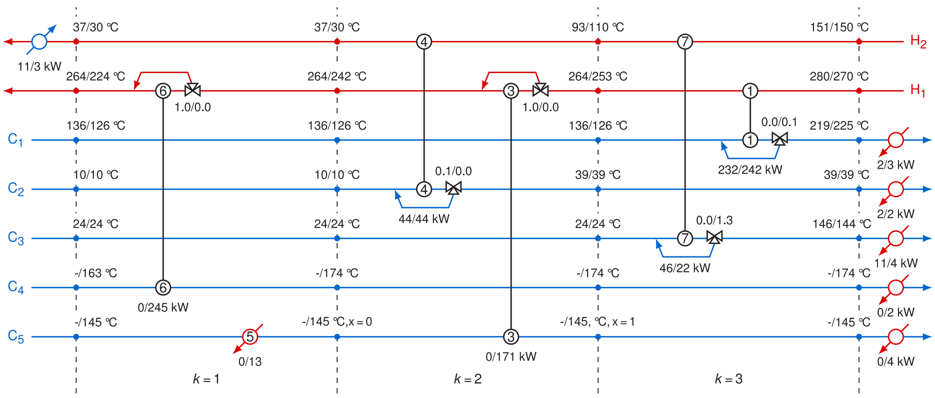

Fig. 6. Retrofitted HEN optimized by the SOO_{TAC} algorithm configuration [5].

Table 1
Comparison of areas between the best found solution and the initial solution.

HEX	Initial design			SOO_{TAC}			$MOO_{TAC,GHG}$		
	$A_e^{op=1}$ m^2	$A_e^{op=2}$ m^2	$\Delta A_{e,not}$ $(m^2\,h)/h$	$A_e^{op=1}$ m^2	$A_e^{op=2}$ m^2	$\Delta A_{e,not}$ $(m^2\,h)/h$	$A_e^{op=1}$ m^2	$A_e^{op=2}$ m^2	$\Delta A_{e,not}$ $(m^2\,h)/h$
Process HEX									
1	14.0	16.0	1.26	13.8	15.2	0.88	16.0	15.1	0.33
2	2.4	2.5	0.06	–	–	–	0.0	11.1	6.97
3	–	–	–	0.0	8.4	5.28	13.9	15.5	1.01
4	–	–	–	15.0	15.0	0.00	13.8	5.0	3.27
5	–	–	–	0.0	0.2	0.13	–	–	–
6	–	–	–	0.0	19.1	12.00	–	–	–
7	–	–	–	13.0	4.3	3.23	0.0	16.2	10.18
Balance utility HEX[a]									
CU_1	–	–	–	–	–	–	–	–	–
CU_2	5.6	3.9	0.63	1.4	0.4	0.37	1.2	0.4	0.30
HU_1	–	–	–	0.1	0.1	0.00	0.0	0.1	0.06
HU_2	–	–	–	0.1	0.1	0.00	0.0	0.1	0.06
HU_3	0.8	0.4	0.15	0.2	0.1	0.04	0.2	0.1	0.04
HU_4	0.0	4.8	3.02	0.0	0.1	0.06	0.0	0.0	0.00
HU_5	0.0	0.5	0.31	0.0	0.1	0.06	0.0	0.1	0.06
$\sum_{\forall e} \Delta A_{e,not}$ $((m^2\,h)/h)$			5.43			22.05			22.28
$\Delta A_{not,rel}$ $((m^2\,h)/(m^2\,h))$			0.18			0.30			0.30

[a]Balance utility HEX number is corresponding to the connected process stream (e.g., CU_1 at the end of H_1).

Table 2
Comparison of results for different objectives configurations (lowest TAC).

Configuration	TAC (CHF/y)	$C_{cap,a}$ (CHF/y)	$C_{op,a}$ (CHF/y)	GHG (t_{CO2e}/y)	Q_{HU} (MWh/y)	Q_{CU} (MWh/y)	OF_{TAC} (–)	$OF_{cap,a}$ (–)	$OF_{cop,a}$ (–)	OF_{GHG} (–)
Initial	141,080	0	141,080	331.68	1451	623	1.000	–	1.000	1.000
SOO_{TAC}[a]	48,198	35,419	12,780	30.14	132	55	2.927	3.983	11.039	11.004
$MOO_{TAC,GHG}$	61,341	54,453	6,888	15.04	62	48	2.300	2.591	20.482	22.053
$MOO_{CAP,GHG}$	67,726	28,737	38,989	81.09	330	314	2.083	4.909	3.618	4.090
$MOO_{CAP,COP}$	50,427	37,299	13,128	30.82	131	67	2.798	3.782	10.746	10.762
$MOO_{CAP,COP}$[b]	49,002	35,153	13,848	33.27	142	62	2.879	4.013	10.188	9.969

[a]Results by Stampfli et al. [5].
[b]Manually inserted topology of SOO_{TAC}[a] into the initial population.

every OP, are compared. The total area needed for the initial design is 30.2 m^2, for the SOO_{TAC} 72.9 m^2, and for the $MOO_{TAC,GHG}$ 74.3 m^2. To determine how well the areas of the HEXs are utilized, the not-in-use area is weighted by its downtime

$$\Delta A_{e,not} = \sum_{\forall op} \left(\left(\max_{\forall op} \left(A_e^{op} \right) - A_e^{op} \right) \frac{\Delta t^{op}}{\sum_{\forall op} \Delta t^{op}} \right). \tag{5}$$

To compare the not-in-use area with other network configurations with different total areas, the not-in-use area is expressed as a ratio to the total area

$$\Delta A_{not,rel} = \frac{\sum_{\forall e} \Delta A_{e,not}}{\sum_{\forall e} \max_{\forall op} \left(A_e^{op} \right)}. \tag{6}$$

By reducing the utility demand, the HEXs need to be more flexible to be able to compensate the different heat recovery in every OP. Therefore, it is expected that the higher the heat recovery and/or the number of HEX units in each OP is, the higher the difference in needed HEX areas between the OPs. This leads to a higher overall not-in-use areas. The results in Table 1 show the same conclusion, whereby the ratio of not-in-use area for the initial design of 0.18 is increased to 0.30 for the SOO_{TAC} and the $MOO_{TAC,GHG}$ designs. Utility demands for the $MOO_{TAC,GHG}$ is halved compared to the SOO_{TAC} solution (see Table 2, however by having one less HEX, the ratio of not-in-use area is insignificantly different.

5.2. Analysis of objectives

By including GHG emission as a second objective in the optimization, a linear dependency on utility demand between both objectives is introduced. This dependency is visible in the results by comparing TAC and GHG emissions (see Fig. 7(a)). Rather than a Pareto front, a single best solution is found. By comparing the annualized capital costs and the GHG emissions in Fig. 7(b) the linear dependency is omitted, and a Pareto front can be identified (red curve). By comparing the SOO_{TAC} result from Stampfli et al. [5] to the $MOO_{TAC,GHG}$ results shows that SOO_{TAC} is also a Pareto optimal solution for the $MOO_{TAC,GHG}$ optimization (green dot). However, with the $MOO_{TAC,GHG}$ no results in this region with similar TAC are found (see Fig. 7(b)). This can be explained by the fact that the $MOO_{TAC,GHG}$ has a higher weight on the utility demand as they are represented in both objectives. Fig. 7(b), shows multiple sets of identifiable DE Pareto fronts. These fronts have all the same HEN topology but different heat load distributions. The range in annualized capital costs is relatively small compared to the range of GHG emissions. This indicates that changing the heat load distribution has a small effect on the HEX areas in contrast to the utility consumption. This concludes that GHG emissions can be reduced without extensive topology modification.

To analyze the influence of the weighting of the utility on the results, operating costs $C_{cap,a}$ are excluded from the TAC objective. The results are visualized in Fig. 8. Since utility demand has a lower weight on the results, operating costs are a higher portion of the TAC. Therefore, in Fig. 8(a), the linear dependency between TAC and GHG emissions is more evident. In Fig. 8(b), it can be seen that the Pareto front is shifted down from the blue dashed curve ($MOO_{TAC,GHG}$) to the red curve ($MOO_{CAP,GHG}$). Thereby, no results in the region of the SOO_{TAC} result (green point) are found. In contrast to the TAC and GHG emission optimization, the SOO_{TAC} result is not part of the Pareto front but dominates a large portion of the results. The results for $MOO_{TAC,GHG}$ and $MOO_{CAP,GHG}$ suggest that cost and emission factors strongly impact the weighting between costs and GHG emissions. By

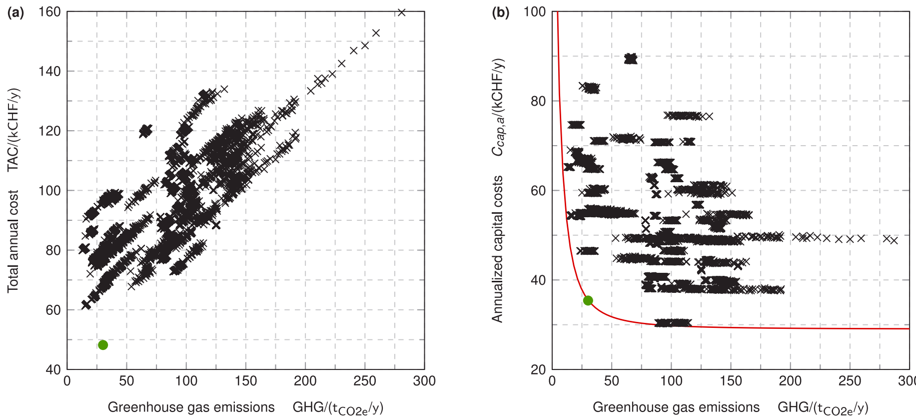

Fig. 7. Optimization results using TAC and GHG emissions as objectives ($MOO_{TAC,GHG}$). The green point indicates the solution of the SOO_{TAC} from Stampfli et al. [5]. In (a), the linear dependency between TAC and GHG emissions is visible. In (b), the Pareto front (red curve) between annualized capital costs and GHG emissions can be identified.

analyzing the ratio of the impact of 1 MWh utility reduction on the TAC and GHG emissions, using the existing plant as a reference, it can be shown that utility has

$$\frac{GHG_{init}}{\xi_{HU}+\xi_{CU}}\,\frac{c_{HU}+c_{CU}}{TAC_{init}} = 1.176$$

more impact on the cost than on the GHG emissions. Thereby, the values for the initial TAC and GHG emissions (TAC_{init}, GHG_{init}) are listed in Table 2 and the values for the cost and emission factors ($c_{HU}, c_{CU}, \xi_{HU}, \xi_{CU}$) are listed in Table A.2.

To have the same impact of utility demand on the result, operating costs instead of GHG need to be considered ($MOO_{CAP,COP}$). The results are visualized in Fig. 9. It shows that the algorithm found a Pareto front close the SOO_{TAC} solution.

In Table 2, the results for the analyzed objective configurations are compared. Due to the higher weight on utility demand for the $MOO_{TAC,GHG}$ optimization, the operating costs and GHG emissions are with 6,888 CHF/y and 15.04 $t_{CO2e/y}$, almost halved compared to the SOO_{TAC} with 12,780 CHF/y and 30.14 $t_{CO2e/y}$. As a result of the lower utility demand, the annualized capital costs for the $MOO_{TAC,GHG}$ are with 54,453 CHF/y higher than the 35,419 CHF/y of the SOO_{TAC}, which results in 61,341 CHF/y TAC compared to 48,198 CHF/y. By excluding the operating costs in the objectives ($MOO_{CAP,GHG}$), the weight on the utility demand is lower than the SOO_{TAC}, leading with 38,989 CHF/y and 81.09 $t_{CO2e/y}$ to the highest operating costs and GHG emissions. However, with 28,737 CHF/y, the lowest annualized capital costs are found, resulting in TAC of 67,726 CHF/y. TAC and GHG emissions are both worse compared to the $MOO_{TAC,GHG}$ solution and therefore this result is unlikely to be implemented.

By optimizing for annualized capital costs and operating costs ($MOO_{CAP,COP}$) the weighting is the same as for the SOO_{TAC}. The results of the optimization confirm this. The solution for $MOO_{CAP,COP}$ has with 37,299 CHF/y slightly higher annualized capital costs than the SOO_{TAC} solution. Operating costs and GHG emissions are with 12,128 CHF/y and 30.82 $t_{CO2e/y}$ the very similar to the SOO_{TAC} solution. This results in a slightly higher TAC of 50,427 CHF/y. To verify the $MOO_{CAP,COP}$ solution, the best found topology of the SOO_{TAC} is manually inserted in the initial population resulting in similar costs and GHG emissions as for the $MOO_{CAP,COP}$ and the SOO_{TAC} solutions.

In general, it cannot be said which objective configuration is best as it is another Pareto problem depending on which objective is more important. The differences in results based on the selection of the configuration of objectives also indicates that changes in cost and emission factors have a large impact on the solution.

5.3. Convergence analysis

In this section the convergence of the MOO algorithm is analyzed. To compare the results, with the SOO_{TAC} solution, the results

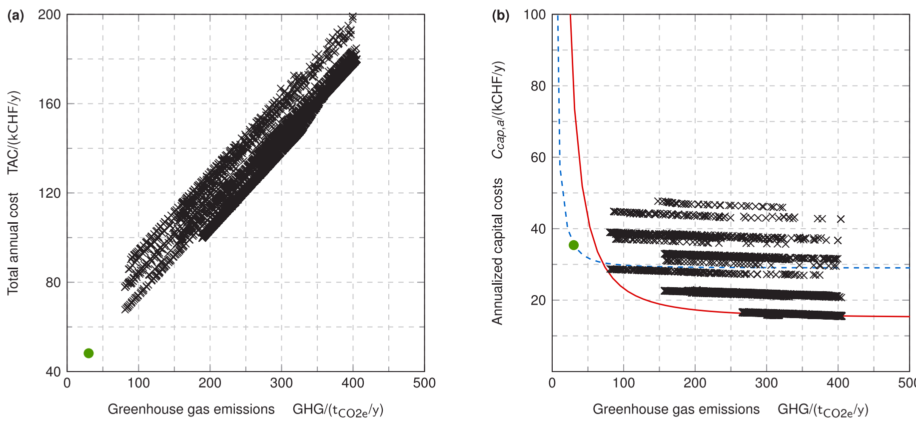

Fig. 8. The optimization results using annualized capital costs ($C_{cap,a}$) and GHG emissions as objectives ($MOO_{CAP,GHG}$). The green point indicates the solution of the SOO_{TAC} from Stampfli et al. [5]. In (b), the new Pareto front between annualized capital costs and GHG emissions (red curve) and the Pareto front from $MOO_{TAC,GHG}$ (blue dashed curve), are visualized.

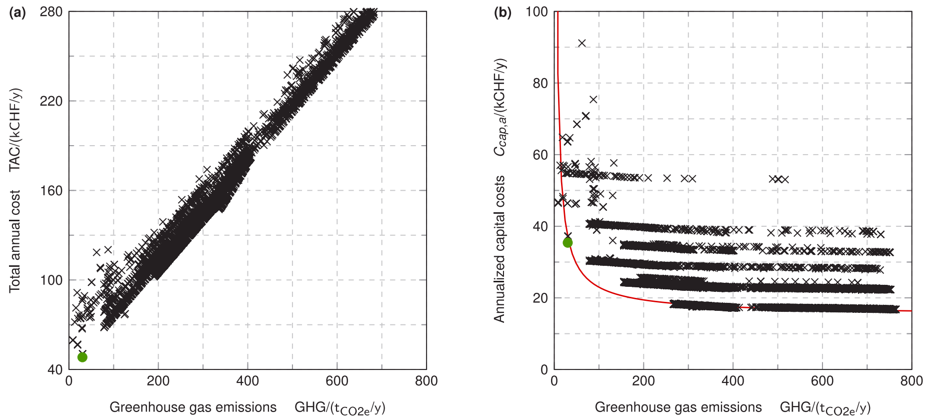

Fig. 9. The optimization results using annualized capital costs ($C_{cap,a}$) and operating costs ($C_{op,a}$) as objectives ($MOO_{CAP,COP}$). The green point indicates the solution of the SOO_{TAC} from Stampfli et al. [5]. In (b), the new Pareto front between annualized capital costs and GHG emissions (red curve) is drawn.

of $MOO_{CAP,COP}$ is selected in order to guarantee the same weighting leading to similar results. Fig. 10 shows the convergence over the number of generations for TAC and GHG. In Fig. 10(a), TAC of the $MOO_{CAP,COP}$ as well as SOO_{TAC} improve rapidly and stagnate over time. In contrast to the SOO_{TAC} which is constantly improving and reaching its best found solution after around 50 generations, $MOO_{CAP,COP}$ stagnates after around 8 generations and reaches its best found solution at around 60 generations. This stagnation can be explained by analyzing Fig. 10(b). It can be seen that the GHG emissions have a very sharp convergence reaching its almost best found solutions already at around 8 generations. This means that after 8 generations the utility consumption and thus also operating costs are only improving slightly. Hence, improvement of TAC after generation 8 are mostly due to improvement of capital costs by changes in topology, HEX areas, and mixer configurations.

6. Conclusions

The hybrid two-level evolutionary-based algorithm for heat exchanger network (HEN) retrofit for multi-period processes using genetic algorithm (GA) for topology optimization and differential evolution (DE) for heat load optimization has been extended from single-objective optimization (SOO) to multi-objective optimization (MOO) by introducing greenhouse gas (GHG) emissions as a second objective. Therefore, the algorithm is extended using a non-dominated sorting genetic algorithm (NSGA-II) and hypervolume indicators to implement a Pareto optimization.

With the introduction of the second objective, the weight on the utility demand is increased because the utility consumption causes operating costs as well as GHG emissions. Hence, the MOO result has 27% higher TAC but 50% lower GHG emissions compared to the SOO result. By excluding the operating costs from the TAC, the weight on utility demand is decreased resulting in 169% higher GHG emissions and 41% higher TAC compared to the SOO result. This can be explained by the fact that with the cost and emission factors of the analyzed case study, the reduction of utility demand has a 18% higher impact on operating costs than GHG emissions. To achieve comparable results to the SOO capital costs and operating costs need to be selected as objectives. In recent years, GHG emissions has itself established as an important decision factor alongside costs and energy consumption. The application to the industrial case study has shown that developed algorithm is useful tool providing the industry with the needed information for the decision-making process during the conceptual phase of a retrofit project.

In conclusion, the selection of the objectives is a Pareto problem. It depends on the project goals if GHG emissions or TAC are more critical and should be prioritized. It is important to highlight the influence of the weighting on the results. This influence also shows that a change in cost or emission factors has a large impact on the solution. Energy

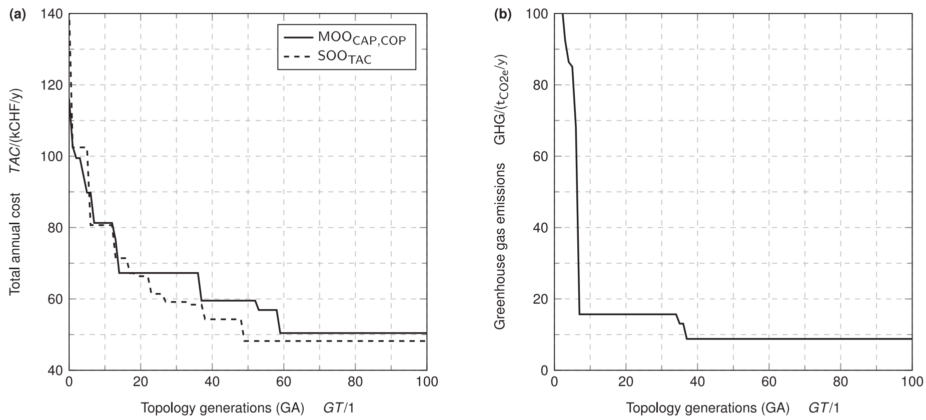

Fig. 10. Convergence of the $MOO_{CAP,COP}$ optimization over the number of topology generations. Whereby, (a) shows the convergence of the TAC in comparison with the SOO_{TAC} algorithm (dashed curve) and (b) shows the convergence of the GHG emissions.

prices might vary between different sites due to other energy provider and GHG emission depend on the technologies used to provide the utilities. Hence, a change in energy prices or the use of different utility systems, have a signigicant influence on the final design of the HEN.

CRediT authorship contribution statement

Jan A. Stampfli: Conceptualization, Methodology, Software, Validation, Formal analysis, Investigation, Data curation, Writing – original draft, Writing – review & editing, Visualization. **Benjamin H.Y. Ong:** Writing – original draft, Writing – review & editing. **Donald G. Olsen:** Data curation, Writing – review & editing, Supervision. **Beat Wellig:** Writing – review & editing, Supervision, Funding acquisition. **René Hofmann:** Resources, Writing – review & editing, Supervision.

Declaration of competing interest

The authors declare that they have no known competing financial interests or personal relationships that could have appeared to influence the work reported in this paper.

Data availability

The algorithm is available online [15,16] and the case study data provided in the Appendix.

Acknowledgments

This research project is financially supported by the Swiss Federal Office of Energy's "SWEET" Programme (Call 1-2020) – Decarbonisation of Cooling and Heating, DeCarbCH. Further financial support is provided by the Lucerne University of Applied Sciences and Arts, Switzerland. This research is part of a collaboration between the Lucerne University of Applied Sciences and Arts and TU-Wien.

Appendix. Process requirements and cost data for the potato chips production case study

Table A.1
Process requirements of the fritter line 1 for the regular chips and the cractive chips OP [5].

Stream	#	T_S	T_T	$T_{extr.}$	CP	h
	–	°C	°C	°C	kW/K	W/(m² K)
Regular chips OP (4,410 h/y)						
Vapor heating	C_1	136	229	500	2.51	400
Boiler air pre-heating	C_2	10	40	300	1.52	100
Make-up oil pre-heating	C_3	24	176	210	0.37	400
Degreaser air heating	C_4	–	–	–	–	–
Degreaser direct steam evaporation	C_5	–	–	–	–	–
Waste gas cooling[a]	H_1	280	30	30	14.81	400
Chips cooling	H_2	151	24	24	0.79	300
Cractive chips OP (2,610 h/y)						
Vapor heating	C_1	125.9	226.1	500	2.45	400
Boiler air pre-heating	C_2	10	40	300	1.48	100
Make-up oil pre-heating	C_3	24	166	210	0.18	400
Degreaser air heating	C_4	163.4	174	500	23.31	100
Degreaser direct steam evaporation	C_5	144.9	145.1	145.1	940.00	5000
Waste gas cooling[a]	H_1	270.1	30	30	14.3	400
Chips cooling	H_2	150	24	24	0.55	300

[a]Soft streams.

Table A.2
Utility data (pseudo-utilities) [5].

Utility	T_S	T_T	h	c_U	ξ_U
	°C	°C	W/(m² K)	CHF/MWh	t_{CO2eq}/MWh
Heating steam (HU)	300	299	5,000	80	0.22[a]
Cooling water (CU)	0	1	2,000	40	0.02[b]

[a]Natural gas boiler ($\eta = 0.9$).
[b]Refrigeration unit (COP = 5.9).

Table A.3
Modification cost factors (including Lang factors [26]: 3 for adding equipment (c_A); 1.1 for removing equipment (c_R)). Only cost for the removal of an equipment is listed, if it is existing (HEX, and admixer) [5].

Equipment	C_0	Q	c_A	c_R	d_f
	CHF	[Q]	CHF/Q	CHF/Q	–
HEX	0	A (m²)	1,731	635	0.61
Split	0	–	40,000	–	1.00
Bypass	0	–	40,000	–	1.00
Admixer	0	–	40,000	14,666	1.00
Re-pipe	0	–	68,000	–	1.00
Re-sequence	0	–	68,000	–	1.00

Depreciation period n = 10 y; interest rate i_r = 5%.

Table A.4
Match cost matrix (including utility streams) in CHF [5].

H\C	C_1	C_2	C_3	C_4	C_5	CU
H_1	0	1,500	2,100	2,100	2,100	0
H_2	900	3,000	600	300	300	0
HU	0	0	0	0	0	0

References

[1] Linnhoff B, Flower J. Synthesis of heat exchanger networks I: Systematic generation of energy optimal networks. AlChE J 1978;24:633–42.
[2] Klemeš JJ. Handbook of process integration (PI): Minimisation of energy and water use, waste and emissions. Cambridge, UK: Woodhead Publishing Limited/Elsevier; 2013, p. 168–200.
[3] Aguitoni MC, Pavão LV, da Silva Sá Ravagnani MA. Heat exchanger network synthesis combining simulated annealing and differential evolution. Energy 2019;181:654–64. http://dx.doi.org/10.1016/j.energy.2019.05.211.
[4] Pavão LV, Miranda CB, Costa CB, Ravagnani MA. Efficient multiperiod heat exchanger network synthesis using a meta-heuristic approach. Energy 2018;142:356–72. http://dx.doi.org/10.1016/j.energy.2017.09.147.
[5] Stampfli JA, Ong BH, Olsen DG, Wellig B, Hofmann R. Applied heat exchanger network retrofit for multi-period processes in industry: A hybrid evolutionary algorithm. Comput Chem Eng 2022;161:107771. http://dx.doi.org/10.1016/j.compchemeng.2022.107771.
[6] Toimil D, Gómez A. Review of metaheuristics applied to heat exchanger network design. Int Trans Oper Res 2017;24:7–26. http://dx.doi.org/10.1111/itor.12296.
[7] Stampfli JA, Olsen DG, Wellig B, Hofmann R. Heat exchanger network retrofit for processes with multiple operating cases : a metaheuristic approach. Comput Aided Chem Eng 2020;48:781–6. http://dx.doi.org/10.1016/B978-0-12-823377-1.50131-2.
[8] Sreepathi BK, Rangaiah GP. Improved heat exchanger network retrofitting using exchanger reassignment strategies and multi-objective optimization. Energy 2014;67:584–94. http://dx.doi.org/10.1016/j.energy.2014.01.088.
[9] Sreepathi BK, Rangaiah GP. Retrofitting of heat exchanger networks involving streams with variable heat capacity: Application of single and multi-objective optimization. Appl Therm Eng 2015;75:677–84. http://dx.doi.org/10.1016/j.applthermaleng.2014.09.067.
[10] Kang L, Liu Y. A systematic strategy for multi-period heat exchanger network retrofit under multiple practical restrictions. Chin J Chem Eng 2017;25:1043–51. http://dx.doi.org/10.1016/j.cjche.2017.01.002.
[11] Ong BH, Lucas EJ, Olsen DG, Roth S, Wellig B. A user workflow for combining process simulation and pinch analysis considering ecological factors. Chem Prod Process Model 2022;17:341–63. http://dx.doi.org/10.1515/cppm-2021-0004.
[12] Fortin F-A, Rainville F-MD, Gardner M-A, Parizeau M, Gagné C. Deap: evolutionary algorithms made easy. J Mach Learn Res 2012;13:2171–5.
[13] Stampfli JA, Olsen DG, Wellig B, Hofmann R. A parallelized hybrid genetic algorithm with differential evolution for heat exchanger network retrofit. MethodsX 2022;9:101711. http://dx.doi.org/10.1016/j.mex.2022.101711.

[14] Chen JJ. Logarithmic mean: Chen's approximation or explicit solution? Comput Chem Eng 2019;120:1–3. http://dx.doi.org/10.1016/j.compchemeng.2018.10.002.

[15] Stampfli JA. J-A-St/Moc_retrofit_ga_de: V1.0 (Version V1.0). Zenodo; 2021, http://dx.doi.org/10.5281/zenodo.4441140.

[16] Stampfli JA. J-A-St/Moc_retrofit_ga_de: V2.0 (Version V2.0). Zenodo; 2023, http://dx.doi.org/10.5281/zenodo.7568479.

[17] Yee TF, Grossmann IE. Simultaneous optimization models for heat integration - II. Heat exchanger network synthesis. Comput Chem Eng 1990;14:1165–84. http://dx.doi.org/10.1016/0098-1354(90)85010-8.

[18] Lambert JH. Observationes variae in mathesin puram. Acta Helv 1758;3:128–68.

[19] Ahmad S, Smith R. Targets and design for minimum number of shells in heat exchanger networks. Chem Eng Res Des 1989;65:481494.

[20] Deb K, Agrawal S, Pratap A, Meyarivan T. A fast elitist non-dominated sorting genetic algorithm for multi-objective optimization: NSGA-II. In: Parallel problem solving from nature PPSN VI. PPSN 2000. Lecture notes in computer science, vol. 1917, Springer Berlin Heidelberg; 2004, p. 849–58. http://dx.doi.org/10.1007/3-540-45356-3_83.

[21] Fortin FA, Grenier S, Parizeau M. Generalizing the improved run-time complexity algorithm for non-dominated sorting. In: GECCO 2013 - Proceedings of the 2013 genetic and evolutionary computation conference. 2013, p. 615–22. http://dx.doi.org/10.1145/2463372.2463454.

[22] Zitzler E, Brockhoff D, Thiele L. The hypervolume indicator revisited: On the design of pareto-compliant indicators via weighted integration. In: Lecture notes in computer science (Including subseries lecture notes in artificial intelligence and lecture notes in bioinformatics). LNCS, vol. 4403, 2007, p. 862–76. http://dx.doi.org/10.1007/978-3-540-70928-2_64.

[23] Fotsch P. Pilotphase Pinch-Methodik 2006/07: Zweifel Pomy-Chips AG. Technical Report, Zurich: Swiss Federal Office of Energy SFOE; 2006, p. 1–71.

[24] CO2-Emissionsfaktoren des Treibhausgasinventars der Schweiz. Technical Report, Berne, Switzerland: Federal Office for the Environment (FOEN); 2022, p. 1–5.

[25] Krebs L, Frischknecht R. Umweltbilanz Strommixe Schweiz 2018. Technical Report, Uster, Switzerland: treeze Ltd., fair life cycle thinking; 2021, p. 1–53.

[26] Lang HJ. Simplified approach to preliminary cost estimates. Chem Eng 1948;55:112–3.

Software 1

Evolutionary-Based Heat Exchanger Network Retrofit for Processes with Multiple Operating Cases

published on Zenodo

This software package is published under the open-source license Apache 2.0 and is online available. The software package includes the two-stage single-objective GA/DE algorithm explained in Article 2, 3 and 4. This software is developed using the programming language Python.

My contribution: Conceptualization, Methodology, Software, Validation.

Stampfli, J. A. (2021). J-a-st/moc_retrofit_ga_de: v1.0. Zenodo.

DOI: *10.5281/zenodo.4441140*

Software 2

Multi-Objective Evolutionary-Based Heat Exchanger Network Retrofit for Multi-Period Processes

published on Zenodo

This software package is published under the open-source license Apache 2.0 and is online available. The software package includes the two-stage multi-objective GA/DE algorithm explained in Article 5 and 6. This software is developed using the programming language Python.

My contribution: Conceptualization, Methodology, Software, Validation.

Stampfli, J. A. (2023). J-a-st/moc_retrofit_ga_de: v2.0. Zenodo.

DOI: 10.5281/zenodo.7568479

Article A

Practical Heat Pump and Storage Integration into Non-Continuous Processes: a Hybrid Approach Utilizing Insight Based and Nonlinear Programming Techniques

published in Energy as a collaboration with Martin J. Atkins, Donald G. Olsen, Micheal R.W. Walmsley, and Beat Wellig

This journal article is an invited contribution to the special issue of the 18th Conference on Process Integration, Modelling and Optimisation for Energy Saving and Pollution Reduction of the Energy journal. The research done for this article proposes hybrid approach to the integration of heat pumps into non-continuous processes. Thereby, a PA approach is used to narrow down the solution space of the MINLP to a NLP problem. The proposed method is applied to a real case study from the dairy industry showing its application for a non-continuous total site problem.

My contribution: Conceptualization, Methodology, Software, Validation, Formal analysis, Investigation, Data curation, Writing –original draft, Visualization, Writing –review & editing.

Stampfli, J. A., Atkins, M. J., Olsen, D. G., Walmsley, M. R., and Wellig, B. (2019b). Practical heat pump and storage integration into non-continuous processes: a hybrid approach utilizing insight based and nonlinear programming techniques. Energy *182, pp. 236–253.*

DOI: `10.1016/j.energy.2019.05.218`

Article B

Batch Process Integration: Management of Capacity-Limited Thermal Energy Storage by Optimization of Heat Recovery

published in Chemical Engineering Transactions as a collaboration with Edward J. Lucas, Donald G. Olsen, Pierre Krummenacher, and Beat Wellig

The research in this journal article was presented in the form of a talk by Jan A. Stampfli at the 19th Conference on Process Integration, Modelling and Optimisation for Energy Saving and Pollution Reduction in Crete, Greece. The research in this article deals with the problem of space constraints for indirect heat recovery using stratified thermal energy storage. Thereby, an LP model is used to optimize the ideal capacity management of a volume-limited storage to maximize HR.

My contribution: Conceptualization, Methodology, Software, Validation, Formal analysis, Investigation, Data curation, Writing –original draft, Visualization, Writing –review & editing.

Stampfli, J. A., Lucas, E. J., Olsen, D. G., and Krummenacher, P. (2019a). Batch process integration: management of capacity-limited thermal energy storage by optimization of heat recovery. Chemical Engineering Transactions *76, pp. 1027–1032.*

DOI: *10.3303/CET1976172*

Article C

Heat Pump and Thermal Energy Storage Integration in Noncontinuous Processes – an Application to the Food Industry

published in Proceedings of the 13th IEA Heat Pump Conference as a collaboration with Edward J. Lucas, Lorenz P. Rast, Raphael Agner, and Beat Wellig

This research was presented in the form of a talk by Raphael Agner at the 13th IEA Heat Pump Conference. This conference proceeding showed the application of the proposed method in Article A to a threshold problem of a candy production plant.

My contribution: Conceptualization, Methodology, Software, Validation, Writing –original draft, Writing –review & editing.

Lucas, E. J., Stampfli, J. A., Rast, L. P., Agner, R., and Wellig, B. (2021). Heat pump and thermal energy storage integration in non-continuous processes – an application to the food industry. In: Proceedings of the 13th IEA Heat Pump Conference*, pp. 1478–1490.*

Article D

Optimization of Volume-Limited Thermal Energy Storage in Non-Continuous Processes

published in Energy as a collaboration with Edward J. Lucas, Benjamin H.Y. Ong, Donald G. Olsen, Pierre Krummenacher, and Beat Wellig

This journal article is an invited contribution to the special issue of the 19th Conference on Process Integration, Modelling and Optimisation for Energy Saving and Pollution Reduction of the Energy journal. The research in this article extends the model from Article B to include fixed temperature variable mass (FTVM) storage. The application of both the stratified and the FTVM storages for two different breweries is shown.

My contribution: Conceptualization, Methodology, Software, Validation, Formal analysis, Investigation, Data curation, Writing –original draft, Visualization, Writing –review & editing.

Stampfli, J. A., Lucas, E. J., Ong, B. H. Y., Olsen, D. G., Krummenacher, P., and Wellig, B. (2020b). Optimization of volume-limited thermal energy storage in non-continuous processes. Energy *203, p. 117805.*

DOI: 10.1016/j.energy.2020.117805

Article E

Integration von Wärmepumpen und Speichern zur Effizienzsteigerung nicht-kontinuierlicher Prozesse

published in 27. Tagung des BFE-Forschungsprogramms Wärmepumpen und Kältetechnik as a collaboration with Beat Wellig, Raphael Agner, and Benjamin H.Y. Ong

This research was presented in the form of a talk by Beat Wellig at the 27. Tagung des BFE-Forschungs-programms Wärmepumpen und Kältetechnik. This research showed an approach for heat pump integration into non-continuous processes. In contrast to the research in Article A, this work explores the opportunities for heat pump integration directly into the process.

My contribution: Writing –original draft, Writing –review & editing.

Wellig, B., Agner, R., Ong, B. H. Y., Stampfli, J. A., Olsen, D. G., and Krummenacher, P. (2021). Integration von wärmepumpen und speichern zur effizienzsteigerung nicht-kontinuierlicher prozesse. In: 27. Tagung des BFE-Forschungsprogramms "Wärmepumpen und Kältetechnik"*, pp. 1–14.*

Article F

Practical Integration of Heat Pumps with Thermal Energy Storage in Non-Continuous Processes

published in Proceedings of the 24th Conference on Process Integration, Modelling and Opimisation for Energy Saving and Pollution Reduction as a collaboration with Raphael Agner, Benjamin H.Y. Ong, Pierre Krummenacher, and Beat Wellig

The research in this conference proceeding was presented in the form of a talk by Benjamin H.Y. Ong at the 25th Conference on Process Integration, Modelling and Optimisation for Energy Saving and Pollution Reduction in Brno, Czech Republic. This Article extends the work from Article E using MP methods to explore the possible indirect HR.

My contribution: Writing –original draft, Writing –review & editing, Supervision.

Agner, R., Ong, B. H. Y., Stampfli, J. A., and Krummenacher, P. (2021). Integration of heat pumps with thermal energy storage in non-continuous processes. In: Proceedings of the 24 th Conference on Process Integration, Modelling and Optimisation for Energy Saving and Pollution Reduction*, pp. 1–10.*

Article G

A Graphical Method for Combined Heat Pump and Indirect Heat Recovery Integration

published in Energies as a collaboration with Raphael Agner, Benjamin H.Y. Ong, Pierre Krummenacher, and Beat Wellig

This journal article is an invited contribution to the special issue of the 24th Conference on Process Integration, Modelling and Optimisation for Energy Saving and Pollution Reduction of the Energies journal. This article explains the method presented in Article F in more detail.

My contribution: Writing –original draft, Writing –review & editing, Supervision.

Agner, R., Ong, B. H. Y., Stampfli, J. A., Krummenacher, P., and Wellig, B. (2022). A graphical method for combined heat pump and indirect heat recovery integration. Energies *15 (8), p. 2829.*

DOI: 10.3390/en15082829

Software A

Capacity Limitation Tool in PinCH 3.5

available through pinch-analyse.ch

The approach developed in Article B and D is implemented in the commercial Software PinCH 3.5. PinCH is a PA tool for practical application in industry. This software is developed using the programming language C#. More information about PinCH can be found on pinch-analyse.ch

My contribution: Conceptualization, Methodology, Software, Validation.

Curriculum Vitae

Jan Andreas Stampfli,
born on 3$^{\text{th}}$ of March, 1991, in Niederbipp, Switzerland, citizen of Subingen and Etziken.

Education

Oct'18–present **Doctor Candidate in Engineering Sciences – Mechanical Engineering** TU-Wien, Vienna, Austria.

Sept'15–Feb'18 **MSc FHZ in Engineering with Specialization in Energy and Envrionment** Lucerne University of Applied Sciences and Arts, Horw, Switzerland.

Sept'12–Aug'15 **BSc FHZ in Mechanical Engineering with Specialization in Renewable Energy & Process Engineering and in Fluid Mechanics & Hydraulic Machines** Lucerne University of Applied Sciences and Arts, Horw, Switzerland.

Sept'11–Aug'12 **Technical Professional Maturity** Gewerblich-Industrielle Berufsfachschule, Solothurn, Switzerland.

Aug'07–Aug'11 **Apprenticeship as technical draughtsman (Konstrukteur EFZ)** EWAG AG, Etziken, Switzerland.

Professional Experience

Mar'23–present **Senior Research Associate** Lucerne University of Applied Sciences and Arts, Competence Center Thermal Energy Systems and Process Engineering, Horw, Switzerland.

Oct'18–present **Guest Lecturer Pinch Analysis** TU-Wien, Vienna, Austria

Mar'18–Feb'23 **Research Associate** Lucerne University of Applied Sciences and Arts, Competence Center Thermal Energy Systems and Process Engineering, Horw, Switzerland.

Sept'17–Jan'18 **Visiting Researcher** The University of Waikato, Energy Research Center, Hamilton, New Zealand.

Sept'15–Aug'17 **Research Assistant** Lucerne University of Applied Sciences and Arts, Competence Center Thermal Energy Systems and Process Engineering, Horw, Switzerland.